



TECHNISCHE
UNIVERSITÄT
WIEN
Vienna | Austria



Diploma Thesis

Water based Lithium-Nickel- Manganese-Cobalt-Oxide-Slurry preparation as Cathodes for Li-Ion Batteries

carried out for the purpose of obtaining the degree of Master of Science (MSc or Dipl.-
Ing. or DI), submitted at TU Wien, Faculty of Mechanical and Industrial
Engineering, by

Marta Habowska

Mat.Nr.: 01529795

under the supervision of

Ao.Univ.Prof. Dipl.-Ing. Dr.techn. Günter Faflek

Institute of Chemical Technologies and Analytics, E164

Affidavit

I declare in lieu of oath, that I wrote this thesis and performed the associated research myself, using only literature cited in this volume.

Vienna, April 2020

ACKNOWLEDGMENTS

I would first like to thank my thesis supervisors Professor Günter Fafilek from the Vienna University of Technology and Dr. Katja Fröhlich from the Austrian Institute of Technology. The door to Prof. Fafilek office was always open whenever had a question about my research or writing.

I would also like to thank the experts and colleagues at Vienna University of Technology and the Austrian Institute of Technology for their great support, guidance and assistance throughout the entire course of this thesis.

Finally, I want to express my very profound gratitude to my parents and to my boyfriend for providing me with unfailing support and continuous encouragement through the process of researching and writing this thesis.

Thank you all.

KURZFASSUNG

Wiederaufladbare Lithium-Ionenbatterien sind eine der vielversprechendsten Energiespeichersysteme die in vielen Anwendungen, z.B. in verschiedenen tragbaren elektronischen Geräten (Mobiltelefone, Laptops, usw.), elektrischen Fahrzeugen Verwendung finden. Aufgrund ihres hohen Wirkungsgrades für die Umwandlung von chemischer in elektrischer Energie findet die Lithium-Technologie große Aufmerksamkeit. Die Entwicklung von sauberen und nachhaltigen Energiesystemen ist von globaler Bedeutung. Die elektrochemischen Eigenschaften von Lithium-Ionenbatterien hängen sehr stark von den verwendeten Materialien, deren Struktur und dem Zelldesign ab. Um die Batterieperformance zu optimieren wird an Elektrodenmaterialien, Elektrolyten, Additiven, Bindern und Membranen geforscht. Das Ziel dieser Arbeit war die Entwicklung von wasserbasierten Bindemitteln (Carboxymethylzellulose - CMC, Fluoroacrylatlatex) für die bekannten Nickel-Mangan-Cobalt-Mischungen (NMC 111, NMC 532, NMC 622) für positive Elektroden. Die derzeitige Technologie nutzt Polyvinylidene-Difluorid - PVDF und das giftige N-methyl-2-pyrrolidone NMP, die durch umweltfreundliche Binde- und Lösemittel ersetzt werden sollen. Die Eigenschaften der hergestellten Elektroden wurden in dieser Arbeit mit den folgenden Methoden untersucht: a) zyklische Lade-/Entladetests mit dem Maccor Battery & Cell Test Gerät im CC-CV Modus (Konstantstrom-Konstantspannung), b) zyklischer Voltammetrie mit Ametek's Geräten und Programm, c) Rasterelektronenmikroskopie (SEM) und energiedispersiver Röntgenspektroskopie/Analyse (EDAX/EDS), d) verschiedene händische mechanische Prüfungen um die Haftungseigenschaften der Beschichtung auf dem Stromkollektor abzuschätzen.

ABSTRACT

Rechargeable lithium-ion batteries are one of the most promising energy storage systems using in various portable electronics (cellular phones, laptops, computers), hybrid electric vehicles (HEVs) and plug-in HEVs (p-HEVs).

Due to the high conversion efficiency between the chemical and the electrical energy, the lithium-ion technology has attracted a great deal of attention. Moreover, the development of clean and sustainable energy system is one of the strategies of global significance. The electrochemical properties of lithium-ion battery depend strongly on its materials, structure and design. To achieve improvement of the battery performance researches carried out studies on electrode materials, electrolytes, additives, binders and membranes. In this work, the main goal was to show properties and working scheme of lithium-ion batteries, which were based on three well known nickel-manganese-cobalt lithium oxides (NMC 111, NMC 532 and NMC 622) materials with water-soluble binder mixtures of carboxymethyl cellulose (CMC) and fluorine acrylic latex. The commercial used organic solvent – based poly(vinylidene difluoride) PVDF processing with harmful and toxic N-methyl-2-pyrrolidone NMP has been substitute by environmentally friendly binder – fluorine acrylic latex. Properties of prepared cathodes were examined in this thesis by:

- cycling charge-discharge tests with Maccor Battery & Cell Test Equipment used in CC-CV (constant current, constant voltage),
- cyclic voltammograms tests with Ametek's program,
- scanning electron microscopy (SEM) and electron dispersive X-ray spectroscopy/analysis (EDAX/EDS),
- some organoleptic tests were used to determine properties of active material coating on current collector.

Table of contents

1. Introduction.....	8
1.1. Li-Ion batteries and their history	9
1.2. Lithium ion cell operation, materials and components.....	10
1.2.1. Main work parameters.....	10
1.2.2. Work and design of Li-ion batteries.....	11
1.2.3. Cathode materials (positive electrode)	14
1.2.4. Anode materials (negative electrode).....	19
1.2.5. Electrolytes.....	21
1.2.6. Current collectors and separators	22
1.2.7. Binders.....	23
2. Water-soluble binders and LiNiMnCoO as cathode material	24
2.1. Sodium carboxymethyl cellulose (CMC) and polyurethane (based on IPDI).....	25
2.2. Sodium carboxymethyl cellulose (CMC).....	29
2.3. NMC 111 with water-compatible (SBR, CMC) and non-aqueous binders (PVDF) ...	31
2.4. Sodium carboxymethyl cellulose (CMC) and styrene-butadiene rubber (SBR)	34
2.5. NMC 111 with water-compatible (SBR, CMC) and non-aqueous binders (PVDF) ...	34
2.6. LiNi _{1/3} Mn _{1/3} Co _{1/3} O ₂ with polytetrafluoroethylene (PTFE).....	39
2.7. “Door opener” to the future of battery?.....	42
3. Experimental	43
3.1. Slurry, electrode and cell preparation.....	43
3.2. Electrode morphology and composition.....	46
3.3. Cycling properties of prepared cells.....	55
3.3.1. Cells from electrode 7 (non-aqueous binder) – NMC 111, comparative sample	56
3.3.2. Cells from electrode 4 (first composition) – NMC 111.....	56
3.3.2.1. Sample 4.1 and 4.3, cycling to 4.2V.....	57
3.3.2.2. Sample 4.8 and 4.14 cycling to 4.5 V.....	60
3.3.3. Cells from electrode 5 (first composition) – NMC532.....	62
3.3.3.1. Samples 5.1, 5.2 and 5.6, cycling to 4.2 V	62
3.3.3.2. Sample 5.3 and 5.10, cycling to 4.5 V.....	64
3.3.4. Cells from electrode 6 (first composition) – NMC 622.....	66
3.3.4.1. Samples 6.2, 6.3, 6.6, 6.7 and 6.10, cycling to 4.2 V	67
3.3.4.2. Sample 6.1	68
3.3.5. Cells from electrode 9 (second composition) – NMC 111	69
3.3.5.1. Sample 9.1.11 and 9.2.1 cycling to 4.2 V.....	70

3.3.5.2.	Sample 9.1.3 and 9.2.5 cycling to 4.5 V	71
3.3.6.	Cells from electrode 8 (second composition) – NMC 532.....	73
3.3.6.1.	Samples 8.1.1 and 8.2.8, cycling to 4.2 V.....	73
3.3.6.2.	Samples 8.1.4 and 8.2.1, cycling to 4.5 V.....	74
3.3.7.	Cells from electrode 10 (second composition) – NMC 622.....	76
3.3.7.1.	Samples 10.1.2 and 10.1.14, cycling to 4.2 V.....	76
3.3.7.2.	Samples 10.1.6 and 10.1.11, cycling to 4.5 V.....	78
3.4.	Comparison of cycling results.....	79
3.5.	Cyclic voltammetry of prepared cathodes.....	85
4.	Experimental results summary and conclusions	88
5.	References.....	95

1. Introduction

It is very hard to imagine our world without energy usage. From the very beginning, humans and their predecessors were using a lot of energy sources, starting with fireplaces and energy coming from combustion process, ending with various kinds of energy now from which electrical energy is the most versatile one. Nowadays, people understand electricity as an energy, which is coming from power plants and many different, devices named as batteries and accumulators. Electricity is used to power stationary devices such as fridges, personal computers and lights or more mobile devices like smartphones, music players or even cars. The technological development allows us to store and utilize more and more energy thanks to sophisticated and advanced galvanic cells. The purpose of this work is to collect the current knowledge about Li-Ion secondary cells, their main working parameters, and main component materials for cathodes, anodes, electrolytes and binders. Moreover, this work will put emphasis on the development of water-soluble binders for electrodes and LiNiMnCoO-based materials for cathodes.

The use of water-soluble binders in Li-Ion batteries and use of water-based slurries with lithium-nickel-manganese-cobalt oxides results in novel impediments. Continuous technological development allows to produce a product of high quality, but mostly uses toxic organic solvents like N-methyl-2-pyrrolidone, which restricts processing and recycling of lithium-ion batteries. This work describes the processing of slurries made with water-soluble binders and lithium-nickel-manganese-cobalt oxides, particularly discussing treatment problems and possible profits coming from application of new materials. A few independent scientific examples of utilization of mentioned materials with their preparation, examination and results will be presented and discussed. The obtained outcome will be described with charts, images or numbers. Similar processes will be carried out for own scientific research on lithium nickel-manganese-cobalt oxides with water-soluble binder. At the end, conclusions from introduced material will be shown.

1.1. Li-Ion batteries and their history

At the beginning of the XIX century, in 1800, Alessandro Volta presented his invention – the Voltaic pile, a simple and working electrochemical primary cell.¹ It consisted of copper and zinc plates with acid as electrolyte. In 1866, Georges-Lionel Leclanché invented the zinc-manganese oxide cell, which later gave birth to dry cell and with its modifications it is still very popular at present. In 1859, Gaston Plante´ invented the acid-lead rechargeable galvanic cell, established as an ‘accumulator’. With its later modifications, the acid-lead cell is still commonly used worldwide.¹ Those inventions are only few examples of a long list of discoveries of different cells, with nickel-cadmium and nickel-metal hydride batteries also included in this list. Inventors usually were looking for lighter materials with a better energy storage property to make their cells continually and persistently smaller and lighter and/or to last longer and/or to work in harsh conditions. That led to lithium – the lightest metal element, with the highest electrochemical potential and energy density, but very reactive chemically. In 1970s, first lithium primary cells (non-rechargeable) were developed² and shortly became popular due to a long working time, very good stability and thanks to waterless electrolytes a wide range of working temperatures. The most popular non-rechargeable lithium batteries are based on the following chemistries: manganese oxide-lithium (‘CR’ batteries), graphite monofluoride-lithium, lithium-iodine (for medical applications), lithium-thionyl chloride, silver chromate-lithium and lithium-iron disulfide.³ Further works ended as secondary cells with metallic lithium as an electrode – for example, lithium-titanium disulfide cell. Their main disadvantage was fast degradation during operation and charging cycles and hazardous composition, proving that the reactive anode is reacting with the electrolyte and affecting dangerous charging process.¹ Cell short circuits b dendrite growth and succeeding fire incidents resulted in important changes of the design. Sony developed the first rechargeable lithium-ion battery and introduced it on the market in 1991. Carbon was the active material of the negative electrode and lithium cobalt oxide -the positive electrode. During discharging, lithium cations leave the anode and the same amount of lithium cations intercalate into the cathode, with all these processes reversed during charging. New batteries do not contain metallic lithium anymore, but they hold various lithium chemical compounds within.² This idea, called the ‘lithium rocking chair battery’ due to the cyclical lithium ions exchange between electrodes during charging and discharging, initiated the

development of many new types of lithium ions batteries, which continues until now.⁴ Modern materials for Li-Ion batteries will be discussed later in this work.

1.2. Lithium ion cell operation, materials and components

1.2.1. Main work parameters

Every battery operation is characterized with some parameters. Among many physical factors, the battery capacity and its voltage are the most practical values for daily use, but from the technical point of view there are several important parameters.^{5,6,7}

Current I – it is the quantity describing the intensity of electrical charges flow, known as an electric current. The measure is Ampere [A]. Li-Ion batteries have security utilities, which limits the maximum current to a safe level for proper operation (due to limits resulting from the cell structure and size).

Open-circuit voltage V_{oc} – this value is measured for a battery when current $I=0$. The measure is Volts [V]. The exact value is depending on electrochemical potentials of anode and cathode and energy gaps between valence bands of liquid and solid electrolytes.

Voltage V – this is the potential difference of the electrodes for an electric current I greater than zero. The measure is Volts [V]. Due to a voltage drop at the battery's internal resistance R , the terminal voltage is different from the open-circuit voltage. During charging, the voltage drop increases the terminal voltage, at discharge, the terminal voltage decreases. The voltage drop is equal to the current times the internal resistance: $V = V_{OC} - I \cdot R$.

Power P – describes energy output from the battery. The measure is Watt [W]. It is calculated from the output current multiplied by the terminal voltage: $P = V \cdot I$.

Capacity C – the quantity describing the electric charge, that can be delivered by a battery at rated voltage. The measure is usually Ampere hours [Ah] rather than in Coulombs [C]. This quantity describes whole cells – bigger cell can store more electric charge than smaller cell with the same chemistry. The capacity is strongly influenced by the discharge rate of cell – along with a greater discharge rates, the cell capacity is reduced.

Specific energy e – describes how much energy is stored in a unit of mass. The measure is Joules per kilogram [J/kg] or Watt hours per kilogram [Wh/kg]. Higher specific energy results in a lighter cell with the same amount of energy stored inside.

Energy density U – is total energy storage per volume unit of a battery or electrode. The measure is Joules per cubic meter [J/m³] or Watt hours per cubic meter [Wh/m³]. This value is widespread and commonly used to compare different batteries and their different chemistries (for example Ni-Cd vs. Li-Ion batteries).

Specific power or power to weight ratio – this property is used to enable the comparison of mobile power sources of different design and chemistries. Usually the measure is Watts per kilogram [W/kg]. For a proper correlation, the discharge rate, cell temperature and specific energy must be considered, making it more complicated than comparing cells using the specific energy and/or energy density parameters.

Charging and discharging rate, C-rate – described as a current (charge or discharge, depending on context, because the C-rate is never negative), divided by the battery's nominal capacity. Usually, the measure is 1 by hour [h⁻¹]. For example, for a 500 mAh battery C-rate 1 C would be a charge (discharge) current of 500 mA, for ½ C it is 250 mA and for 10 C it is 5000 mA. It is widely used to determine conditions of charging and discharging processes without involving battery capacity and current.

1.2.2. Work and design of Li-ion batteries

The Li-Ion cell design is relatively simple. Every cell consists of 'working parts', which are anode, cathode and electrolyte (lithium salts dissolved in non-aqueous solvent, ion conducting polymers or solid electrolytes), and 'inactive parts' like casing, separators, current collectors, connectors, etc. Ready-to-work cell is in a charged state. During discharging, electrons leave the negative electrode through an external circuit. The negative electrode becomes oxidized and is therefore the anode. The electrons flow across an electric load to the positive electrode, which becomes reduced and the cathode.⁸ The ionic current inside the cell matches the external electric current, because the perfect electrolyte is just an ionic conductor rather than a conductor for electrons. Cations (in this case lithium cations) leave the anode and enter the electrolyte. The cations migrate across the electrolyte to the cathode material where it intercalates. Figure 1 displays this principle of operation for the discharging. During charging, all processes are reversed – the negative electrode is reduced (cathode), and the positive

electrode is oxidized (anode). Lithium ions also travel in a backward direction through electrolyte.⁵

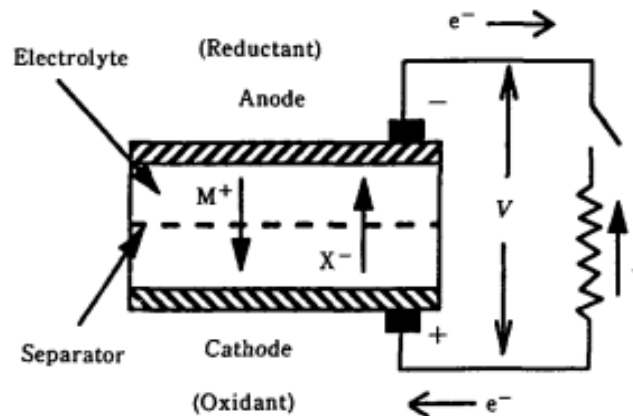


Figure 1. The diagram of lithium-ion cell work.⁵

The operation of one of the first secondary lithium ions cells will be shortly discussed: the lithium-titanium disulfide cell based on a lithium metal anode. Theoretically, the electrochemical reaction occurring during discharge can be written in the simple equation: $x \text{Li} + \text{TiS}_2 \rightarrow \text{Li}_x\text{TiS}_2$, where $0 < x \leq 1$.

Ti(IV) is reduced to Ti(III), and metallic Li(0) is oxidized to Li(I), enters the electrolyte and after intercalating the cathode balances the charge change in a reduced titanium disulfide.¹ This is well presented in Figure 2.

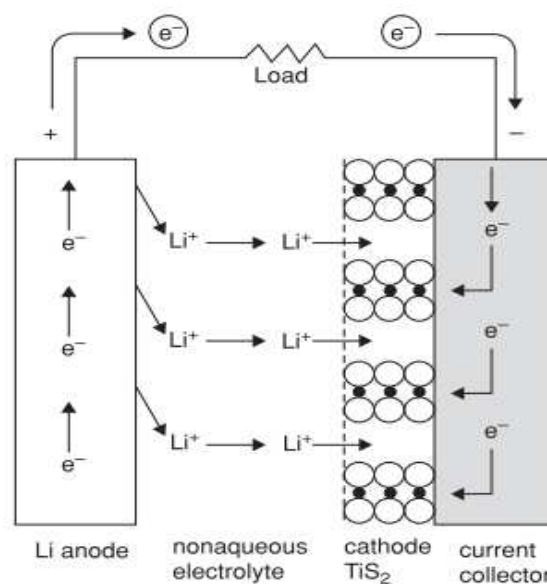
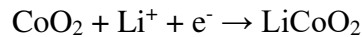


Figure 2. The diagram of LiTiS₂ cell work.¹

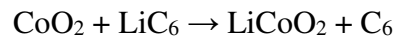
The description of operation of batteries based on lithium containing chemical compounds instead of metallic lithium, as anode will be discussed based on the example of a lithium cobalt oxide-graphite cell. During discharge, the anodic half-reaction is given by:



and the cathodic half-reaction by



The reaction equation for a whole cell during discharge is:



Both electrodes exchange lithium ions and are intercalation electrodes (named usually as ‘sink electrodes’). Co(IV) is reduced to Co(III) and the Li-graphite complex is oxidized to Li^+ and free graphite. Li^+ -ions enter the electrolyte and after intercalation into the cathode it balances the charge change in the reduced cobalt oxide.⁹

Lithium-ion batteries have many advantages when compared to other batteries:

- high open circuit voltage (especially when compared to aqueous batteries like lead-acid, nickel-cadmium, nickel-metal hydride);
- high energy density, which means that the same amount of energy can be stored in lighter battery;
- high specific density, which means that the same amount of energy can be stored in a smaller battery;
- relatively cheap and easily assembled;
- nearly no memory effect;
- efficient operation.¹⁰

Their main disadvantage is a danger of cell short-circuit with fire or cell damage, which can lead to electrolyte leakage, air contact with electrodes or short-circuit, all three potentially bring a serious risk of fire and environmental pollution. In addition, due to a high popularity, the environmental impact and possibility of recycling of spent and obsolete batteries are subject of increased interest.

The term „battery” is often applied, but in electrochemical point of view, the basic unit being referred to is the „cell”. A battery may consist of one or more cells. In

Figure 3 one can see the scheme of a cell in cylindrical form, showing all internal parts and their arrangement. The cathode, the anode and the electrolyte are the major components of a cell. During discharge, the positive electrode is the cathode and the oxidizing electrode, which accepts electrons from the external circuit. It is reduced during the electrochemical reaction. The negative electrode – the anode or fuel electrode is reducing and itself it is oxidized during the electrochemical reaction. The ion conducting liquid or gel-based solution, in which cathode and anode have been placed, is the electrolyte. As a conducting medium, it allows lithium ions to travel between electrodes.¹¹

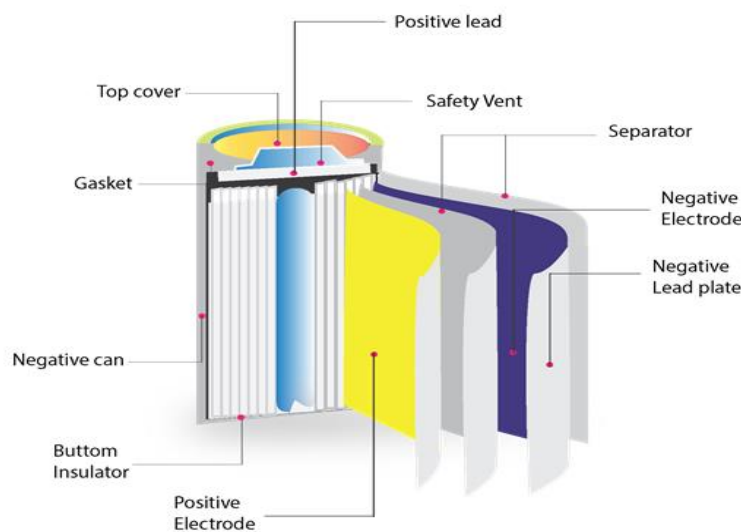


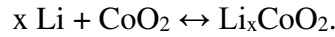
Figure 3. Cell design – cylindrical form.¹²

1.2.3. Cathode materials (positive electrode)

The cathode materials (referred to discharge) are divided into two main groups – layered compounds of transition metals and other compounds with different structures. Both materials should have a low chemical potential of lithium in the cathode, should allow a large number of lithium ions to be inserted/extracted per unit weight/volume and show a low lattice expansion and therefore low stress of active material (good durability) during discharging and charging. They should also offer a good electronic and lithium ions conductivity, be thermally and chemically stable and react with electrolyte neither chemically nor electrochemically. Other desired properties are full chemical reversibility, low price and environmental friendliness.¹³ All cathode materials work as Li-ions acceptors during discharge – lithium cations balance valence change of

material when reduced. Those properties are easily attainable when crystalline structure does not change while reacting with lithium ions.

Cobalt dioxide CoO₂ (LiCoO₂) is a layered transition metal oxide electrode material. It is very popular since 1990s in mobile devices powered with Li-Ion cells developed by Sony.¹⁴ The chemical equation for reaction is



This material has good electric conductivity, high reversibility in working conditions, high energy density and allows for good Li-ions diffusion.¹⁵ This is well presented in Figure 4. It is rather expensive and unstable in charged state.¹⁶ Practical capacity of LiCoO₂ is limited to about 130 mAh/g due to the limitation, that only about 0.5 Li cations per 1 mole of Co can be reversibly cycled. Higher proportions can affect the crystalline structure. Modifications of the surface with other oxides like Al₂O₃, ZrO₂ and TiO₂ or phosphates improved the structure stability and allowed up to 40% increase in practical capacity.¹³

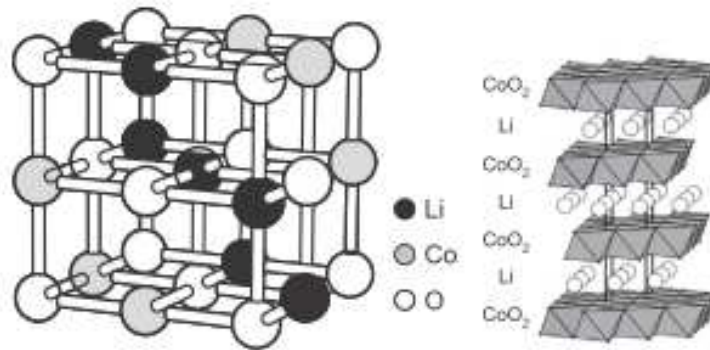
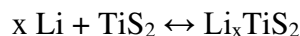


Figure 4. The rock-salt structure of LiCoO₂ (left) and layered structure of intercalated material (right).¹³

Nickel dioxide NiO₂ (LiNiO₂) is a layered transition metal oxide electrode material. It was proposed as an alternative to LiCoO₂, due to a better stability in charged state and far lower price. The main disadvantage is that the synthesis is difficult for maintaining good properties of the whole complex structure of this material.^{13,16}

Titanium disulfide TiS₂ (LiTiS₂) is a classical layered intercalation electrode. During reaction with Li-ions, its layered structure expands perpendicularly to TiS₂ layers, which changes lattice parameter from 5.7 Å in TiS₂ to 6.2 Å in LiTiS₂. The chemical equation for reaction is



This is well presented in Figure 5.⁵

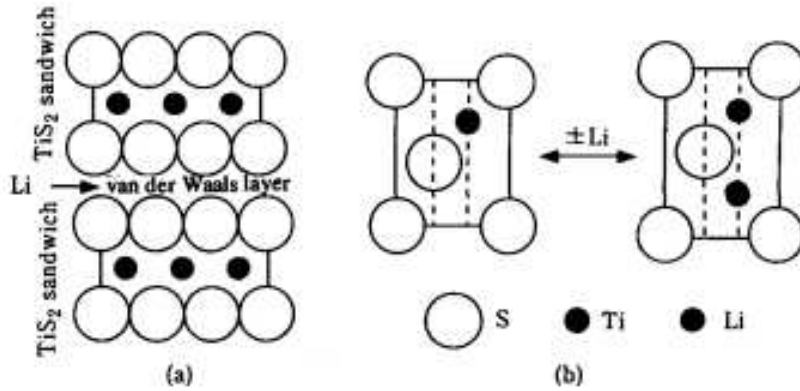


Figure 5. The diagram of lithium cations migration in TiS_2 layers (a) and in single primitive cell (b).⁵

Nickel-cobalt dioxide ($\text{LiNi}_{1-y}\text{Co}_y\text{O}_2$) is a layered transition metals oxide electrode material. $\text{LiNi}_{1-y}\text{Co}_y\text{O}_2$ exists as stable structure for $0.1 \leq y \leq 1$. In comparison to pure cobalt or nickel oxides materials, this composition promotes the layered structure, allows for cost reduction and offers a better cycling property – high reversibility and cyclability. Moreover, the specific capacity can be substantially increased, with a maximum of 220 mAh/g for $\text{LiNi}_{0.9}\text{Co}_{0.1}\text{O}_2$ material. Further exchanging nickel in $\text{LiNi}_{1-y}\text{Co}_y\text{O}_2$ for aluminum, leads to $\text{LiNi}_{1-y-z}\text{Co}_y\text{Al}_z\text{O}_2$, a layered materials family (NCA), which has a better stability in the lithium cations deintercalated state (charged battery).^{13,16}

Other promising cathode materials are spinel oxides of transition metals (mainly manganese) and olivine phase (**LiFePO_4**) based materials. Due to its high-power capability and relatively low cost it is commonly used in automotive applications. This means that it can accept a regenerative braking charge and can provide an acceleration discharge very quickly. The LFP is used in lithium ion batteries for hybrid electric vehicles (HEVs) and electric vehicles (EVs). This material offers excellent thermal stability, a high reversibility of Li^+ insertion/extraction, relatively low cost, and a low level of toxicity. The main drawbacks of LFP cathode material are low electric conductivity and a slow lithium diffusion.¹⁷

Nickel-manganese-cobalt dioxide ($\text{LiNi}_{1/3}\text{Mn}_{1/3}\text{Co}_{1/3}\text{O}_2$) is a layered transition metals oxide electrode material. It comes from the $\text{LiNi}_{1/2-y}\text{Mn}_{1/2-y}\text{Co}_{2y}\text{O}_2$ family, in this case with $y=1/6$ known as NMC. It has a very complex structure, which minimizes the stress in sheets in charged, discharged and intermediate states (as it contains 3 metal

ions in different oxidation states) and allowing free lithium ions movement in the lattice.¹⁸ The advantage of this material is the good price compared to the working parameters. The practical capacity is about 170 mAh/g, it has stable potential, high thermal stability and availability. The lower cost is compromised by a bit lower maximum rates of discharge.¹⁹

The secret of NMC lies in combining manganese and nickel. Manganese forms a spinel structure to achieve low internal resistance but offers a low specific energy. Nickel is known for its high specific energy but poor stability. Cobalt ions stabilize the amount of nickel (II) ions in lithium positions, lowering nickel ions migration, allowing better cycling properties and two-dimensional stability of the layered structure. The main working ion is nickel, which can be di-, tri- and tetravalent under cycling conditions (divalent in discharged conditions), but also cobalt is partly involved in the redox process (mainly trivalent and sometimes tetravalent in charged state). Combining the metals enhances each other strengths.²⁰ The characteristics of NMC are visible in Figure 6.

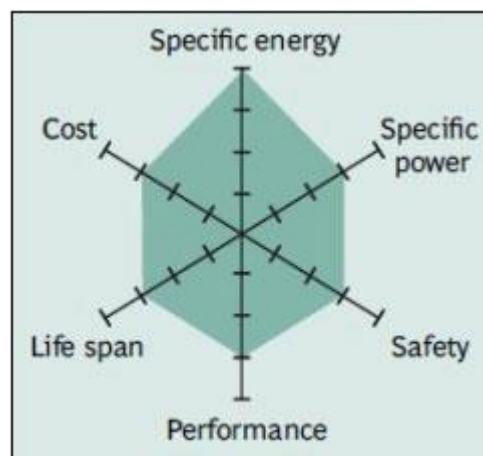


Figure 6. Spider diagram of NMC.²¹

Moreover, thermal stability of the whole structure is higher than in commonly used cobalt and/or nickel dioxide layered materials. Due to inclusion of manganese, which remains tetravalent under cycling conditions, the whole structure is more thermally stable. The NMC battery with its low self-heating rate and excel in specific energy is the preferred candidate for electric vehicle (EV) and energy storage systems (ESS). The family of NMC is growing and other combinations using various amounts of cathode materials are possible. The typical combination is one-third nickel, one-third

manganese and one-third cobalt, also known as NMC 111. Lithium-Nickel-Manganese-Cobalt Oxide with 5 parts nickel, 3 parts cobalt and 2 parts manganese (NMC 532) is another combination of cathode material.²² The most advanced version of NMC batteries are $\text{LiNi}_{0.6}\text{Mn}_{0.2}\text{Co}_{0.2}\text{O}_2$ (NMC 622) and $\text{LiNi}_{0.8}\text{Mn}_{0.1}\text{Co}_{0.1}\text{O}_2$ (NMC 811). According to Jame Frith, “the recently introduced NMC 622 battery, used by Renault in their Renault Zoe model, is most promising material by SK Innovation and LG Chem against the already commercially well-established NMC 111 and NMC 532”. In Lee Jon-ha’s opinion, NMC 811 batteries will help to develop new batteries that can extend the range of electric cars up to 700 km by 2020 (Korea Times).²³

The comparison of the specific energy of lead-, nickel- and lithium-based systems shown in Figure 7. Due to high cost of cobalt, battery manufacturers change from cobalt systems to nickel-based cathodes. Nickel systems have lower cost, higher energy density and longer cycle life than the cobalt-based cells but they have a slightly lower voltage.²⁴

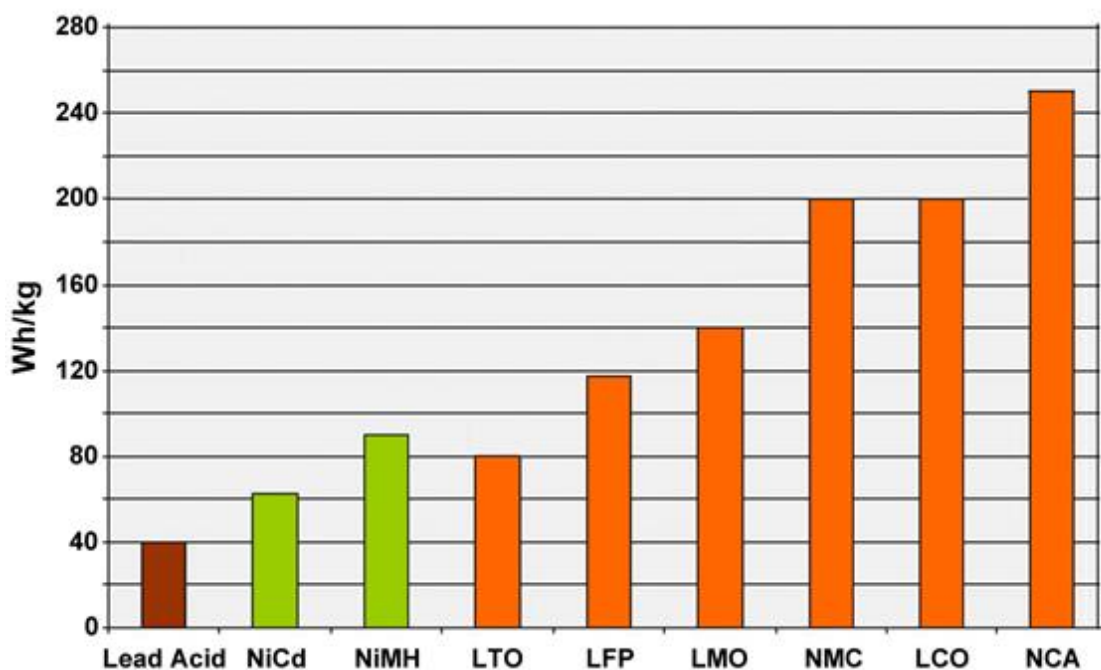


Figure 7. The comparison of the specific energy of lead-, nickel- and lithium-based systems.²⁴

The comparison of capacity commonly used commercial NMC powder has been showed in Table 1.

Table 1. The capacity of the NMC.²⁵

Electro-chemical data, voltage range 2.8-4.25V	NMC Powder Specifications			
	NMC111	NMC 532	NMC 622	NMC 811
Capacity [mAh/g]	154.8	166.1 - 187.0 (4.5V)	175.8	1.4 (4.3V)

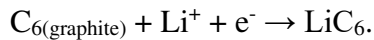
1.2.4. Anode materials (negative electrode)

The anode materials (referred to discharge) are divided into two main groups – intercalation materials and others. Both materials should have very high chemical potential of lithium in the anode, should allow a big amount of lithium ions to be inserted/extracted per unit weight/volume and show a low lattice contraction/expansion stress of active material (good durability) during discharging and charging. It also should have a good electronic and lithium ions conductivity, be thermally and chemically stable and should not react with electrolyte chemically or electrochemically.¹³ Other desired properties are full chemical reversibility, low price and environmental friendliness.⁵ All anode materials work as Li-ions acceptors during charging – lithium cations balance charge changes of the material. Those properties are easily attainable when the structure does not change while reacting with lithium ions.

Metallic Lithium (Li) would be an ideal anode material for rechargeable batteries due to lowest standard potential (-3.040 V vs. the standard hydrogen electrode), extremely high theoretical specific capacity (3860 mA h g^{-1}) and low density (0.59 g cm^{-3}). Uncontrollable dendritic Li growth and low Coulombic efficiency (CE) during Li deposition/stripping have prevented practical applications in batteries over the past 40 years.^{26, 27} Two problems are critical for Li anodes – one is safety hazards because of potential internal short circuits and high surface area, and another is short cycle life.²⁸

Graphite, the most popular anode material, consists of many graphene layers arranged in a bulk 3D crystalline structure. The theoretical discharge capacity of

graphite is 372 mAh/g.²⁹ During charging, lithium ions intercalates into the graphite matrix and chemical equation is:



Due to inserted lithium, graphite expands up to 11% by volume perpendicular to graphene sheets. This electrode has a very low potential (almost equal to lithium) combined with a very good electrical conductivity, which resulted in a high popularity in mobile devices powered with Li-Ion cells since 1990s.¹⁶ The main disadvantage of graphite (and other carbonaceous based anode materials) is a process known as an exfoliation of graphene sheets. It leads to irreversible separation of graphene layers from the crystalline structure due to the wrong choice of electrolyte composition. This causes a drop in performance of the whole cell.^{1,16} The exfoliation occurs with improperly selected solvent (for example propylene carbonate). Solvated lithium ions intercalated into the graphite structure and rips it apart. The right choice of solvent (for example ethylene carbonate) results in formation of a passive coating on the anode surface, named as solid electrolyte interphase (SEI) which is a lithium ion conductor. Therefore, only un-solvated lithium ions can pass into the lattice, which prevents it from being exfoliated due to solvent co-intercalation.¹⁶ With all requirements taken into consideration, graphite as an anode material is a good material, with a proper stability, very high reversibility and good lifespan. Other carbonaceous anode materials can have higher discharge capacity than graphite, but their structure and large surface area influence important properties. All carbon-based materials containing lithium in their structure have reactivity like metallic lithium aggravated by a huge specific surface area, so this must be considered during designing and working with those anodic materials.⁵

Titanium oxides containing bonded lithium ions, like $\text{Li}_4\text{Ti}_5\text{O}_{12}$, are also insertion type anodic materials. As oxides, they are chemically stable, have smaller volume changes during charging/discharging and high reversibility, which are their advantages. They have lower capacity (about 175 mAh/g), high potential versus lithium (about 1.5 V) and can oxidize solvents under inappropriate conditions (this results in gas emissions, which also negatively affects the capacity).¹⁶

Silicon and tin as anodic materials form alloys with lithium. They have very high specific capacities, but they show extremely high-volume changes at alloy formation

with lithium (up to 200-300%). This limits their current usage, because the cell must contain volume buffer materials to retain mechanical integrity.^{1, 16}

Table 2. list various lithium insertion compounds already commercially available. Highly oxidized $M^{4+/3+}$ and $M^{3+/2+}$ redox couples are the leading candidates for positive electrodes. The development of suitable hosts with compatible anodes for the next generation Li-ion cells request several considerations: chemical and structural stabilities, voltage, rate capability, service life, capacity electrode and thermal safety. According to Dr Ch. Julien and co-workers both the LiFePO_4 positive electrode and the $\text{Li}_4\text{Ti}_5\text{O}_{12}$ negative electrode have demonstrated safe and rapid charge and discharge over many cycles.³⁰

Table 2. Configuration of the three types of Li-ion cells related to their application.³⁰

Application	Positive electrode	Negative electrode	Remarks
High energy	LiCoO_2	Graphite, Si, SnO_x	$M = \text{Mn, Al, Cr}$ named "LMO"
	$\text{LiNi}_y\text{Co}_z\text{M}_{1-y-z}\text{O}_2$	CoO_x , FeO_x , CuO_x	
	LiMn_2O_4	NiO_x , etc.	
High power	$\text{LiMn}_{2-y}\text{Al}_y\text{O}_{4+5}$	hard carbon,	named "NMC" "LFP/LTO" cell
	$\text{LiNi}_y\text{Mn}_y\text{Co}_{2-y}\text{O}_2$	graphite	
	LiFePO_4	$\text{Li}_4\text{Ti}_5\text{O}_{12}$	
Long cycle life	$\text{LiMn}_{2-y}\text{Al}_y\text{O}_{4+5}$	Graphite	named "LFP"
	LiFePO_4	$\text{Li}_4\text{Ti}_5\text{O}_{12}$	
	$\text{LiFe}_{1-y}\text{Mn}_y\text{PO}_4$	$\text{Li}_4\text{Ti}_5\text{O}_{12}$	

1.2.5. Electrolytes

Due to the high reactivity of lithium metal with water, most popular electrolytes are non-aqueous, non-protonic organic liquids with dissolved lithium salts or solid electrolytes with good lithium-ion conductivity. Main features of solvents are high dielectric constant (which favors dissociation of lithium salts), low volatility, low viscosity (enables faster movement of ions) and good stability towards all battery composites. Usually used solvents are various organic carbonates, both cyclic (like ethylene carbonate, with higher viscosity) and linear (like diethyl carbonate, with lower viscosity and higher volatility).^{31,32} Those two different types of carbonates are mixed to achieve desired properties of electrolyte. Main disadvantages of organic solvents are their flammability and volatility, which limits the temperature range in which they stay safe. They can be very dangerous during for example short circuit of cell, which results

in rapid heating and may end in a serious fire.^{5,31} Also, those solvents react with electrode materials, for example the graphite anode, to the SEI (solid electrolyte interphase) on the graphite surface which is a good lithium ion conductor. A similar phase can be formed on the cathode, which is named CEI – cathode electrolyte interphase. This film is formed during the first charge/discharge of the battery and prevents further reaction of the solvent with graphite.³² The most suitable lithium salts are lithium hexafluorophosphate LiPF_6 (with good ion conductivity, electrochemical stability and good SEI-forming ability, but lower thermal stability), lithium perchlorate LiClO_4 (high conductivity, but poor electrochemical stability) and lithium tetrafluoroborate LiBF_4 .^{5,31}

The next type of electrolytes are solid inorganic lithium ion-conducting electrolytes, like lithium iodide LiI , used in the lithium-iodine primary cell. Their advantages are low discharge rate, incombustibility, no risks of leak and protection from short circuits in battery.⁵ However, they are hard to implement commercially, generally fragile and have low mechanical flexibility. On the other hand, solid organic gel and particularly dry polymer electrolytes comprise some advantages of solid electrolyte cells and liquid electrolyte batteries.³¹ While the gel polymer electrolyte is a liquid electrolyte kept in a polymer matrix, a dry state polymer electrolyte is a solvent-free lithium ion containing and conducting material. A very popular polymer is poly(ethylene oxide) or PEO in short, which can ‘dissolve’ lithium salts into its matrix as solid solution. Lithium cations are stabilized by oxygen atoms negative charge, while anions (preferably large sized, to promote salt dissolution in PEO due to Lewis acid-base interaction) are maintained in the whole polymer-cations complex. The most popular lithium salts for this application are LiBF_4 , LiClO_4 , $\text{CF}_3\text{SO}_3\text{Li}$.³³ The flexible structure, high moldability and great safety and stability are main advantages, but disadvantage is the high temperature (above polymer melting point, for PEO $>70^\circ\text{C}$) required to allow fast transport of lithium ions.

1.2.6. Current collectors and separators

The typical LIB cell contains a positive current collector (e.g. an aluminum foil), and a negative current collector (e.g. a copper foil). The layers of active material (AM) are coated on them. Between positive and negative electrodes, there is usually a separator, which is a sheet of a porous polymer membrane, forming an electrode stack.

The electrode stack is soaked with the electrolyte solution, based on organic solvents such as ethylene carbonate (EC) and ethyl methyl carbonates (EMC).^{34,35} The energy density of lithium-ion batteries can be increased by using a thin Cu current collector, due to the fact that the weight of Cu current collector is higher than the Al.³⁶

The role of the ion permeable separator is to avoid an internal short circuit between the two electrodes. The selection of the separators follows several criteria: high chemical, thermal and mechanical stability and sufficient ionic conductivity for Li.³⁷ The separator is often made of plastic or ceramic. Inorganic separators can adsorb much more electrolyte than polymer separators with the same volume. Commercial polymer membranes offer pore size in the range 0.03-0.1 μm with 30-50% porosity.

A special type of PP/PE/PP separator was invented by Celgard. The combination of PP and PE provides the function of a thermal fuse for the cell. This is achieved by the different melting points of PE and PP. As the temperature approaches the melting point of the polymers, 135 °C for PE and 165 °C for PP, porosity is lost. The lower melting point of PE layer is intended to shut down the cell if an over-temperature condition is reached, while the PP layer is designed to maintain the integrity of the film.³⁸

1.2.7. Binders

The binder is an electrochemically inactive material which adheres electrode particles together and joins it with the current collectors (adhesion). Its features should be stability (thermal, chemical and electrochemical), high tensile strength (cohesion, adhesion), flexibility (it should buffer volume changes of electrode materials) and right viscosity of slurries made with it.^{39,40} Currently, the most popular binder is PVDF - poly(vinyl difluoride), used as a solution in N-methyl-2-pyrrolidone (NMP). Good adhesive properties and stability of PVDF favors its use in Li-Ion batteries, but PVDF makes recycling of those batteries dangerous for environment.^{39,41} As a result, because of the detrimental properties, toxicity, harmfulness of NMP and high price of both PVDF and NMP, the goal is to introduce other binders and their solvents. This leads to use of water-soluble and water-compatible polymer binders, like sodium carboxymethyl cellulose (CMC), styrene-butadiene rubber (SBR), fluorine acrylic latex (like TRD202A) and their mixtures. Their usage enables easier recycling process of Li-Ion batteries, lowers total cost of electrode slurries and improves the environmental impact.⁴²

2. Water-soluble binders and LiNiMnCoO as cathode material

The environmental concern combined with desire to lower total cost of lithium-ion batteries are the main driving forces for alteration binder's composition for electrode slurries preparation process. Poly(vinyl difluoride) is a very good binder material with relatively low density, great flexibility, good stability and great adhesive strength. PVDF advantages cope with its two main disadvantages – high price (compared to other proposed binders) and the fact, that the relatively aggressive solvent, N-methyl-2-pyrrolidone (NMP) is needed for the preparation process. NMP is a very widely used dipolar aprotic solvent, with very good properties – it is miscible with polar solvents like water, ethanol, acetone, ethyl acetate and apolar solvents like diethylether and benzene, it can dissolve many of currently used polymers. Moreover, NMP has a high boiling point and relatively low volatility, but it is toxic and possibly carcinogenic. The main problem of using PVDF as a binder is the necessity of use of NMP as a solvent to prepare the electrode slurry NMP would also be needed during the recycling process of lithium ion batteries (when the binder is removed before recycling of electrode materials). Other methods of removing the PVDF binder is firing it. However, combustion would create fluorinated organic material or HF. The mentioned disadvantages of using PVDF dissolved in NMP gradually shifted interest to other, water-soluble binders. Recycling of batteries with water-soluble binders can be far easier and more environmental-friendlier due to a simpler reprocessing by using water for removing the binder.

Proposed new binder materials are sodium carboxymethylcellulose (CMC), styrene-butadiene rubber (SBR), fluorine acrylic latex (like TRD202A) and their mixtures. All mentioned polymers are water-compatible and soluble in water. Sodium carboxymethylcellulose (CMC) is a frequently used ingredient especially in food industry as an emulsion stabilizer, viscosity modifier, thickening agent and binder. It is non-toxic and hypoallergenic. CMC properties depend on the degree of cellulose hydroxylgroup substitution with carboxymethyl groups and on cellulose chain length. The styrene-butadiene rubber (SBR) is commonly used as a natural rubber substitute (for example in pneumatic tires, shoe soles or gaskets), coating and waterproofing agent (for example in the paper industry, building materials), also as a binder and reinforcing agent. Both, CMC and SBR dissolve in water. Using the water-soluble binders requires

some adjustments to the processing of electrode slurries and lithium-ion batteries assemble. While modern commercial negative electrode materials are more and more frequently prepared with polymers dispersed or dissolved in water (mainly SBR), lithiated oxide materials for the positive electrode are problematic under their processing conditions. Water tends to leach lithium cations from the oxide materials and this leads to corrosion of the aluminum current collectors. Both reactions reduce batteries efficiency and durability.

Nickel-manganese-cobalt dioxide (known as NMC) is a layered transition metals oxide electrode material. The chemical formula for the whole family of NMC compounds is $\text{LiNi}_{1/2-y}\text{Mn}_{1/2-y}\text{Co}_{2y}\text{O}_2$ (with $y=1/6$ in case of most popular $\text{LiNi}_{1/3}\text{Mn}_{1/3}\text{Co}_{1/3}\text{O}_2$). The working potential is similar to other cathode materials, which allows to use the cell for the same applications.¹⁶ Other advantages of this material are a relatively good price together with favorable working parameters. It has high working capacity about 150-170 mAh/g after some charge/discharge cycles, a stable potential, low toxicity, high availability of raw materials and a very good price.^{16,29} The main disadvantages of this material are the tendency to react with water with leaching of lithium ions from the active material and low electrical conductivity, which affects high rates performance and requires therefore a higher amount of conductive agent like carbon black.³⁹

The first of the mentioned disadvantages leads to tests with proper binders and/or with coating substances for the active oxide material and/or slurry additives.

The current knowledge about the effects of binders on LiNiMnCoO as cathode material in lithium batteries, collected from work of different research groups, will be discussed in the following chapters.

2.1. Sodium carboxymethyl cellulose (CMC) and polyurethane (based on IPDI)

The group of N. Loeffler tested water dispersions of sodium carboxymethyl cellulose (CMC) and heat-cured polyurethane based on blocked isophoronediiisocyanate (IPDI) as a binder for graphite (SLP 30) anode and $\text{LiNi}_{1/3}\text{Mn}_{1/3}\text{Co}_{1/3}\text{O}_2$ (NMC) cathode³⁹ They prepared slurries by mixing binder material with water, adding conductive agent and finally the active electrode material. Proportions for cathode slurry were 90 wt% of active material, 7 wt% of conductive agent and 3 wt% of binder and

proportions for anode slurry were 93 wt% of active material, 4 wt% of conductive agent and 3 wt% of binder. In addition, different proportions of CMC to polyurethane were tested (Table 3 below). The prepared slurries were applied on metal foils (aluminum – cathode, copper – anode). Slurries without CMC had too low viscosity and proper electrodes could not be tested. After application, foils were dried in atmospheric ovens and tested or used for cell preparation. Thermogravimetry and cyclic voltammetry proved that the polyurethane material is stable under working temperature and electrochemical conditions of the cathode and anode. The cycling tests were performed for different cathodes (Ref C, C1, C2), which results are shown in Figure 8. The best results at 1 C rate after 100 cycles had C2 cathode (2% polyurethane), with 93% retention of capacity, and C1 cathode (1% polyurethane) which showed 86% capacity retention. This demonstrates the good performance of polyurethane as a binder. Moreover, the mentioned results suggest that NMC oxide material was chosen properly, because it had a good lifetime even in an unfavorable water-based slurry composition. The common problem of aluminum corrosion, which is lowering capacity in water-based metal-oxide cathodes, was less affecting the C2 cathode, which suggests that the IPDI-polyurethane may prevent the corrosion process. SEM images of the mentioned cathodes proved that a higher polyurethane amount decreased the corrosion rate – observed pits under oxide particles were far smaller in C2 formulation than in Ref C. The SEM images are presented in Figure 9. This process could occur thanks to the polyurethane coating, which reduced oxide material contact with water, which efficiently reduced the corrosion rate. The electrochemical tests of various cathodes indicate undisturbed performance of differential capacity after 5 and 50 cycles (see Figure 10) – this also proves that PU coating do not affect negatively electrode performance. The battery made by pairing C1 with the anode material showed 90% capacity retention after 200 cycles, very high efficiency and nearly no signs of electrolyte degeneration.

Table 3. The composition of the binder (mixtures) for the prepared electrodes.³⁹

	CMC (%)	Polyurethane (%)	Total amount of binder (%)	Acronym Cathode/Anode
a)	3	0	3	RefC/RefA
b)	2	1	3	C1/A1
c)	1	2	3	C2/-
d)	0	3	3	-/-

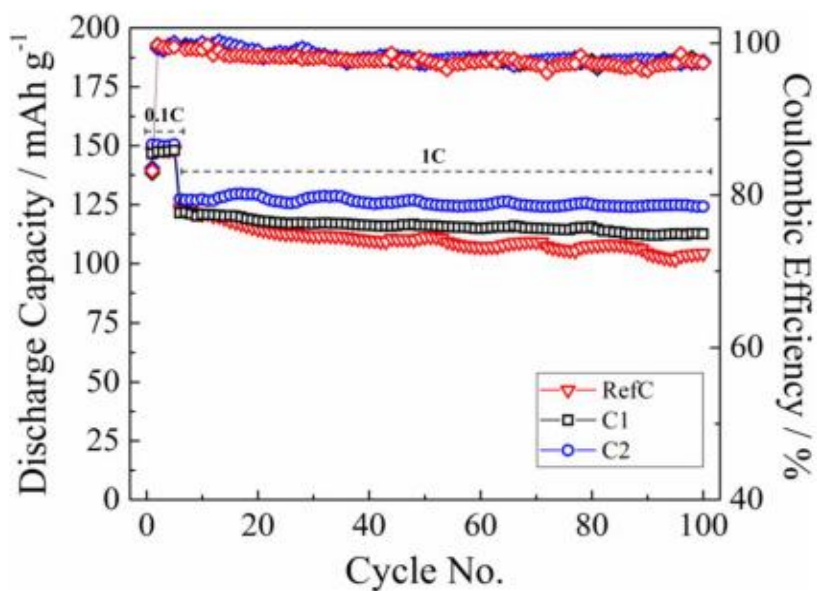


Figure 8. The discharge capacity and coulombic efficiency of cathode materials.³⁹

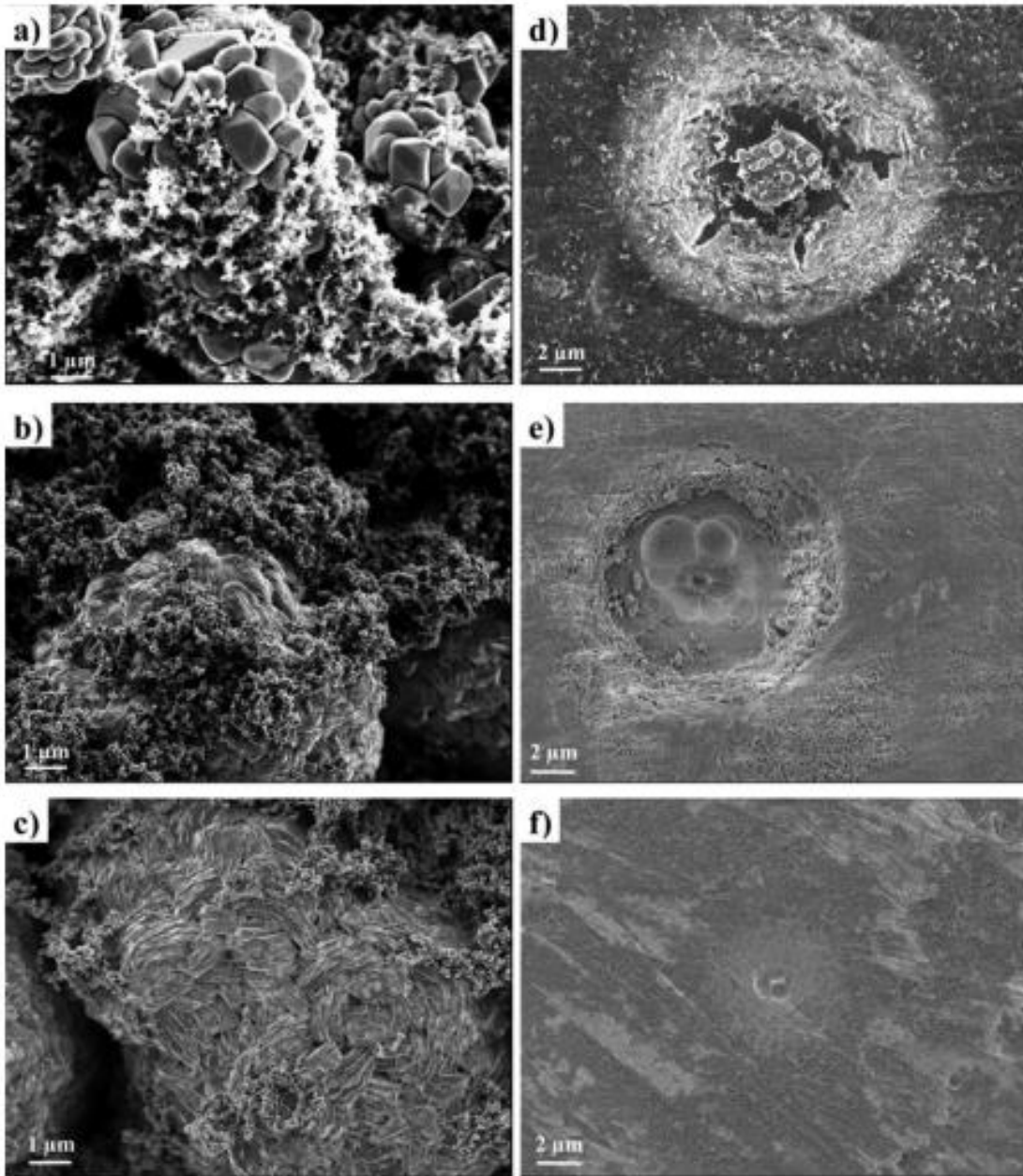


Figure 9. The SEM images of cathodes and its aluminum foil after coating removal:
RefC (a, d), C1 (b, e), C2 (c, f).³⁹

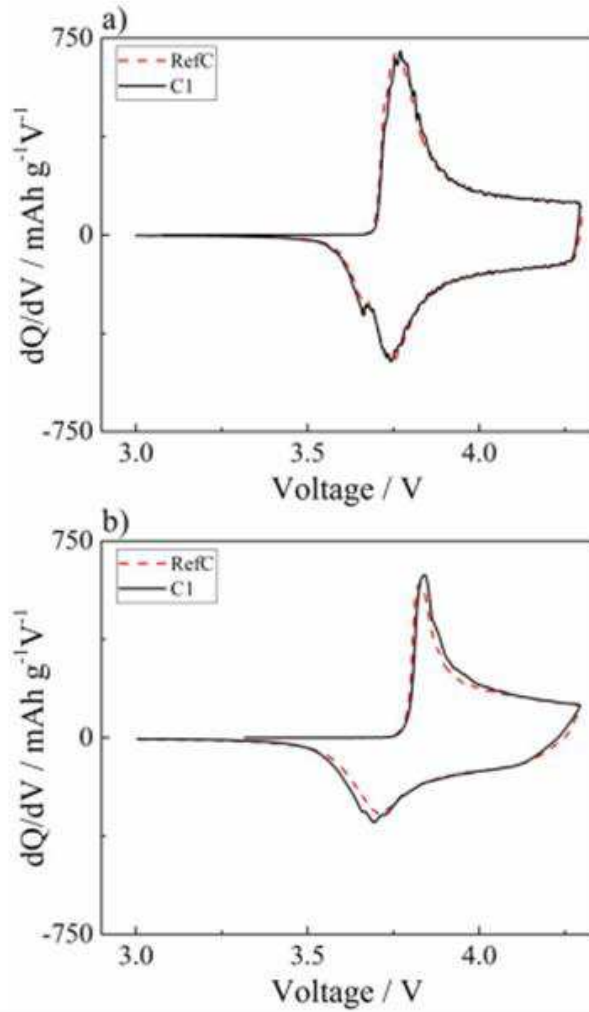


Figure 10. The differential capacity curves from (a) 5th and (b) 50th cycles for RefC and C1 cathodes.³⁹

2.2. Sodium carboxymethyl cellulose (CMC)

Again, the group of N. Loeffler tested water dispersions of sodium carboxymethyl cellulose (CMC) as a sole binder for graphite (SLP 30) anode and $\text{LiNi}_{1/3}\text{Mn}_{1/3}\text{Co}_{1/3}\text{O}_2$ (NMC) cathode.⁴⁰ They prepared slurries by mixing binder material in water, adding the conductive agent and finally adding the active electrode material. The proportions for cathode slurry were 88 wt% of active material, 7 wt% of conductive agent and 5 wt% of binder and proportions for anode slurry were 90 wt% of active material, 5 wt% of conductive agent and 5 wt% of binder. The prepared slurries were applied on aluminum coated with carbon dispersion to prevent corrosion – effects of using non-coated foil are shown below in Figure 11. After application, the foils were dried in atmospheric ovens

and tested or used for cell preparation. Thermogravimetry and cyclic voltammetry proved that the used CMC is stable under working temperature and electrochemical conditions of the cathode and anode. The aluminum foil coated with carbon layer was not affected by corrosion due to protection from alkaline slurry of the metal oxides, but unfortunately, there were no images to prove that fact, and only good experimental results suggest that the cathode current collector was secured. The complete cell, with electrodes made with only CMC binder, showed good working properties, as seen in Figure 12. After 1000 cycles at 1 C rate, the capacity loss was about 16%, and after 2000 cycles whole capacity loss was approximately 30%, with a coulombic efficiency near 100%.

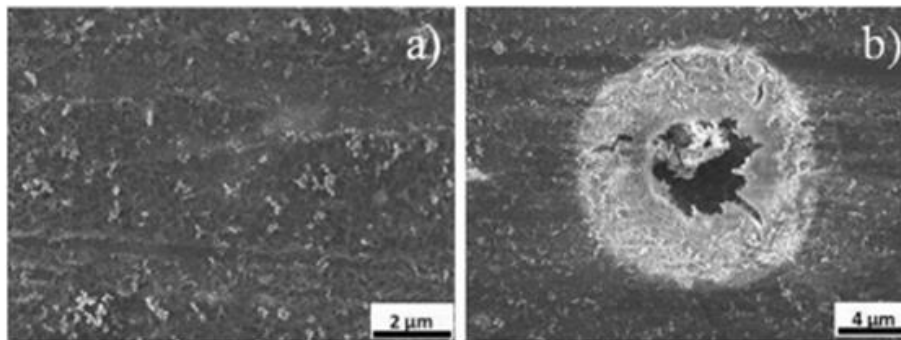


Figure 11. The SEM images of the corroded aluminum foil surface (a) and individual corrosion pit (b).⁴⁰

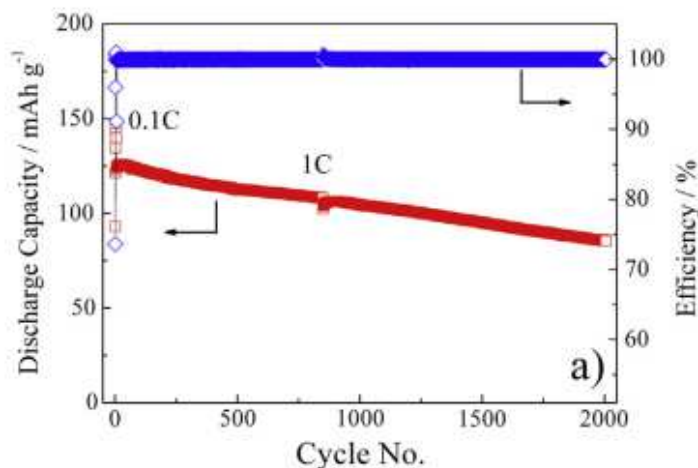


Figure 12. The discharge capacity and coulombic efficiency of full cell.⁴⁰

2.3. NMC 111 with water-compatible (SBR, CMC) and non-aqueous binders (PVDF)

The group of K. Notake investigated water dispersions of hybrid polymer (TRD202A) and fluoropolymer with sodium carboxymethyl cellulose (CMC) as binders for own-synthesized NMC cathode material uncoated and coated with Al_2O_3 . They also tested the same material with polyvinylidene difluoride (PVDF) binder for comparison.⁴¹

Part of the obtained material, characterized as $\text{Li}[\text{Ni}_{0.18}\text{Li}_{0.2}\text{Co}_{0.03}\text{Mn}_{0.58}]\text{O}_2$, was later coated with an Al_2O_3 layer to prevent the active oxide material from contact with water during the electrode preparation process. They prepared slurry by mixing binder material with water, adding the conductive agent (acetylene black) and finally adding the active electrode material. The proportions for water-based cathode slurry were 91 wt% of active material, 5 wt% of conductive agent, 3 wt% of hybrid TRD202A binder and 1 wt% of carboxymethyl cellulose. The proportions for non-aqueous cathode slurry were 91 wt.% of active material, 5 wt% of conductive agent and 4 wt% of PVDF binder. The prepared slurries were applied on an aluminum foil as a current collector. After application, the foils were dried in a vacuum oven and tested or used for cell preparation. All cycling experiments showed no voltage changes in function of capacity in both types of cells during charging and discharging, with very similar curves. In addition, the long-term stability of fully charged cell was checked. After 28 days, both cells showed nearly identical discharge curve (as seen in Figure 13), with slightly better operation of the TRD202A-based cell (lower capacity loss after holding time). The obtained XRD patterns of raw uncoated active material and the same material after processing it into slurries suggest that synthesized active material is stable under preparation conditions with both solvents – organic and water. After the first cell formation cycles, the group performed cycling tests for cathodes with 0.1 C rate of discharge and charge. Both cathodes showed similar performance over about 80 cycles, with stable discharge capacities of approximately 275 mAh/g. Figure 14 shows the long-term performance of the prepared cells. Despite a very small capacity fade at the end of testing, the TRD202A-based cell was not seemingly inferior compared with the PVDF-based cell. Furthermore, both cells were compared with higher discharge rates (0.1, 0.2, 0.5, 1, 2, 3 C). It showed that the NMC-based cell performance is nearly

unaffected by water-based binder (Figure 15). The coated NMC material was examined with TEM microscopy before using it in tests. The surface layer on NMC has different lattice constant than interior of material (shown in Figure 16) and is estimated to be uniform with thickness of about 3-5 nm. Figure 17 show the cycling charge/discharge test results. Both curves are nearly identical, with a slightly better capacity retention in case of non-aqueous binder cathode after 30 cycles and discharge capacity about 260 mAh/g. The uncoated samples with aqueous binders show slow degradation of material, which was reflected by the diminishing discharge capacity of cathode (about 7.5%) after 25-30 cycles. These results reveal the advantage of the Al₂O₃ coating, which prevents contact between water and oxide material during the preparation process and leads to better long-time performance of cathode. The Al₂O₃ coating does not limit the lithium ions migration into the oxide material during the electrode operation. The performance of non-aqueous binder sample and aqueous binder with coated NMC sample are similar.

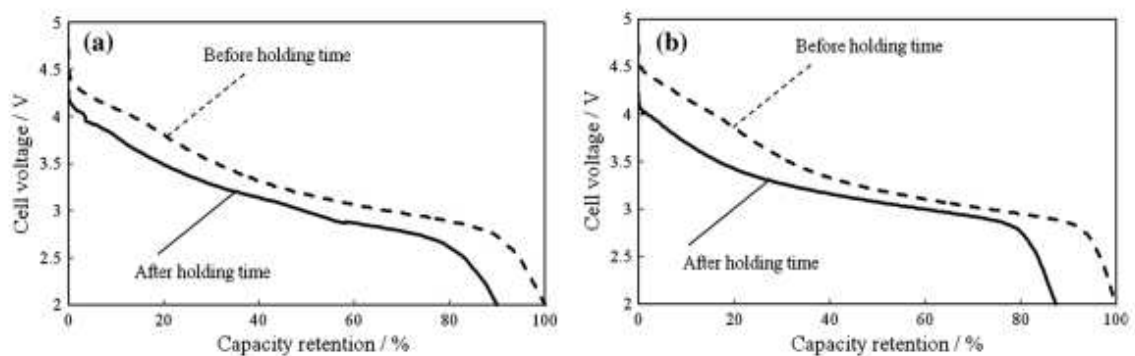


Figure 13. The discharge curves of cells made with electrodes containing (a) TRD202A binder and (b) PVDF binder after holding in full-charge state for 28 days.⁴¹

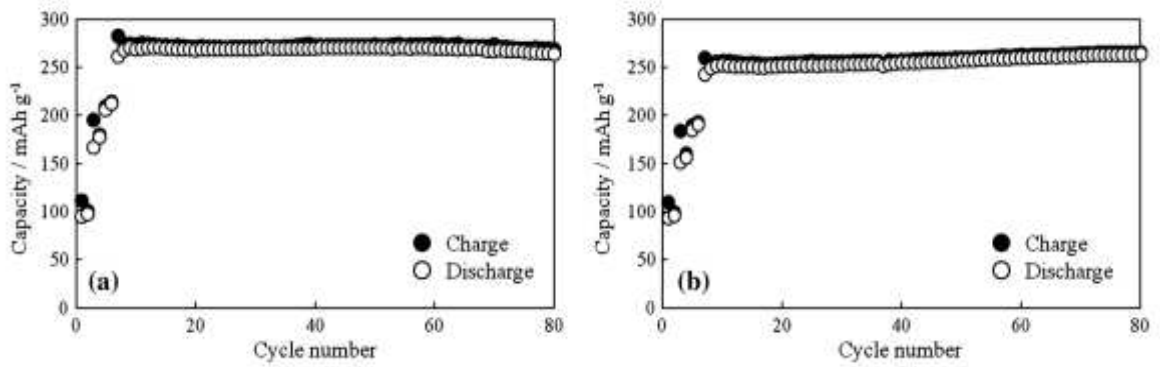


Figure 14. The cycling performance of cells made with electrodes containing (a) TRD202A binder and (b) PVDF binder.⁴¹

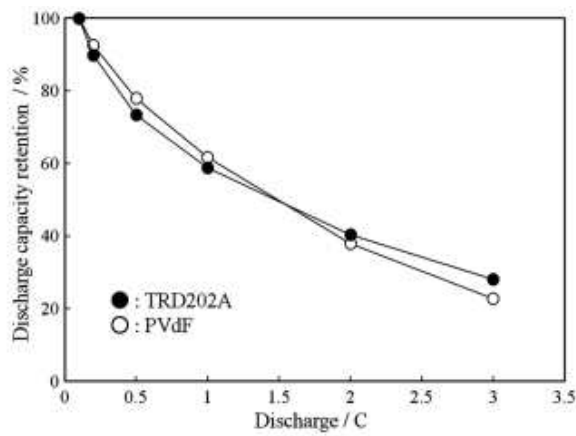


Figure 15. The performance of cells during different discharge rates.⁴¹

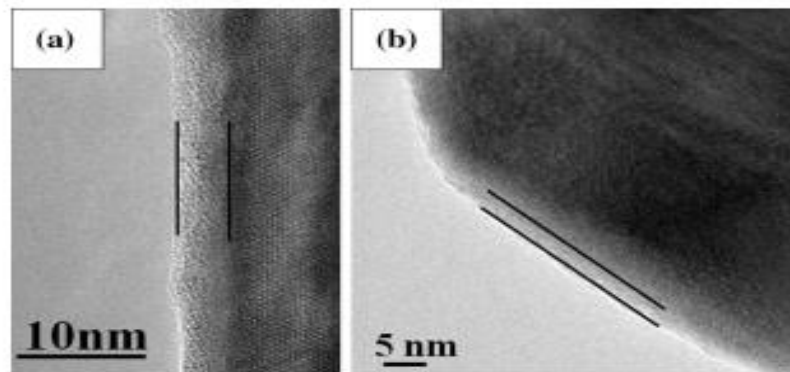


Figure 16. The TEM images (a, b) of Al₂O₃ coated NMC material. Different structure on surface can be seen.⁴¹

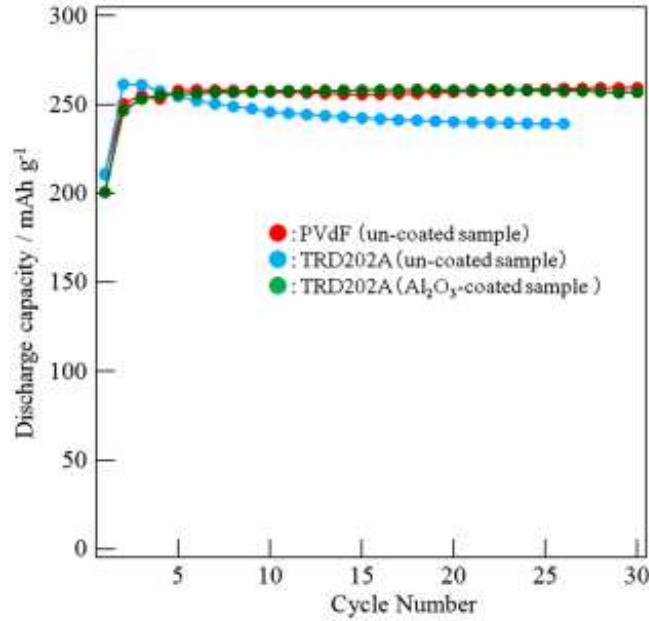


Figure 17. The cycling performance of cathodes made with uncoated $\text{Li}[\text{Ni}_{0.18}\text{Li}_{0.2}\text{Co}_{0.03}\text{Mn}_{0.58}]\text{O}_2$ and PVdF binder, uncoated $\text{Li}[\text{Ni}_{0.18}\text{Li}_{0.2}\text{Co}_{0.03}\text{Mn}_{0.58}]\text{O}_2$ and aqueous binders and Al_2O_3 coated $\text{Li}[\text{Ni}_{0.18}\text{Li}_{0.2}\text{Co}_{0.03}\text{Mn}_{0.58}]\text{O}_2$ and aqueous binders⁴¹

2.4. Sodium carboxymethyl cellulose (CMC) and styrene-butadiene rubber (SBR)

The group of S. Lim studied the water dispersions of sodium carboxymethyl cellulose (CMC) and styrene-butadiene rubber (SBR) as binders for graphite anode.⁴³ They prepared slurries by mixing CMC with water, adding graphite and finally adding SBR suspension. Different proportions of CMC and/or SBR to graphite were tested using cryo-SEM microscopy to determine their structures, which confirmed the observed rheological properties. Better dispersion and slurry stability were observed for higher concentrations of CMC and/or SBR. Those effects depend on adsorption on graphite surface, which is influenced by the concentrations of binder materials.⁴³

2.5. NMC 111 with water-compatible (SBR, CMC) and non-aqueous binders (PVDF)

The group of M. Memm checked water dispersions of sodium carboxymethyl cellulose (CMC) and styrene-butadiene rubber (SBR) as binders for $\text{LiNi}_{1/3}\text{Mn}_{1/3}\text{Co}_{1/3}\text{O}_2$ (NMC) cathode and NMC cathodes modified with additives and compared them with

organic solvent-based cathodes.⁴⁴ Two samples of alternative cathode material were prepared, first one with addition of Al_2O_3 replacing 4.6% of NMC and second one with addition of SiO_2 replacing 2% of NMC. The slurries were prepared by mixing solid materials by spatula, water in steps and finally adding the water-SBR emulsion. The proportions for cathode aqueous slurry were 94 wt% of active material, 2 wt% of conductive agent and 3 wt% of CMC and 1 wt% of SBR. The proportions for cathode organic slurry were 93 wt% of active material, 4 wt% of conductive agent and 3 wt% of PVDF. The prepared slurries were applied on aluminum foils. After application, the foils were dried on a hotplate and after that used for cell preparation. The NMC slurry was tested to calculate the amount of leached lithium cations, which proved that Li^+ loss was negligible (about 0.63% in 50%/50% water/NMC suspension). SEM pictures showed no visible differences in agglomerates structure on aluminum foil, but in a larger overview their surfaces were visibly different (see Figure 18). It showed a smooth surface for the NMP-based cathode but holes and cracks on the water-based NMC cathode. Those damages were explained by hydrogen gas formation during preparation due to reaction between aluminum and the alkaline slurry. Furthermore, the research group prepared some slurries with additives – with 3wt%, 4.6wt% and 13.6 wt% of Al_2O_3 and 2wt%, 3wt% and 13.6 wt% of SiO_2 and used them to make different cathodes. With higher additional oxide content, the pH value of the slurry was lower and the aluminum foil showed no pitting corrosion under laser microscopy, but its surface was still rougher when compared to pristine foil (see Figure 19). The performance of SiO_2 addition was better than Al_2O_3 in case of lowering pH value – less addition of oxide was needed to achieve the same pH value, allowing for a higher active material content in the cathode material. For cathodes examinations, the cells were prepared with different cathodes coupled with a lithium metal anode. The discharge curves for cells made with water-based NMC cathode materials containing 4.6 wt% Al_2O_3 and 2 wt% SiO_2 are shown in Figure 20, which presents nearly identical curves for 0.2 C rate and 1 C rate. This confirms a similar performance with lower concentration of SiO_2 in cathode material compared to Al_2O_3 . The specific discharge capacities are 146 mAh/g and 120 mAh/g for both cathodes, respectively. Also, the capacity retention during different cycles at 0.2 C; 0.5 C; 1 C; 2 C and 5 C rates are very similar, with about 83% retention at 1 C rate for both materials. At higher rates, slightly better performance of SiO_2 addition was observed (see Figure 21).

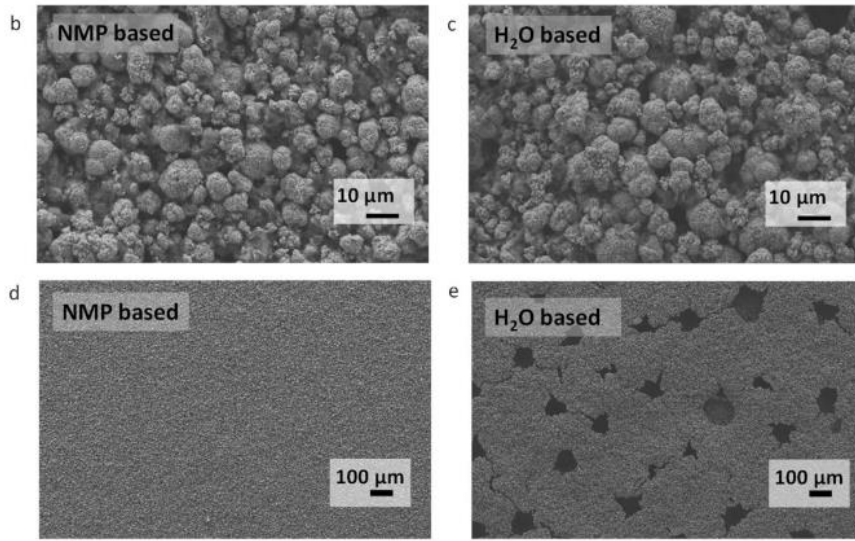


Figure 18. The SEM images of dried cathodes (d) NMP-based and (e) water-based and magnification of their surfaces – (b) and (c) respectively.⁴⁶

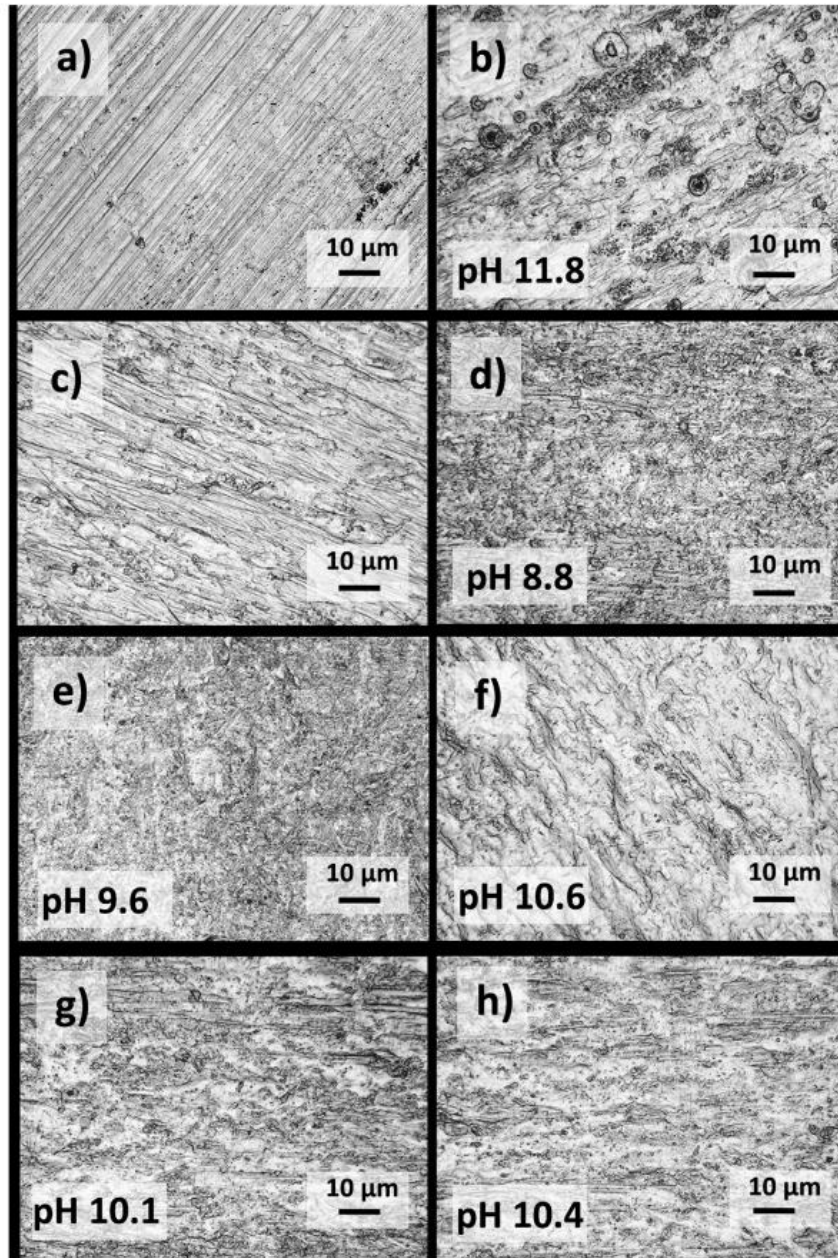


Figure 19. Laser microscopy images of (a) pristine aluminum foil, (b) foil after removal of coating with NMC water-slurry without additives, (c) foil after removal of coating with NMC NMP-slurry, (d) foil after removal of coating with NMC with 13.6% of Al_2O_3 , (e) foil after removal of coating with NMC with 4.6% of Al_2O_3 , (f) foil after removal of coating with NMC with 3% of Al_2O_3 , (g) foil after removal of coating with NMC with 3% of SiO_2 and (h) foil after removal of coating with NMC with 2% of SiO_2 .⁴⁶

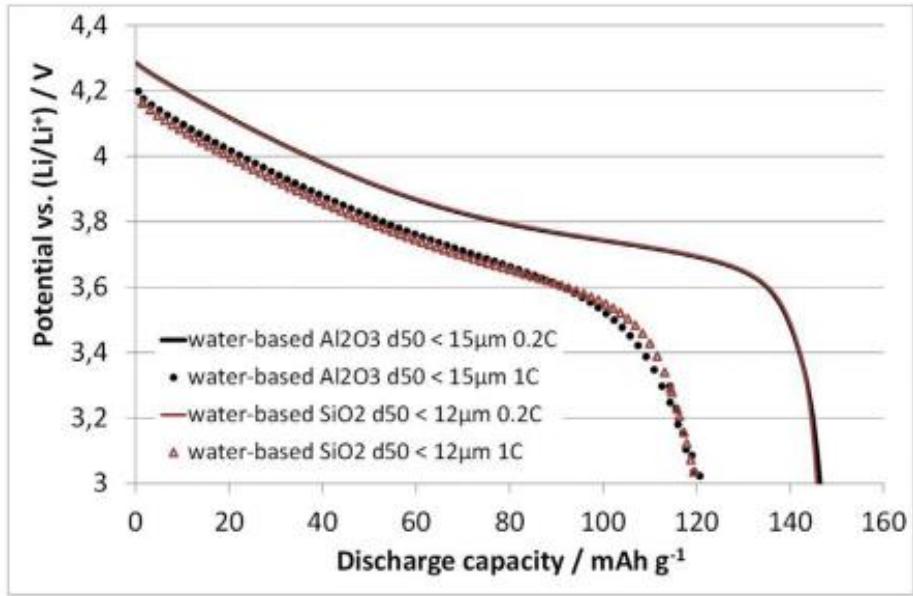


Figure 20. Discharge curves for cells made with water-based NMC cathodes with 4.6% Al_2O_3 and 2% SiO_2 .⁴⁶

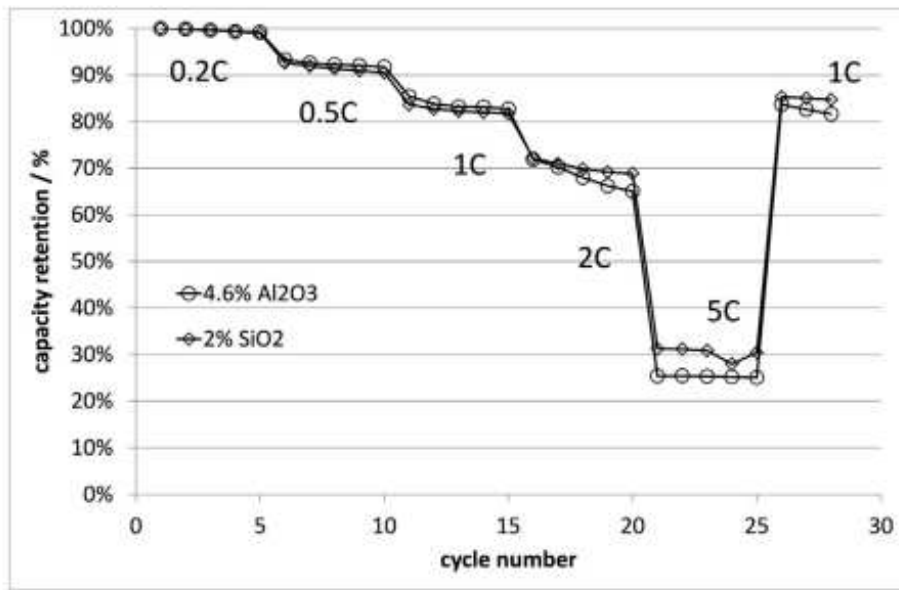


Figure 21. Capacity retention for water-based NMC cathodes with 4.6% Al_2O_3 (circles) and 2% SiO_2 (diamonds).⁴⁶

2.6. $\text{LiNi}_{1/3}\text{Mn}_{1/3}\text{Co}_{1/3}\text{O}_2$ with polytetrafluoroethylene (PTFE)

The group of L. Li studied the properties of $\text{LiNi}_{1/3}\text{Mn}_{1/3}\text{Co}_{1/3}\text{O}_2$ (NMC) obtained in laboratory and sintered at different temperatures.⁴⁵ The material was characterized as $\text{LiNi}_{1/3}\text{Mn}_{1/3}\text{Co}_{1/3}\text{O}_2$, with different sintering temperatures (800 °C – NMC 800, 850 °C – NMC 850 and 900 °C – NMC 900). The cathodes were prepared by pressing previously dry-premixed NMC, acetylene black (conductive agent) and polytetrafluoroethylene (PTFE, binder) on a nickel grid. Proportions for cathode were 70 wt% of active material, 20 wt% of conductive agent and 10 wt% binder. After application, cathodes were dried prior to cell preparation. For their examinations, cathodes were combined with a lithium metal anode. SEM was used to check the structure of the prepared samples. The results are presented in Figure 22, which clearly shows that higher temperature of sintering leads to bigger particles (smallest for 800 °C, about 100-200 nm and biggest for 900 °C, about 300-400 nm). All three cathodes showed similar performance for about 50 cycles (see Figure 23), with stable discharge capacities of approximately 140-160 mAh/g for NMC800 and NMC900, and noticeably higher for NMC850, about 170-180 mAh/g. Figure 24. shows the long-term performance of prepared cells. Again, NMC800 and NMC900 samples showed similar operating properties (with capacity retention of about 83-88% after 50th cycle), while NMC850 showed a better performance, with higher initial discharge capacity and capacity retention after 50th cycle of about 94%.

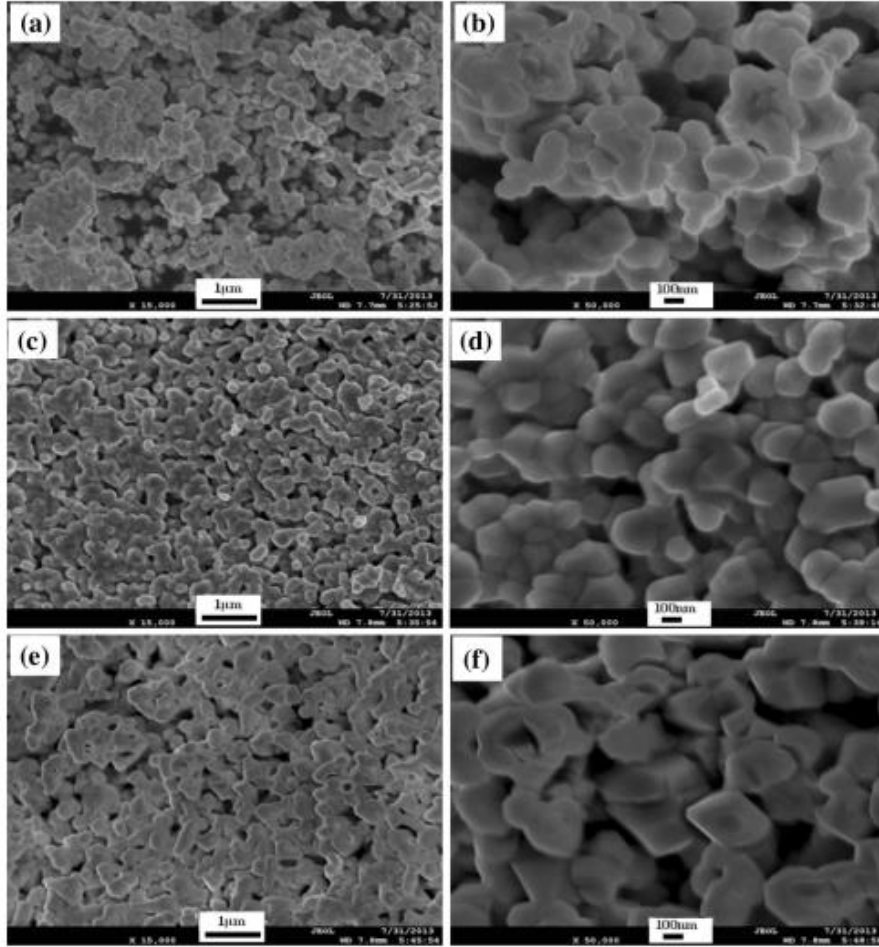


Figure 22. The SEM images of samples obtained at (a, b) 800 °C, (c, d) 850 °C and (e, f) 900 °C.⁴⁷

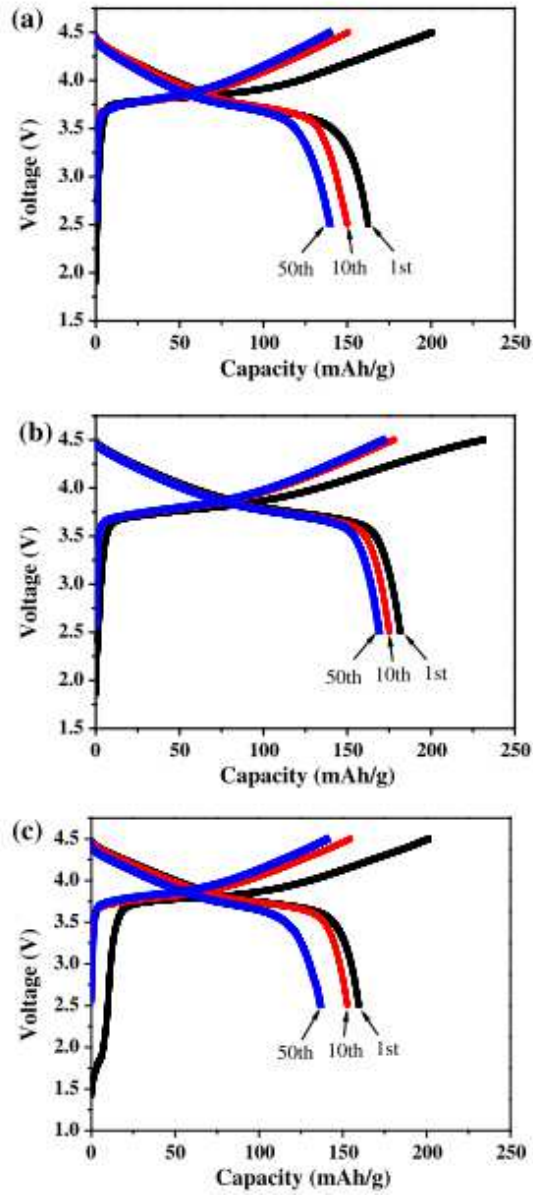


Figure 23. Discharge curves for 1st, 10th and 50th cycle for NMC samples obtained at (a) 800 °C, (b) 850 °C and (c) 900 °C.⁴⁷

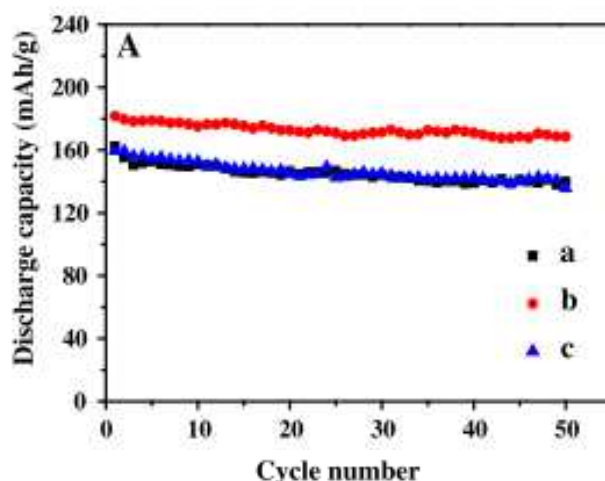


Figure 24. Cycling performance (as discharge capacity) for NMC samples obtained at (a) 800 °C, (b) 850 °C and (c) 900 °C.⁴⁷

2.7. “Door opener” to the future of battery?

Water-compatible binders can be competitive in relation to currently used water-free binders. As mentioned above, with scientific proofs, water-based binders can achieve at least the same properties at operation conditions as their water-free competitors. Sodium carboxymethyl cellulose (CMC), styrene-butadiene rubber (SBR), hybrid acrylic-fluoropolymer (TRD202A) and polyurethane (IPDI-based) can be used as stable and durable binders, which are environmentally friendly and relatively cheap compared to other processing formulations with NMP-based binders. Moreover, when properly used, they provide better processability due to use of neutral solvent and due to good protective characteristics for the active material and the current collector, excellent rate capabilities, initial capacity and capacity retention in long-term use.

The nickel-manganese-cobalt oxides can be competitive in relation to currently used cathode materials. As mentioned above, with scientific proofs, NMC-oxides can achieve at least the same working properties as their challengers. Compounds with different ratios of nickel, manganese, cobalt and lithium can be used as stable and durable cathode materials, which are more environmentally friendly and cheaper in comparison to other active material proposed for cathode formulations like pure cobalt-oxide. Moreover, when used in right way, they show very good processability, adequate stability in proper formulations of aqueous-slurries and suitable capacity retention in long-term use. Considerations and investigations of many researcher have led scientists

from AIT Institute and TU WIEN to carry out scientific research on water-soluble binders whose results will be presented in the 2nd part of the work.

3. Experimental

3.1. Slurry, electrode and cell preparation

Commercially available materials were used to prepare slurries for further processing to electrodes: conductive carbon black C-ENERGY SUPER C65, carboxymethyl cellulose CMC, fluorine acrylic latex JSR TRD202A and three types of NMC powders: NMC111, NMC532 and NMC622. Mentioned materials were used to make two types of cathodes slurries with different composition. First composition was: 94.5 wt% of NMC powder, 3 wt% of carbon black, 1.5 wt% of CMC and 1 wt% of latex and samples with marks beginning with 4 (NMC 111), 5 (NMC 532) and 6 (NMC 622). The second composition was: 92.5 wt% of NMC powder, 5 wt% of carbon black, 1.5 wt% of CMC and 1 wt% of latex and samples with marks beginning with 9 (NMC 111), 8 (NMC 532) and 10 (NMC 622). For comparison, an electrode was made with PVDF as a binder and NMP as a solvent (sample 7). Some labels, showing data about the mentioned ingredients are presented below.

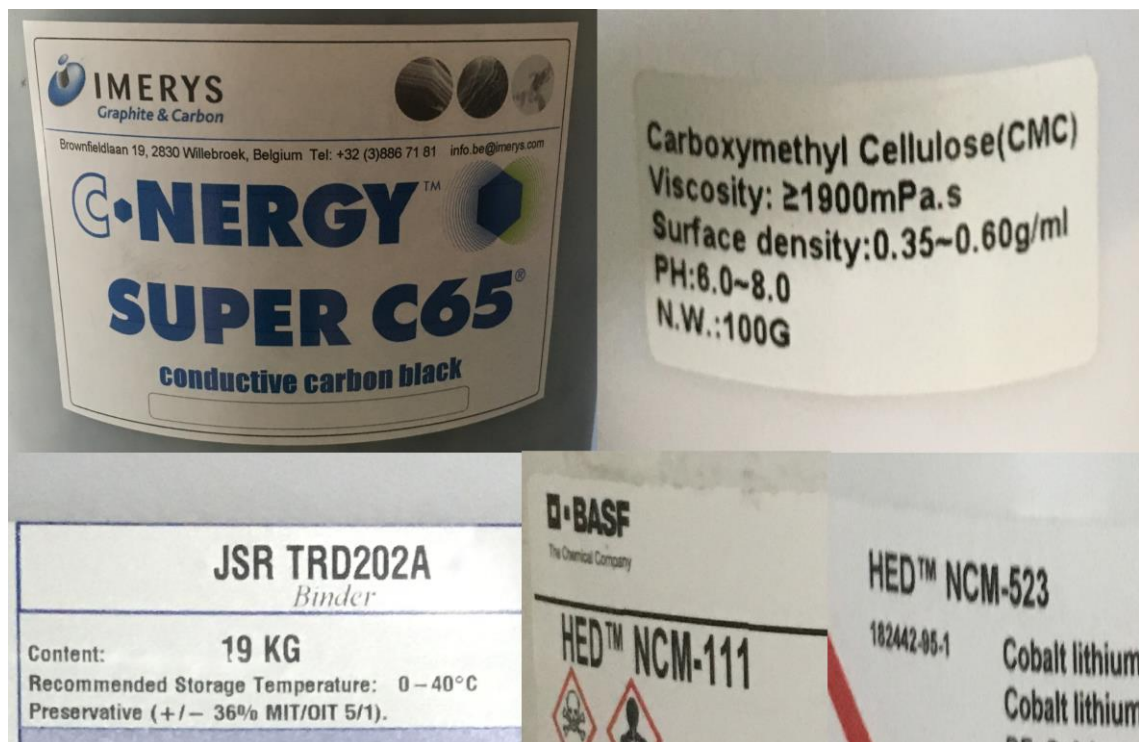


Figure 25. Product labels of some components for electrode slurries.

For the first composition, electrode slurries were prepared in the following presented order. Firstly, weighed amount of carbon black (0.75 g) was added to 18.75 g of 2 wt% water solution of CMC and stirred for 3 hours (250 rpm) by IKA stirrer - Figure 26. Next, weighed amount of NMC powder (23.625 g) was added to dispersion and further stirred for 1.5 hours (300 rpm). Finally, 0.625g of fluorine acrylic latex was added, and whole dispersion was stirred for 30 minutes (250 rpm). Identical processing to slurry was used for second composition, with differences in carbon black weight (1.25 g instead of 0.75 g) and NMC powder (23.125 g instead of 23.625 g). Obtained slurries were used to make electrodes by spreading it with 120- μ m doctor blade (MTI Corp., AFA-II Automatic Thick Film Coater) on aluminum foil with speed of 7 mm/s - Figure 27. Prepared electrodes were left for 24 h to let them dry in atmospheric conditions - Figure 28. Then they were dried in vacuum oven in 120 °C for 14 h and were put into calendaring machine (MTI Corp., HR01 Hot Rolling Machine, Figure 29). After roll-pressing, it was possible to cut electrodes for coin-cells with appropriate device (MTI Corp., Electrode Cutter, Figure 30), and they were weighed and measured to determine their thickness.

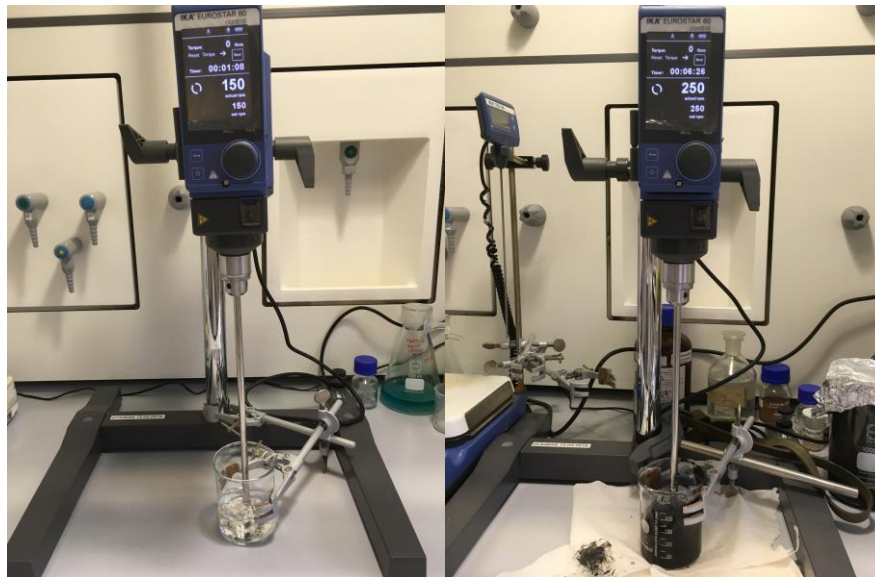


Figure 26. IKA stirrer with CMC solution (left) and nearly processed slurry (right).

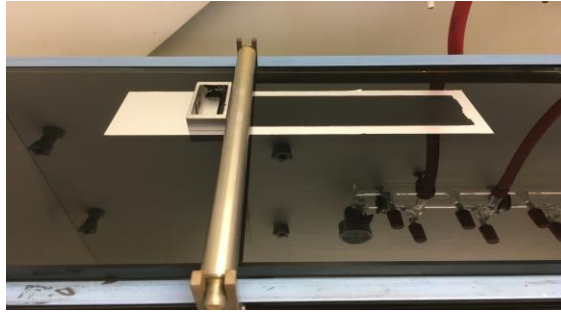


Figure 27. Casting slurry on aluminium foil with doctor blade.



Figure 28. Dried cathodes.



Figure 29. Calendring machine.

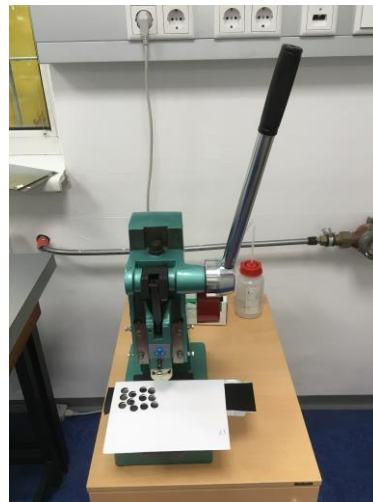


Figure 30. Coin-cell electrode cutter.

Coin-cell electrodes were dried again in glass oven (Buchi, Glass Oven B-585, Figure 31) and used to assemble lithium coin-cells in glove-box - Figure 32. The anode

was made of metallic lithium. The electrolyte was 1 mol/L LiPF₆ in EC/DMC in 30:70 w/w with 2 wt% of VC. Prepared cells can be seen in Figure 33.

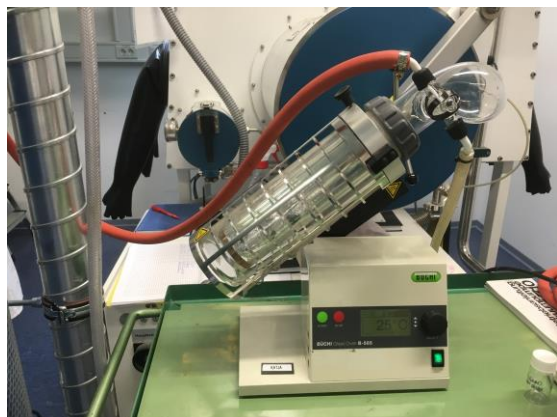


Figure 31. Glass oven.



Figure 32. Glove box.

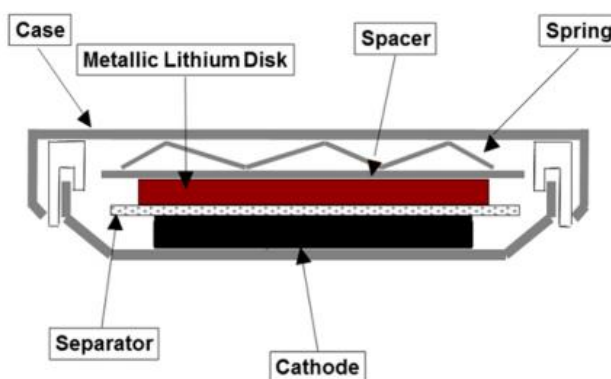
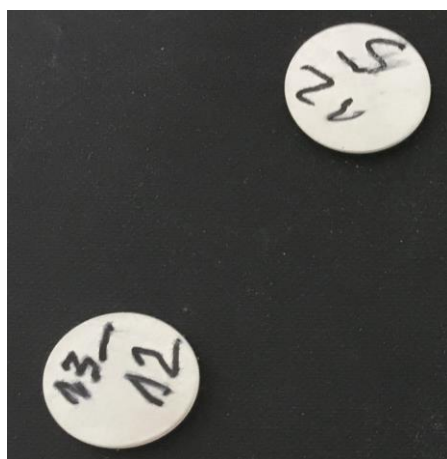


Figure 33. Prepared coin cells for the electrochemical testing and schematical cross-sectional view.⁴⁶

3.2. Electrode morphology and composition

Some samples from electrodes were taken to check their morphology and to verify their composition with SEM microscopy (scanning electron microscopy) and EDS or EDAX (energy dispersive X-ray spectroscopy/analysis). Those two methods are commonly used together, because they share the same apparatus. While SEM is used to reveal samples morphology and texture, EDAX is used to determine the chemical composition of the sample. The most common SEM mode is the detection of secondary electrons, which are emitted by atoms, excited by the electron beam. The amount of detectable secondary electrons depends also on sample shape. Usage of special detector

to collect those electrons, leads to images of the specimen surface topography. A similar method is used in EDAX analysis. A high-energy beam of electrons is used to excite atom electrons in the sample. This can cause electron ejection from inner electron shell, resulting in electron hole, which is filled by higher-energy electron from higher-energy shell, and this leads to energy emission in form of an X-ray. X-rays intensity and their energy can be measured with an energy-dispersive spectrometer. Those energies are characteristic for different atoms as their energies between different electron levels are characteristic for the electronic shell structure of the emitting atoms. Thus EDAX can be used to check elemental composition of samples.

Prior to examination, samples must be well dried, because high vacuum conditions during SEM or EDAX analysis will cause rapid water boiling and this could lead to destruction of the sample. In addition, due to low electric conductivity of sample components, materials must be coated with a thin gold layer to increase surface conductivity and allow discharge of electrons to ground. For that reason, samples were coated with gold in the sputter device visible in Figure 34.

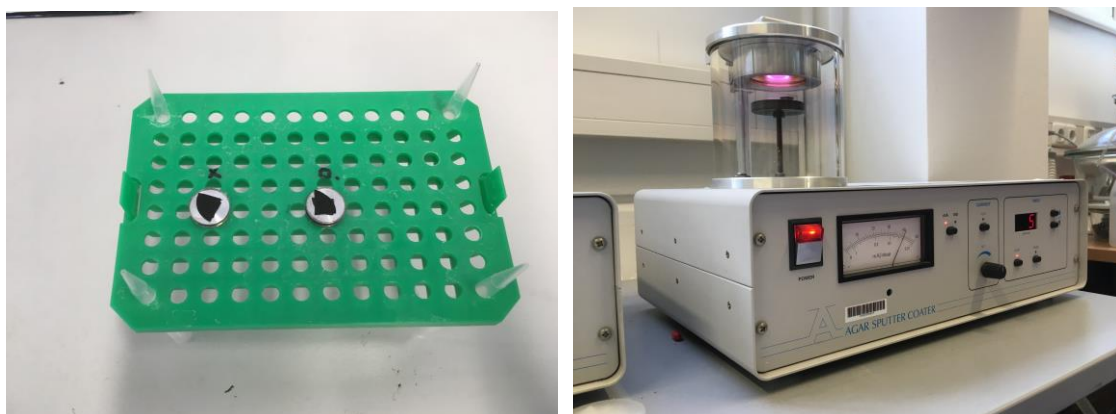


Figure 34. Samples of electrode materials and working Agar Coater Sputter (sputter-coater).

Samples of electrodes coated on an aluminum foil current collector with the active materials NMC532 (5) and NMC622 (6) were objects of SEM and EDAX examination. For the tests, 6 samples were selected:

- 2 samples cycled to 4.2 V (0.1 C formation cycles and 0.2 C cycling): 5.3, 6.3;
- 2 samples cycled to 4.5 V (0.1 C formation cycles and 0.2 C cycling): 5.10, 6.4;
- 2 uncycled samples: 5.4, 6.15.

In the text, only part of calculated compositions and results will be discussed and analyzed.

Low magnification SEM images are shown in Figure 35. Morphologies of all samples show regular electrode structure. Electrodes have rather smooth surface, which is result of the calendaring process. As can be seen in Figure 35, all six electrodes samples have small cavities (even sample 6.4 in the upper left corner of the image) in the coating. Three of them have rather circular holes (5.4, 5.3, 5.10), with diameter from 30 to 100 μm , sample 6.15 shows circular and irregular holes with diameters from 50 to 160 μm , sample 6.3 shows small circular holes with diameters from 20 to 40 μm and sample 6.4 shows very small circular holes with diameters around 10 μm . Formation of these cavities was also observed in two cited papers.^{40,44} This was explained by hydrogen gas formation during water-based slurry casting and drying on aluminium foil. The high pH and water of the slurry caused a corrosion reaction of the current collector, which resulted in hydrogen bubbles and formation of cavities. During the drying process, those structures were maintained. This effect might alter electrochemical properties of the active material, resulting for example in lower long term electrode stability and faster decay of charge/discharge capacity.

Medium magnification SEM images - Figure 36. of electrodes show some interesting properties of some cavities. While in sample image 6.4 no cavities are visible, other samples reveal cavities with different sizes. Samples 5.10 and 6.3 have cavities with diameters ranging from 30 to 50 μm . At the bottom, spherical particles of electrode material are visible. Samples 5.4, 5.3 and 6.15 have cavities with dimensions from 50 up to 100 and 150 (5.3) μm . At the bottom of some of those cavities, the surface appears smooth, which suggests that it is current collector foil. A prove for this are high magnification SEM images and EDAX examination at the bottom surface in holes, which was performed for sample 5.3. The examined hole-area is marked with a red rectangle and named 'spec1' in Figure 37. It shows only few electrode particles in the center and some filaments (maybe binder residuals). EDAX examination results of this area reveal very high aluminum atomic content (67.93%), which indicates that the observed smooth surface at the cavity bottom is aluminum foil.

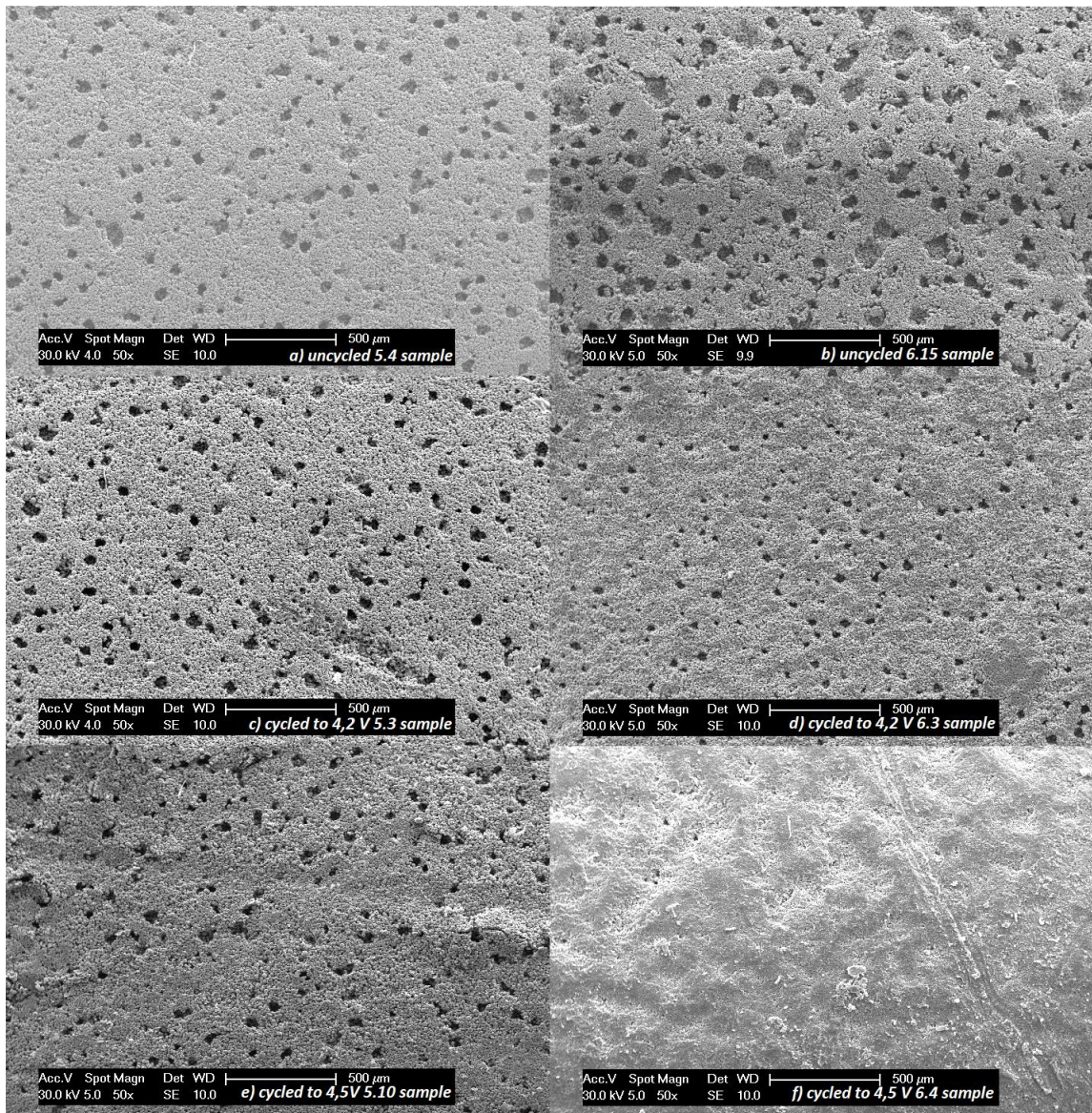


Figure 35. Low magnification SEM images of samples of uncycled electrodes a) 5 (5.4) and b) 6 (6.15), cycled to 4.2 V electrodes c) 5 (5.3) and d) 6 (6.3) and cycled to 4.5 V electrodes e) 5 (5.10) and f) 6 (6.4).

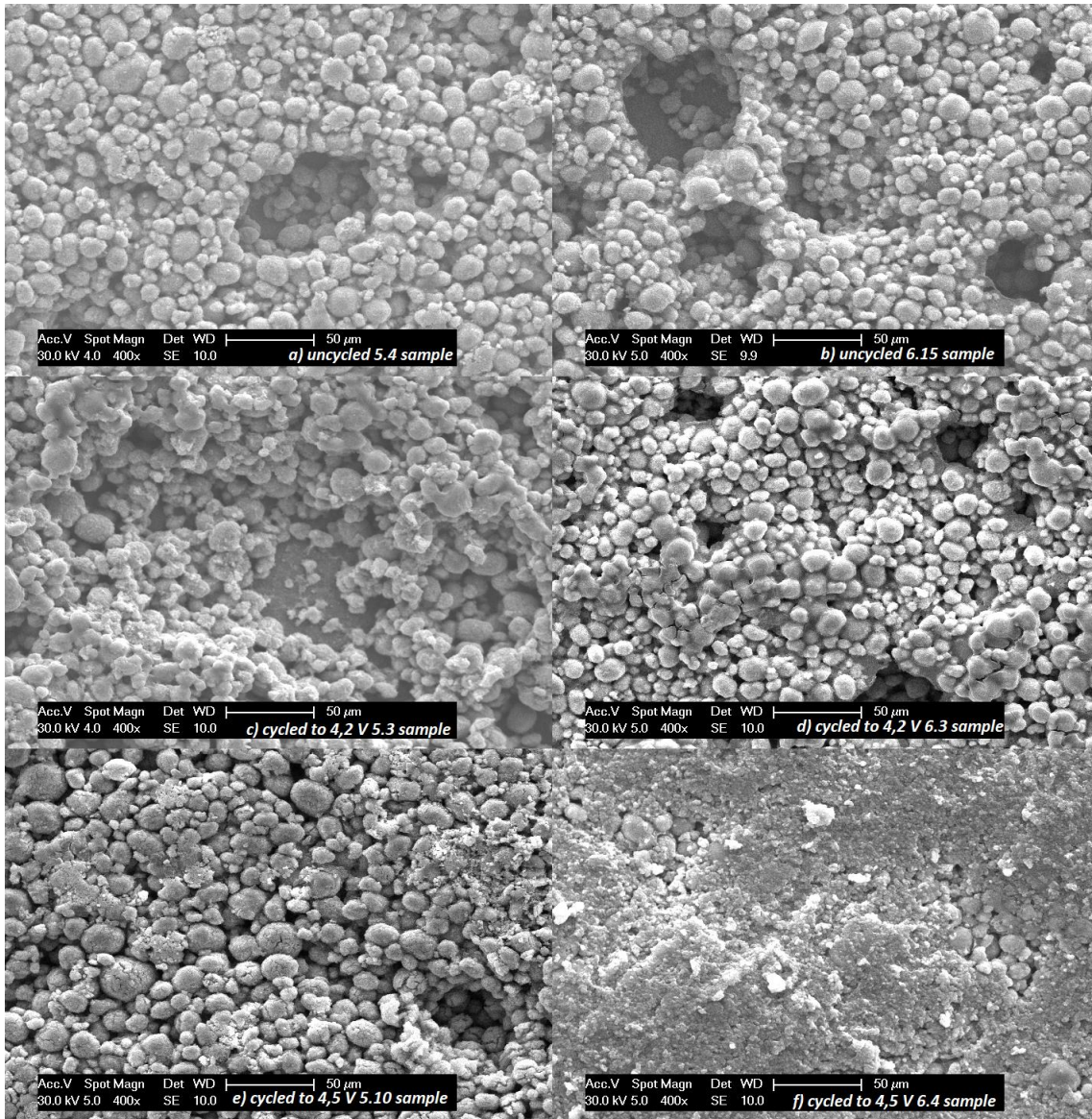


Figure 36. Medium magnification SEM images of samples of uncycled electrodes a) 5 (5.4) and b) 6 (6.15), cycled to 4.2 V electrodes c) 5 (5.3) and d) 6 (6.3) and cycled to 4.5 V electrodes e) 5 (5.10) and f) 6 (6.4).

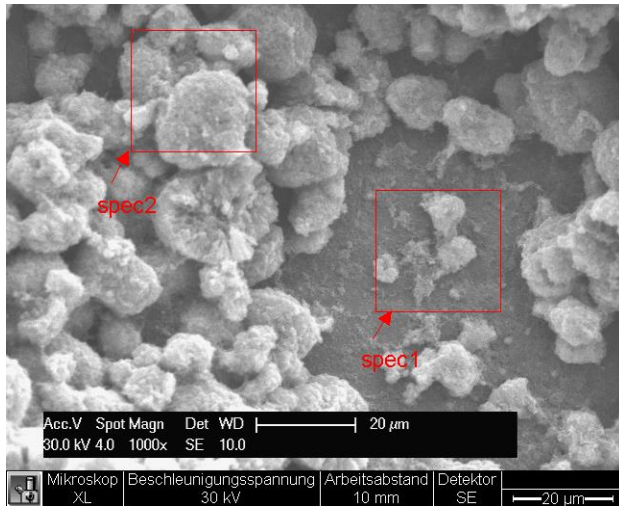


Figure 37. High magnification SEM image of 5.4 cycled sample with marked area of EDAX examination ('spec1').

Very high magnification SEM images of the same sample (Figure 38) shows nearly bare, smooth surface with very small particles and chain-like structures of organic binder. EDAX examination result is 73.4% atomic content of aluminum and 25.43% atomic content of oxygen, which clearly confirms that the observed area is the current collector aluminum foil, which may be partially affected by reaction with the alkaline water during casting water-based electrode slurry (aluminum corrosion leads to formation of aluminum oxides and hydroxides).

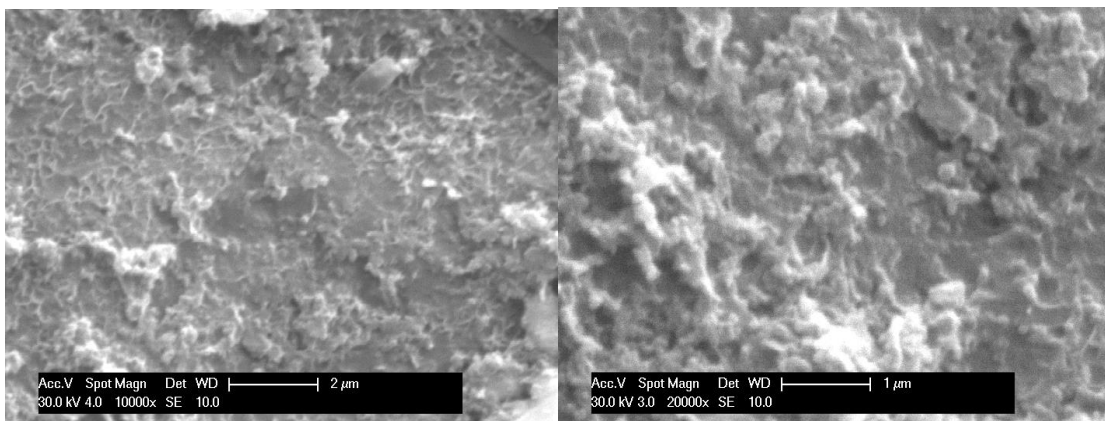


Figure 38. Very high magnification SEM images of 5.4 cycled sample.

In the text, only part of the calculated EDAX compositions and results will be discussed. Main reason of this is fact, that NMC material parameters are mainly connected to nickel, manganese and cobalt content, so other elements (carbon – from conductive agent and binders, oxygen – from NMC material, binders and others, aluminium – from current collectors and gold – from conductive coating for SEM and

EDAX examination) will be omitted during EDAX results discussion. As SEM and EDAX are surface investigations, results are sample morphology (SEM) and surface composition (EDAX). Changes in active material composition can occur during charge-discharge cycling. Proportions between nickel, manganese and cobalt were recalculated for constant amount of nickel – 5 for electrode 5 (NMC 532 material) and 6 for electrode 6 (NMC 622 material). Nickel, manganese and cobalt in electrode composition originate only from initial active material powder and cannot be created during operation of the cell. An increase in amount of manganese or cobalt mean that nickel amount decreases.

Firstly, examination results of electrodes based on NMC 532 active material will be discussed. For electrode 5, three EDAX tests of uncycled samples and three tests of cycled samples were performed, but two samples were cycled to 4.2 V and one sample was cycled to 4.5 V. Results are presented in Table 4. Uncycled samples show rather lower content of manganese versus nickel – instead of 3, Mn amount varies from 2.64 to 2.87, with an average value of 2.76. Cobalt content versus nickel is roughly 2 and varies from 1.92 to 2.07, with an average value of 1.98. Nearly ideal cobalt content and lowered manganese content suggests that during slurry preparation, some amount of manganese on active material surface is probably lost due to leaching in contact with water. After cycling to 4.2 V, both samples showed higher manganese and cobalt ratio versus nickel from 3.09 to 3.16 and from 2.10 to 2.13 respectively. These results suggest that during operation manganese and cobalt is enriched at the surface or nickel is lost. After cycling to 4.5 V, sample showed similar manganese and higher cobalt content versus nickel, 2.72 and 2.05 respectively. These results suggest that the surface is enriched in cobalt during cycling to 4.5 V (in comparison with uncycled electrode) or some manganese is lost (in comparison with electrode cycled to 4.2V).

Table 4. Composition of the samples of electrode 5 (NMC 532) uncycled and after cycling.

Sample status	Sample name	NMC532		
		Metals in active material (proportions)		
		Ni	Mn	Co
Uncycled	5.4 (unc07.1)	5	2.64	1.95
Uncycled	5.4 (unc07.2)	5	2.87	1.92
Uncycled	5.4 (unc072)	5	2.76	2.07
cycled to 4.2 V	5.3 (cyc04.2)	5	3.09	2.10
cycled to 4.2 V	5.3 (cyc09)	5	3.16	2.13
cycled to 4.5 V	5.10 (51007)	5	2.72	2.05
mean uncycled		5	2.76	1.98

Secondly, examination results of electrodes based on NMC622 active material will be discussed. For electrode 6, two EDAX tests of uncycled samples and three tests of cycled samples were performed, but two samples were cycled to 4.2 V and one sample was cycled to 4.5 V (see Table 5). Uncycled samples show different content of manganese versus nickel – instead of 2, manganese amount varies from 1.65 to 2.21, with an average value of 1.93, which is just slightly lower than expected value of 2. Cobalt content versus nickel is higher than 2 and varies from 2.20 to 2.44, with an average value of 2.32. Nearly ideal mean manganese content and raised cobalt content suggest that during slurry preparation, at the surface of the active material some amount of nickel and manganese is probably lost due to leaching in contact with water. After cycling to 4.2 V, both samples showed slightly increased manganese and bit lowered cobalt content versus nickel, from 2.09 to 2.15 and from 2.03 to 2.24 respectively. These results suggest that during operation, the surface is slightly enriched in manganese and a bit of cobalt is lost. After cycling to 4.5 V, sample showed lowered manganese and a higher cobalt content versus nickel, 1.84 and 2.21 respectively. Probably the surface is depleted in manganese during cycling to 4.5 V (in comparison with uncycled and cycled to 4.2 V electrode) and cobalt amount is lower than in uncycled electrode.

Table 5. Composition of the samples of electrode 6 (NMC 622) uncycled and after cycling.

Sample status	Sample name	NMC 622		
		Metals in active material (proportions)		
		Ni	Mn	Co
uncycled	6.15 (61507_1)	6	1.65	2.44
uncycled	6.15 (61507_2)	6	2.21	2.20
cycled to 4.2 V	6.3 (6305_1)	6	2.15	2.24
cycled to 4.2 V	6.3 (6305_2)	6	2.09	2.03
cycled to 4.5 V	6.4 (6405)	6	1.84	2.21
mean uncycled		6	1.93	2.32

EDAX examination results show unstable chemical composition of the surface layer. All samples have atomic content of carbon ranging from 25.33% to 56.67%, which may be consequence of carbon conductive agent and/or water-soluble organic binder presence in electrode material composition. When cycled to 4.2 V potential, electrode 5 (NMC 532) experienced increase in manganese and cobalt content or loss in nickel content. When cycled to 4.5 V, the same electrode suffered manganese and probably nickel loss. When cycled to 4.2 V potential, electrode 6 (NMC 622) experienced some cobalt loss and probably nickel loss (by increase in manganese content). When cycled to 4.5 V, the same electrode suffered loss in manganese and cobalt content. Those changes can be explained by reaction of oxide active material with solvent and/or electrolyte during battery cycling. At the beginning, ready to use uncycled cathode material is protected with binders. After formation cycles, increased charge/discharge rate (from 0.1 C to 0.2 C) and periodic changes in volume of oxide active material leads to stress of whole electrode complex, also straining cathode electrolyte interphase. Those changes can lead to impoverishment of NMC powder in nickel and/or manganese and/or cobalt. Further ongoing alterations can lead to loss of properties of active material, especially to drop in charge/discharge capacity, which severely affects cell stability, durability and suitability for use.

As SEM and EDAX examinations required opening of closed cells, it was also possible to check the adhesion strength of the coating on the aluminum foil. Results are visible on Figure 39 below. Both uncycled cells showed rather good resistance to scratching or handling, while four cycled samples were much more prone to any

mechanical operations, which is visible as detachment from foil surface. It may suggest that during cycling, binder is losing its properties, especially adhesive and bonding strength, which may affect cell stability and properties. After separation of the active material coating from current collector during cycling, cell capacity may be severely affected.



Figure 39. Cathodes from opened and tested cells, cycled (left) and uncycled (right).

3.3. Cycling properties of prepared cells

Cells samples made with every prepared cathode were taken to check their electrochemical properties during cycling in Maccor Battery & Cell Test Equipment



Figure 40. Maccor Battery & Cell Test Equipment.

Series 4600, visible in Figure 40. Tests are performed in CCCV charging manner (constant current, constant voltage) and discharging with rate of 0.1 C (during formation of the cell) or 0.2 C (during ‘work’ cycling). During charging current remains constant and after reaching the desired cell voltage limit, this voltage was maintained with decreasing charging current. All cells were tested with two different charging voltages limits – 4.2 V and 4.5 V. Cycling parameters like voltage, electric current and time were

recorded by the device, and were further used to calculate the number of charge/discharge cycles, charge/discharge capacity and cell efficiency. Results are shown in charts, mainly as capacity (charge/discharge) over cycle, voltage over time or electric efficiency over time. Some electrodes were cycled to perform other examinations (like EDAX and SEM) and their cycling properties may be omitted in this paper.

3.3.1. Cells from electrode 7 (non-aqueous binder) – NMC 111, comparative sample

Electrode 7 samples were used to perform cycling tests. Sample 4.1 was the subject for cycling. Results are visible in Figure 41. For 100 cycles, the cathode specific capacity (of cathode material) is about 155 mAh/g. This value corresponds well to practical capacity (170 mAh/g), with specific capacity calculated for pure NMC-oxide material in cathode slurry formulation around 165 mAh/g. In the chart, there is no trend towards a lower specific capacity – it is rather stable. Active material has no chance of reacting with water, due to non-aqueous slurry based on NMP-soluble binder.

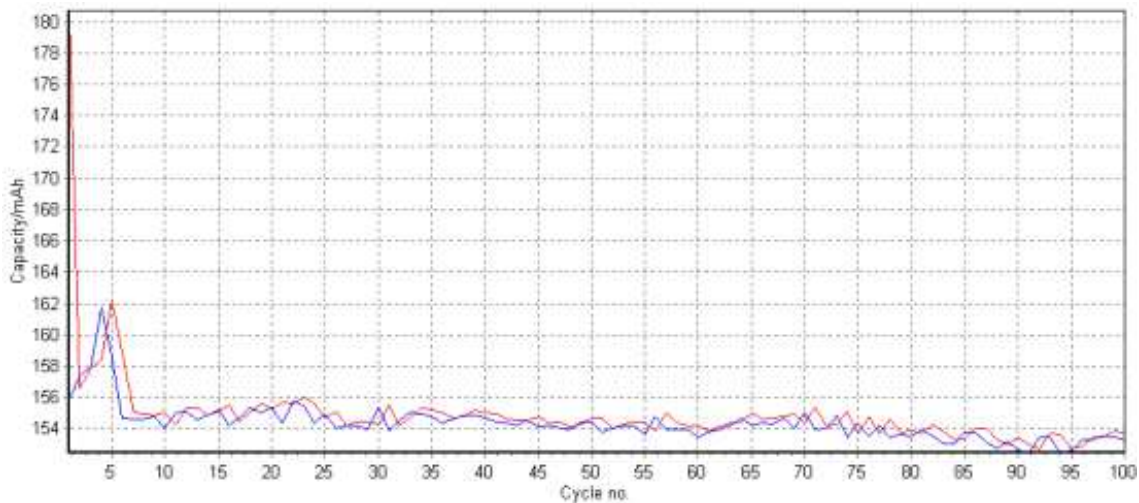


Figure 41. Electric capacity over time, electrode 7 sample (PVDF non-aqueous binder).

3.3.2. Cells from electrode 4 (first composition) – NMC 111

Four electrode 4 samples were taken for further examination. Samples named 4.1, 4.3, 4.8. and 4.14 were subject for cycling to 4.2 V or 4.5 V and other tests.

3.3.2.1. Sample 4.1 and 4.3, cycling to 4.2V

Electrode 4 samples were used to perform cycling tests. Sample 4.1 was the subject for 4.2 V cycling. Results have been shown in Figure 42, 43 and 44. For about 90 cycles, cathode specific capacity (of cathode material) is about 130 mAh/g. This value corresponds well to results of other groups using aqueous binders with specific capacity calculated for pure NMC-oxide material in cathode slurry formulation around 137 mAh/g, which is a rather good result.^{39,40} Unfortunately, after 90 cycles, capacity drops to about 55% of previous level to about 70 mAh/g and gradually decreases to 20 mAh/g after 120 cycles. Electric efficiency ranges from 85 to 100 %, with an average value of 94%. This behavior suggests that active material degrades during charging and discharging, probably reacting with residual water, because slurry was water-based.

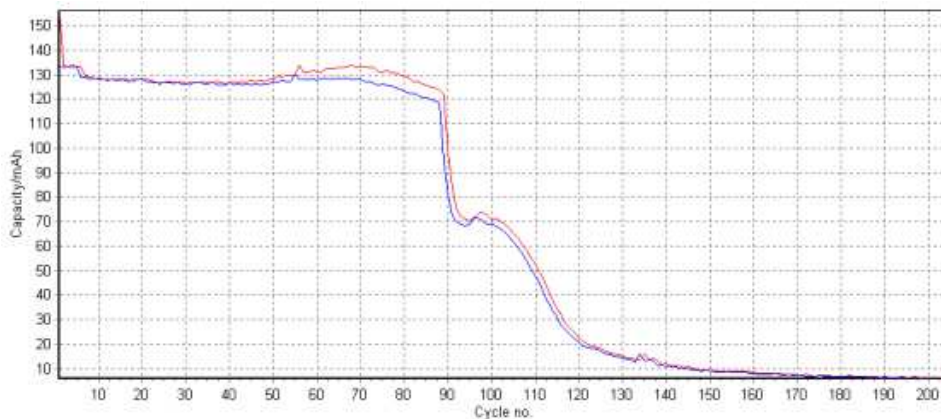


Figure 42. Electric capacity over time, electrode 4 sample 4.1, cycling to 4.2 V.

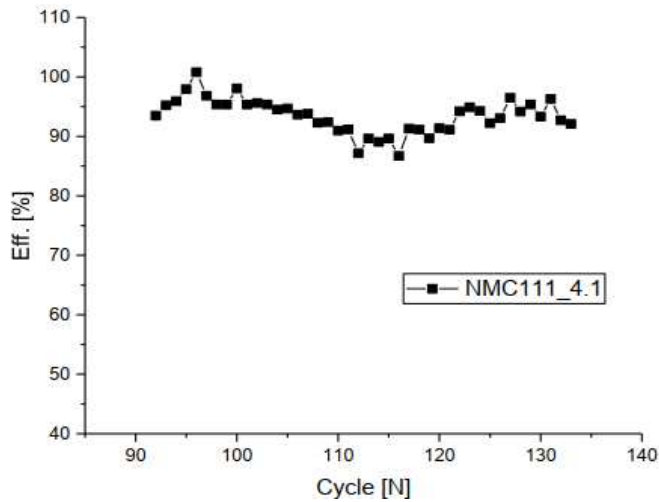


Figure 43. Electric efficiency over time, electrode 4 sample 4.1, cycling to 4.2 V.

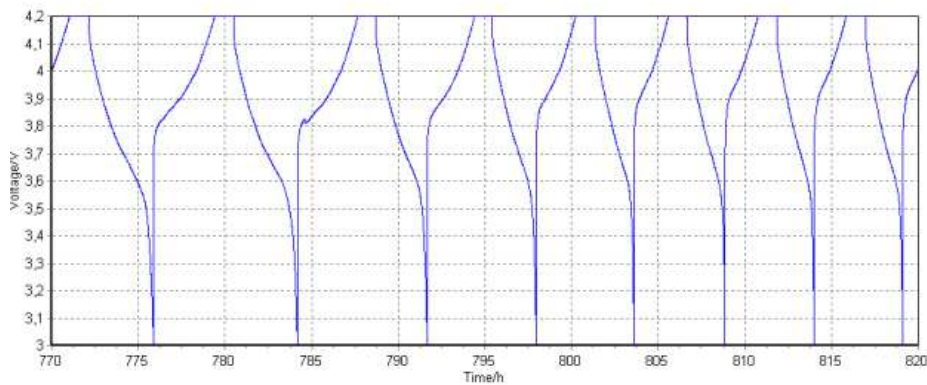


Figure 44. Cell voltage over time for cycles 100 to 110, electrode 4 sample 4.1, cycling to 4.2 V.

Sample 4.3 was the subject for 4.2 V cycling. Results are visible in Figure 45. and 46. For about 60 cycles, cathode specific capacity (of cathode material) is about 130 mAh/g. This value corresponds well to results of other groups using aqueous binders, with specific capacity calculated for pure NMC-oxide material in cathode slurry formulation around 137 mAh/g, which is rather good result.^{39,40} Unfortunately, after 60 cycles, capacity gradually decreases to 50 mAh/g after 100 cycles. Electric efficiency ranges from 90 to 100 %, with an average value of 97%. This decrease is rather uniform and steady.

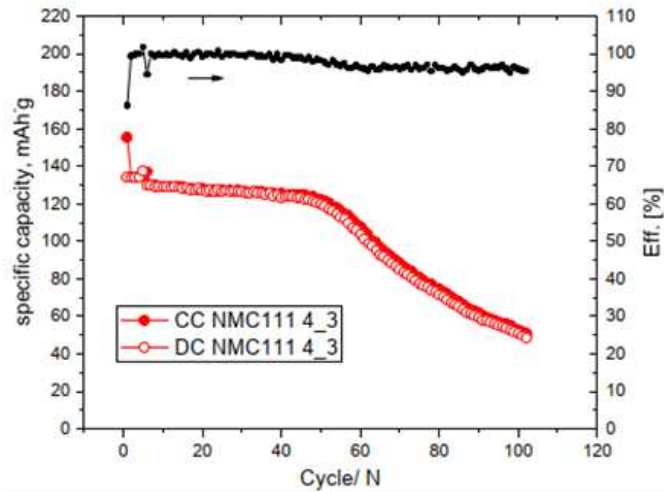


Figure 45. Electric capacity and electric efficiency over time, electrode 4 sample 4.3, cycling to 4.2 V.

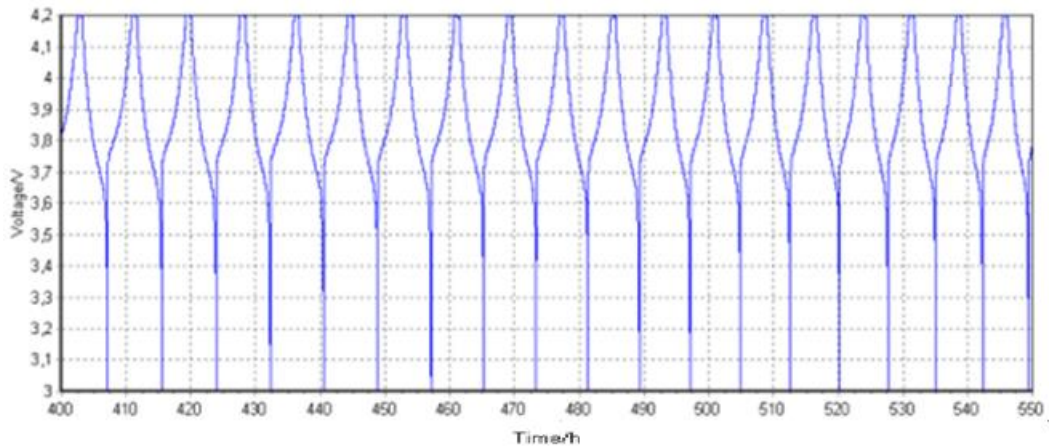


Figure 46. Cell voltage over time for cycles 40 to 60, electrode 4 sample 4.3, cycling to 4.2 V.

Slow, uniform capacity loss may be associated with active material steady degradation due to electrochemical and physical changes during cycling, like changes of chemical composition, also connected with periodic changes in volume of charged/discharged oxide active material, which stresses the whole cathode structure complex, held entirely by binders. Those changes are slow, but relentless, gradually lowering cell electric capacity. For the 4.1 sample it can be observed for about 90 charge/discharge cycles and for second sample 4.3 about 55 charge/discharge cycles. Further ongoing alterations can lead to loss of charge/discharge capacity, which eventually drop down to zero. A rather sharp decrease around 90th may be caused by mechanical failure, while further decrease may originate from steady degradation of

active material. Fast capacity drop (within 10-15 cycles) is higher than slow capacity loss mentioned earlier and leads to complete cell degradation. This process is clearly much faster than slow capacity loss and the chart shows notable decrease in capacity during one cycle. It suggests that during cycling, binder loses its properties, especially adhesive and bonding strength, which lead to separation and peeling of coating of active material due to continuous stress overload. After peeling of coating from current collector during cycling, capacity of the cell is lost by the lack of electrical contact between collector and coating (which is seen as a huge decline of electrode capacity during a single cycle). Capacity loss is also visible in charge-discharge cycles where the cell voltage over time charts become more inclined and the time to reach the voltage thresholds decreases.

3.3.2.2. Sample 4.8 and 4.14 cycling to 4.5V

Electrode 4 samples were used to perform cycling tests. Sample 4.8 was the subject for 4.5 V cycling, which was investigated in parallel. Results are visible in Figure 47, 48. and 49. For about 110 cycles, cathode specific capacity (of cathode material) is about 158 mAh/g. This is a very good result compared with the calculated specific capacity for pure NMC-oxide material in cathode slurry formulation of around 167 mAh/g. The measured value corresponds also well to results of other groups using non-aqueous binders⁴⁵ and to the conventional reference sample. Unfortunately, after 110 cycles, capacity decreases fast to about 20 mAh/g after 125 cycles. Electric efficiency ranges from 97 to 100 % for 80 cycles, with an average value of 98%.

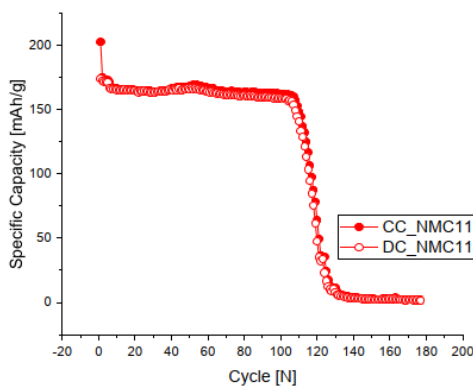


Figure 47. Electric capacity over time, electrode 4 sample 4.8, cycling to 4.5 V.

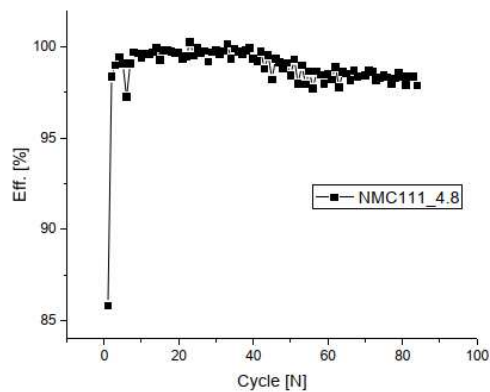


Figure 48. Electric efficiency over time, sample 4.8, cycling to 4.5 V.

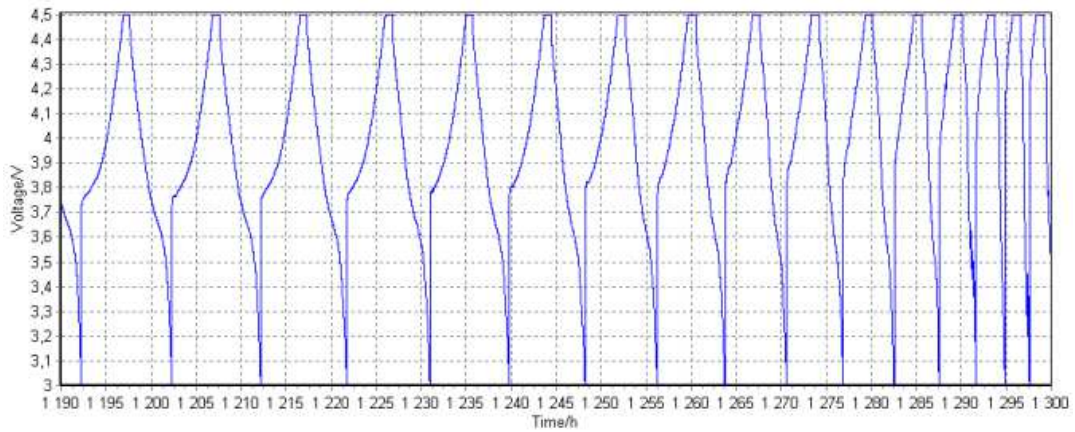


Figure 49. Cell voltage over time for cycles 100 to 120, electrode 4 sample 4.8, cycling to 4.5 V.

Sample 4.14 was the subject for 4.2 V cycling. From the chart in Figure 50, it can be seen that cathode specific capacity (of cathode material) is about 162 mAh/g for about 110 cycles. Again, this capacity is a very good result compared with the theoretical value of 171 mAh/g, the literature data⁴⁵ and our reference sample. After 80 cycles, capacity is still at the same level as at the beginning. Electric efficiency ranges from 96 to 100 % for 80 cycles, with an average value of 98%. After 60 cycles, efficiency started to decrease slowly, which is also visible in a growing difference between charge and discharge capacity.

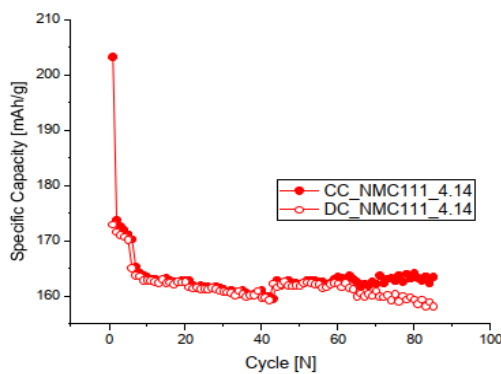


Figure 50. Electric capacity over time, electrode 4 sample 4.14, cycling to 4.5 V.

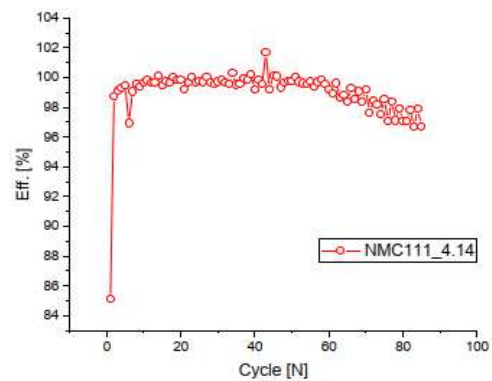


Figure 51. Electric efficiency over time, electrode 4 sample 4.14, cycling to 4.5 V.

The behavior of both samples 4.8 and 4.14 suggests that active material degrades during charging and discharging, probably reacting with residual water, because slurry

was water-based. In the presence of water, high mechanical stress during slurry preparation causes a partial detachment of carbon coating. For sample 4.8 it can be observed that changes are slow, but relentless, gradually lowering cell electric capacity. For about 110 charge/discharge cycles, the major fraction of particles is located inside the agglomerates, which protected the whole structure from mechanical stress. After 110 charge/discharge cycles loss of properties of active material takes place, especially to drop in charge/discharge capacity, which eventually drop to zero. Probably exposure to water and mechanical stress only takes place on particles at the outer layer of agglomerates. Fast capacity drop (under 10-15 cycles) is stronger than slow capacity loss mentioned earlier and leads to complete cell degradation. This process is clearly much faster than slow capacity loss and the chart shows notable decrease in capacity during one cycle. It suggests that during cycling, binder loses its properties, especially adhesive and bonding strength, which lead to separation and peeling of the active material coating due to continuous stress overload. After peeling of the coating from the current collector during cycling, capacity of the cell breaks down within a single cycle because of the lack of electrical contact between collector and coating. Cell voltage over time chart reveals fast capacity loss, as curves are very similar to each other at the beginning, becoming far more inclined with time lapse and whole charge-discharge cycle takes less time to complete.

3.3.3. Cells from electrode 5 (first composition) – NMC532

Five electrode 5 samples were taken for further examination. Samples named 5.1, 5.2, 5.3, 5.6. and 5.10 were subject for cycling to 4.2 V or 4.5 V and other tests.

3.3.3.1. Samples 5.1, 5.2 and 5.6, cycling to 4.2 V

In order to go forward with the electrode manufacturing, another cathode formulation (with NMC 532 instead of NMC 111) was used to perform cycling tests. Samples 5.1, 5.2 and 5.6 were subject for 4.2 V cycling. Results are presented in Figures 52 and 53, 54 and 55 respectively. For about 85, 30 and 45 cycles, cathode specific capacity (of cathode material) is about 150 mAh/g. This value is between results of other group using non-aqueous binders,⁴⁵ our reference sample and results of other groups using aqueous binders.^{39,40} The specific capacity calculated for pure NMC-oxide material in our cathode slurry formulation is around 158 mAh/g. Unfortunately, for all three samples after 85, 30 and 45 cycles, capacity decreases fast to about 10

mAh/g in about 5 cycles. Electric efficiency ranges from 85 to 100 % for all three samples, with an average value of 96%.

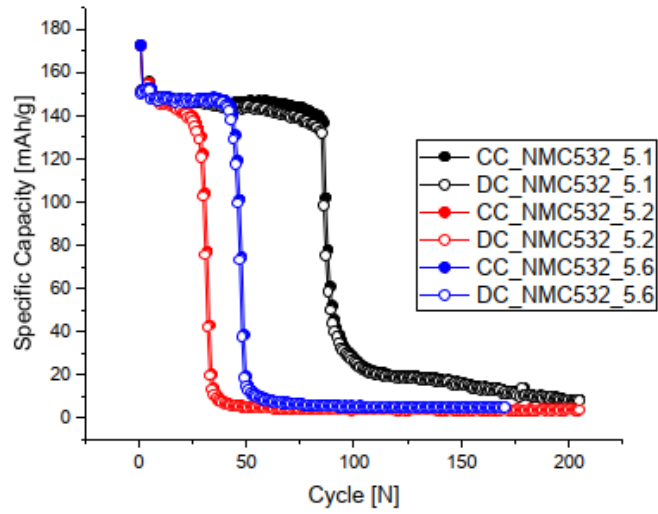


Figure 52. Electric capacity over time, electrode 5 samples 5.1, 5.2 and 5.6, cycling to 4.2 V.

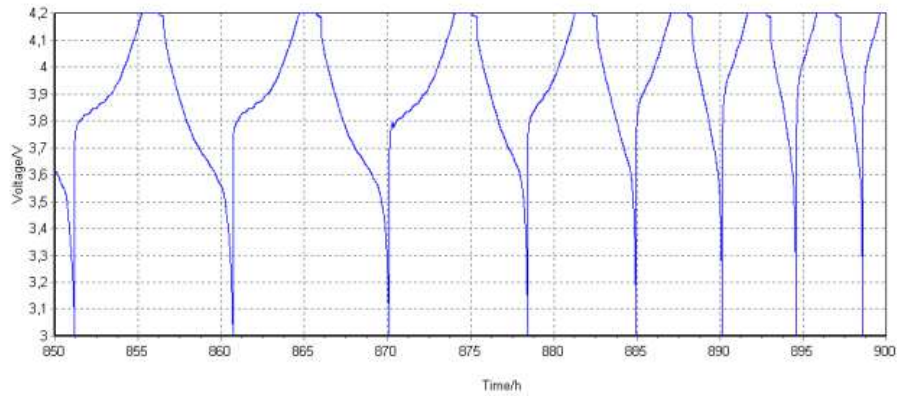


Figure 53. Cell voltage over time for cycles 85 to 90, electrode 5, sample 5.1, cycling to 4.2 V.

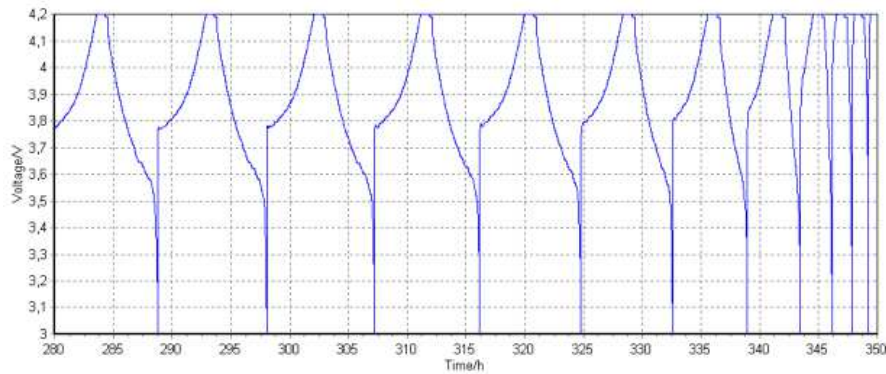


Figure 54. Cell voltage over time for cycles 25 to 35, electrode 5, sample 5.2, cycling to 4.2 V.

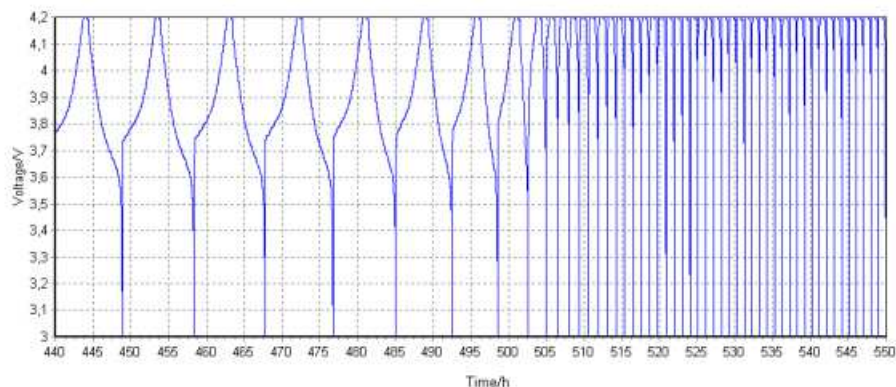


Figure 55. Cell voltage over time for cycles 35 to 45, electrode 5, sample 5.6, cycling to 4.2 V.

All samples with NMC 532 cycling to 4.2 V are sensitive to water, that lead to degradation of active material during charging and discharging cycles. The active material particles are exposed to high shear rates due to contact with water. Nearly instant capacity drop (under less than 10 cycles) is repeatedly stronger than slow capacity loss mentioned earlier and leads to complete cell degradation. This suggests that during cycling, separation and peeling of active material coating due to continuous stress overload occurs. It may be exaggerated by reaction with residual water in cathode coating material, which usually results in hydrogen gas bubbles forming. After peeling of coating from current collector during cycling, cell capacity falls to zero due to the loss of electrical contact between collector and cathode coating. Cell voltage over time charts present fast fading of the capacity, as curves are very similar to each other at the beginning, becoming much more inclined with time lapse and whole charge-discharge cycle takes less time to complete.

3.3.3.2. Sample 5.3 and 5.10, cycling to 4.5 V

Samples 5.3 and 5.10 were the subject for 4.5 V cycling procedure. Results are presented in the figures 56, 57, 58 and 59. For sample 5.3 the cathode specific capacity is about 180 mAh/g within 110 cycles. This is a very good result compared with the calculated specific capacity of 190 mAh/g for pure NMC-oxide material in this cathode slurry formulation. This value is even higher than data from material using non-aqueous binders⁴⁵ and from our reference sample. Unfortunately, after 50 cycles, capacity decreases fast to about 20 mAh/g after 70 cycles. Electric efficiency ranges from 92 to

100 % for 50 cycles, with an average value of 98%, then drops to about 94% average value.

Cycling performance was also investigated for sample 5.10. The second experiment confirmed results achieved earlier for sample 5.3. The chart shows an observable decrease in capacity during one cycle.

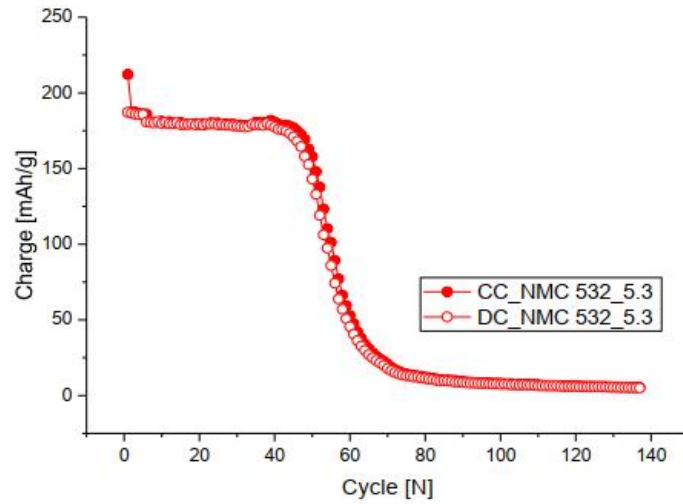


Figure 56. Electric capacity over time, electrode 5 sample 5.3, cycling to 4.5 V.

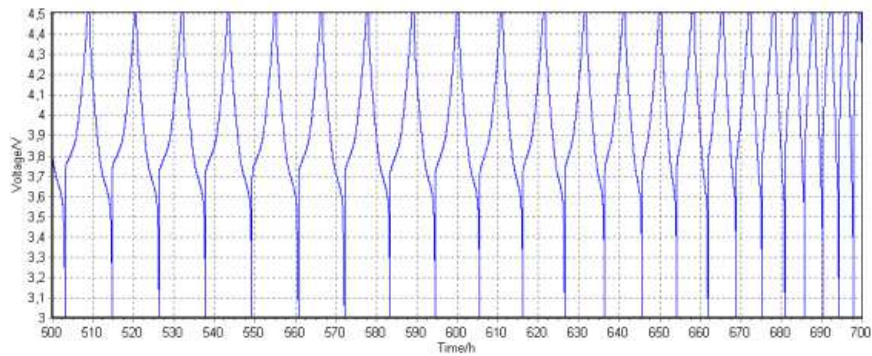


Figure 57. Cell voltage over time for cycles 40 to 50, electrode 5 sample 5.3, cycling to 4.5 V.

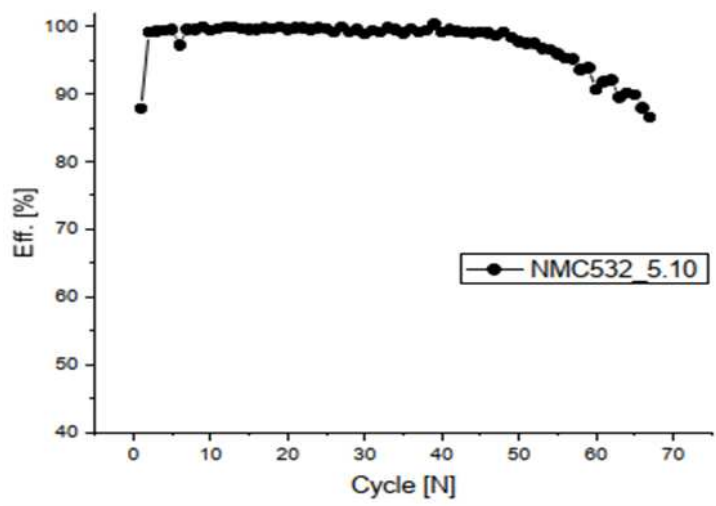


Figure 58. Electric efficiency over time, electrode 5 sample 5.10, cycling to 4.5 V.

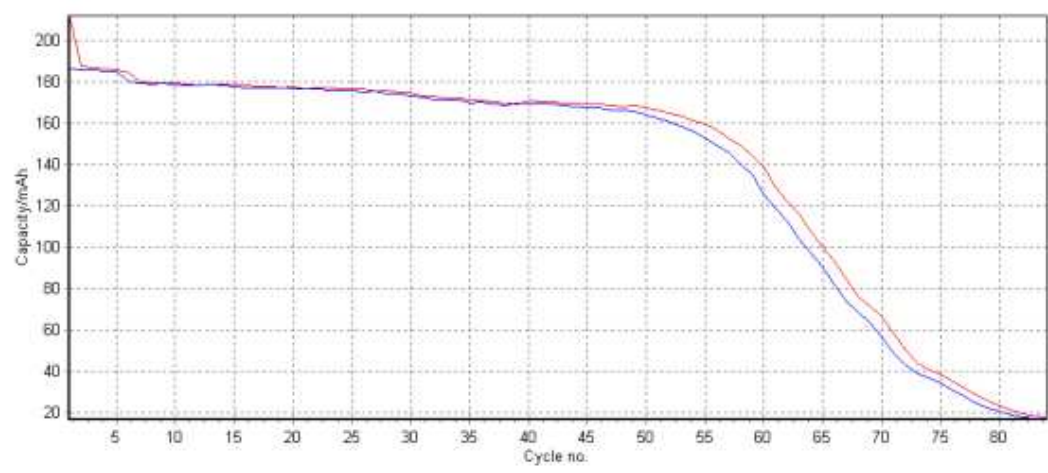


Figure 59. Electric capacity over time, electrode 5 sample 5.10, cycling to 4.5 V.

The key factor in assessing the performances of the cathode is the structural stability of the active material. This aspect is guaranteed only if the uniformity of the coating is ensured all over the electrode. The good battery performance for samples 5.3 and 5.10 for the first 50-55 cycles indicates that the coating does not hinder the flow of lithium ions and electrons during charge/discharge cycles. After this number of cycles, cathodes experience a deterioration of performance. This test is showing degradation phenomena, caused by prolonged contact with water prior to cycling, become more evident after long cycling.

3.3.4. Cells from electrode 6 (first composition) – NMC 622

Seven electrodes of samples no. 6 (NMC-622), namely 6.1, 6.2, 6.3, 6.6, 6.7, 6.10 and 6.11 were used in next experiments for cycling to 4.2 V or 4.5 V.

3.3.4.1. Samples 6.2, 6.3, 6.6, 6.7 and 6.10, cycling to 4.2 V

Cells 6.2, 6.3, 6.6, 6.7 and 6.10 made using NMC 622 materials were tested in regular working conditions and exposed to 4.2V. Results of tests are presented in Figure 60 and 61.

For about 50-60 cycles, cathode specific capacity (of cathode material) remains at about 145 mAh/g. This value is between results of other group using non-aqueous binders,⁴⁵ the reference sample and results of other groups using aqueous binders.^{39,40} The calculated specific capacity for pure NMC-oxide material in cathode slurry formulation is about 154 mAh/g. After 50-60 cycles a notable capacity fading has been observed to about 15 mAh/g. Electric efficiency ranges from 75 to 100 % for all samples, with an average value of 91%.

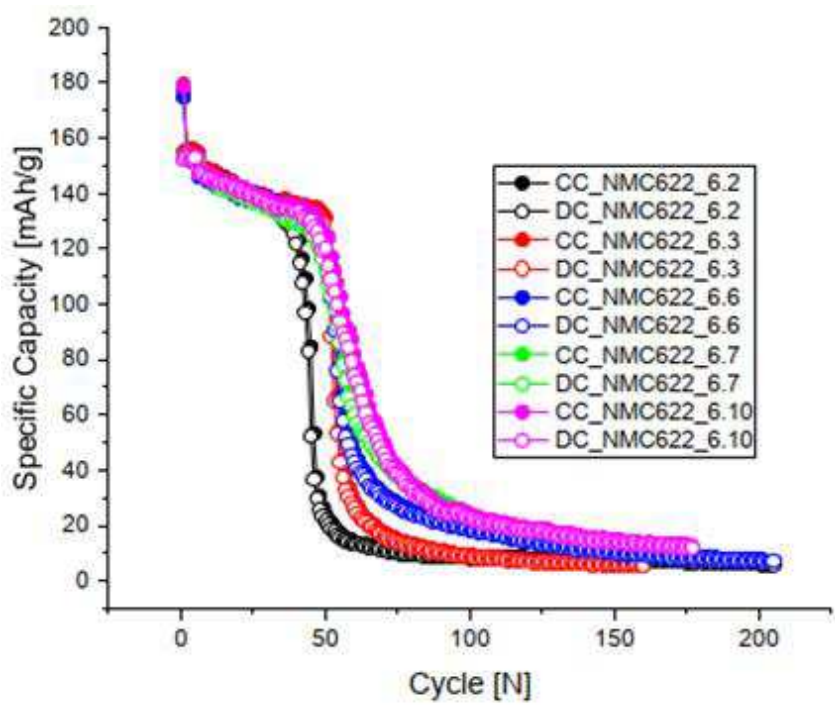


Figure 60. Electric capacity over time, electrode 6 samples 6.2, 6.3, 6.6, 6.7 and 6.10, cycling to 4.2 V.

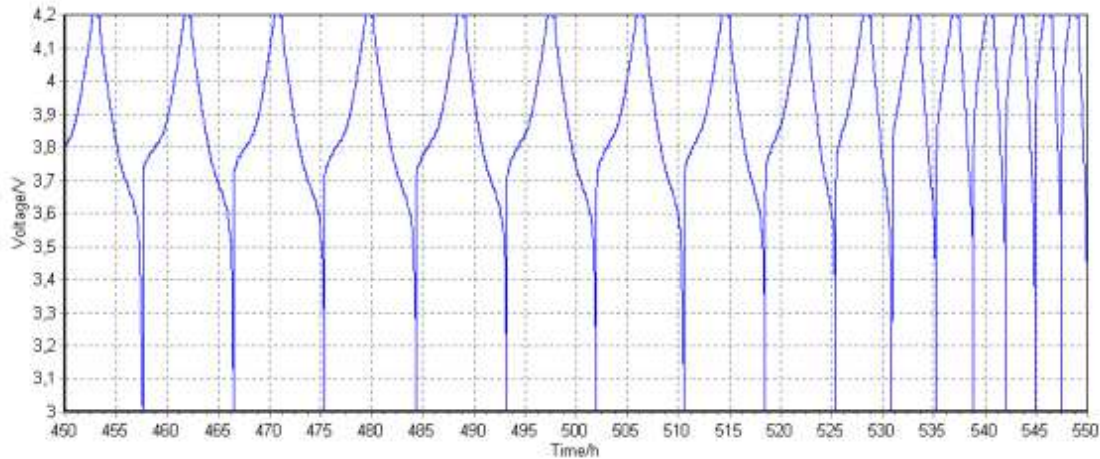


Figure 61. Cell voltage over time for cycles 55 to 60, electrode 6 sample 6.3, cycling to 4.2 V.

The achieved results suggest that during cycling, binder loses its properties, especially adhesive and bonding strength, which can lead to separation and peeling of coating of active material due to continuous stress overload. Cycling procedure leads to loss of electrical contact between collector and coating (which leads to a significant loss of electrode capacity during a single cycle).

Most of water-based binder systems cannot achieve the tape green density (packing density) of a solvent based binder system. These systems also require the use of strong dispersants to help achieving dense green tapes and frequently foaming problems will result.⁴⁷

3.3.4.2. Sample 6.1

The second experiment for sample 6 has been carried out based on the identical electrode material as for the first experiment. The experimental conditions of cycling were changed to 4.5 V. Testing cycles are presented in Fig. 62 and 63. For about 30 cycles, cathode specific capacity is about 160 mAh/g. The electrochemical performance until 30 cycles corresponds well to results of other group using non-aqueous binders.⁴⁵ After 30 cycles, capacity decreases fast in about 10 cycles to about 15 mAh/g.

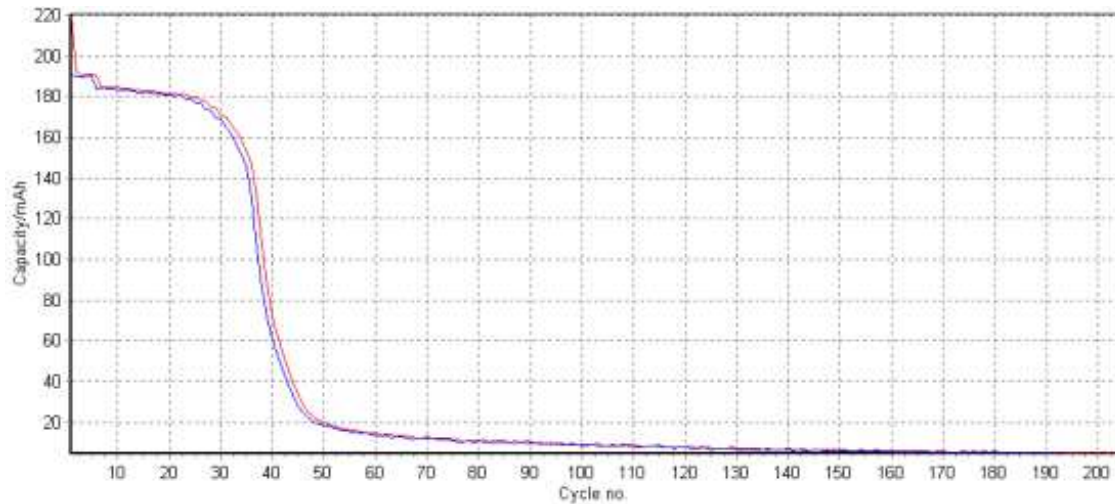


Figure 62. Electric capacity over time, electrode 6 sample 6.1, cycling to 4.5 V.

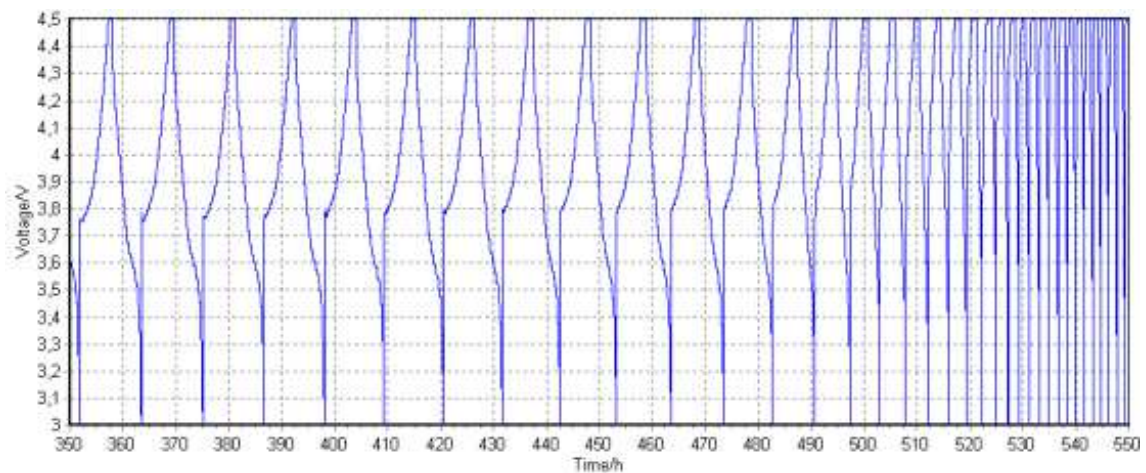


Figure 63. Cell voltage over time for cycles 25 to 45, electrode 6 sample 6.1, cycling to 4.5 V.

The achieved results are very similar to earlier results with sample 6 exposed to 4.2V.

3.3.5. Cells from electrode 9 (second composition) – NMC 111

The second series of experiments were carried out with the following composition for cathodes (92.5 wt% of NMC powder, 5 wt% of carbon black, 1.5 wt% of CMC and 1 wt% of latex). The cycling tests with the electrode 9 samples were performed with conditions identical to the first experiment series. The main objective of these experiments was to check the water-based cathodes richer in carbon and compare achieved results with first composition. Four electrode 9 samples were taken for further examination. Samples named 9.1.3, 9.1.11, 9.2.1 and 9.2.5 were subject for cycling to 4.2 V or 4.5 V and other tests.

3.3.5.1. Sample 9.1.11 and 9.2.1 cycling to 4.2 V

Sample 9.1.11 was the subject for 4.2 V cycling. Results are shown in Figure 66. For about 125 cycles, cathode specific capacity (of cathode material) is about 130 mAh/g. In the considered cycling test after 130 cycles, capacity show a huge drop to about 1 mAh/g, but a bit slower than similar behaviors of other samples (decrease within about 20 cycles). For this sample capacity fading can be observed over about 110 charge/discharge cycles.

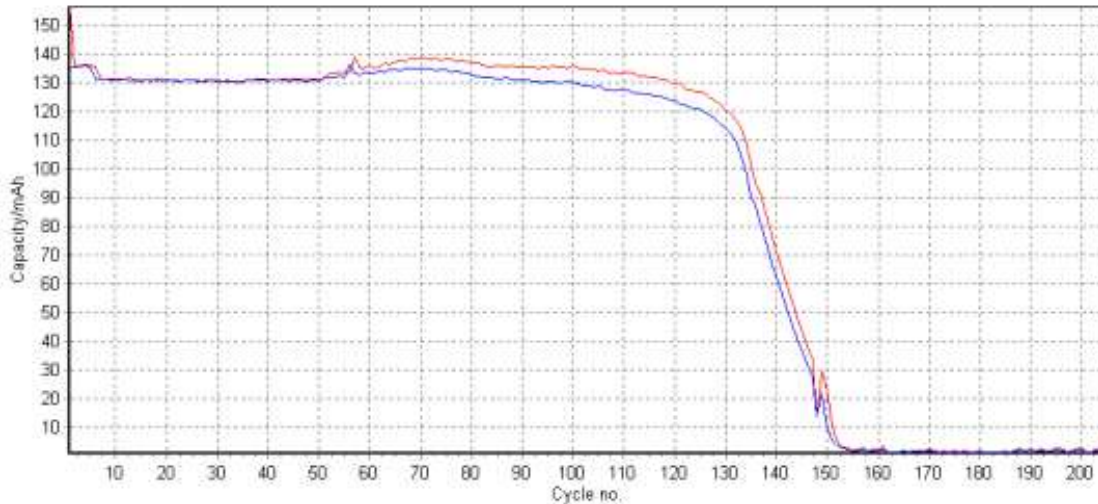


Figure 66. Electric capacity over time, electrode 9 sample 9.1.11, cycling to 4.2 V.

Quite similar and comparable results were observed from charge/discharge testing up to 4.2 V for sample 9.2.1. Results are displayed in Figure 67 and 68.

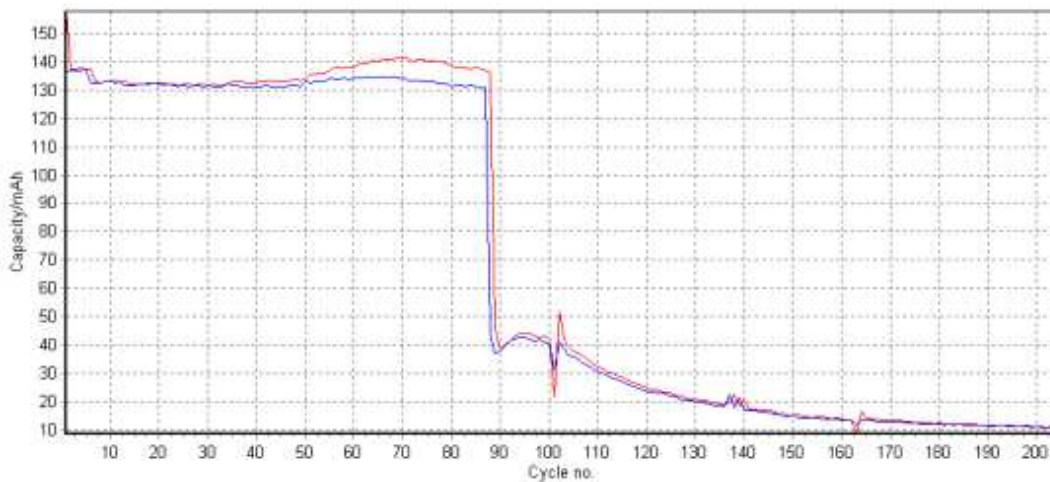


Figure 67. Electric capacity over time, electrode 9 sample 9.2.1, cycling to 4.2 V.

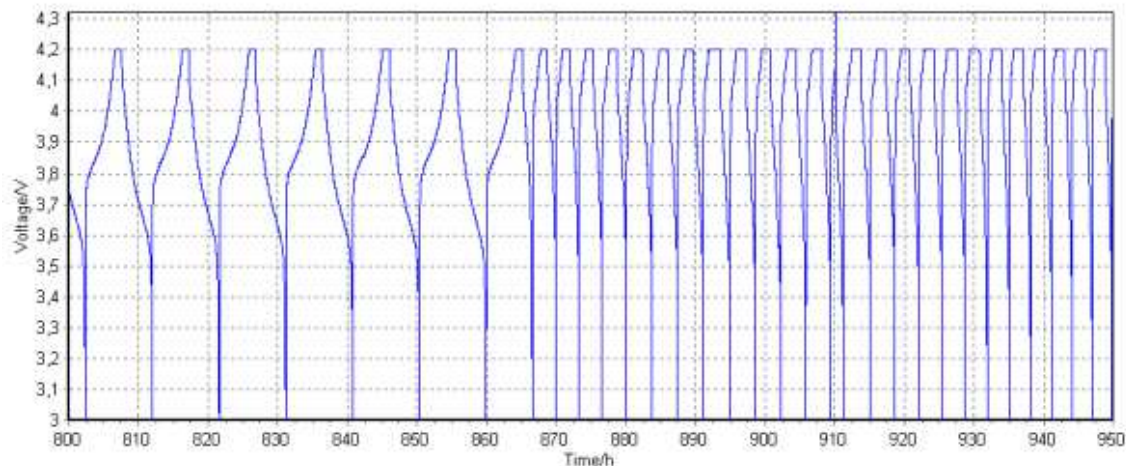


Figure 68. Cell voltage over time for cycles 80 to 105, electrode 9 sample 9.2.1, cycling to 4.2 V.

3.3.5.2. Sample 9.1.3 and 9.2.5 cycling to 4.5 V

In the next two experiments (sample 9.1.3 and 9.2.5) our attention was focused on the same water-based cathode materials working under another Voltage range 4.5 V. Results were published in Figures 69-72. For both samples cathode specific capacity is about 165 mAh/g. This value corresponds well to results of other group using non-aqueous binders.⁴⁵ After 60 cycles, it was observed, that capacity decreases fast in about 10 cycles to about 15 mAh/g.

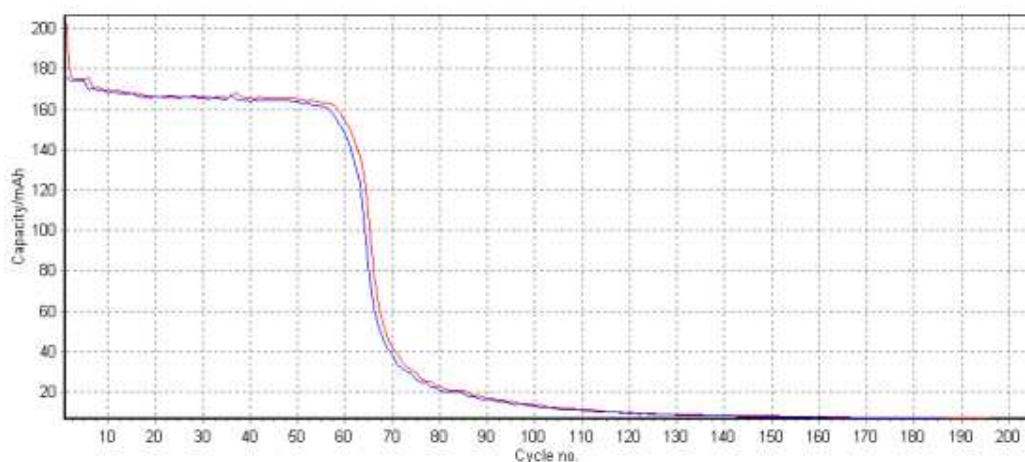


Figure 69. Electric capacity over time, electrode 9 sample 9.1.3, cycling to 4.5 V.

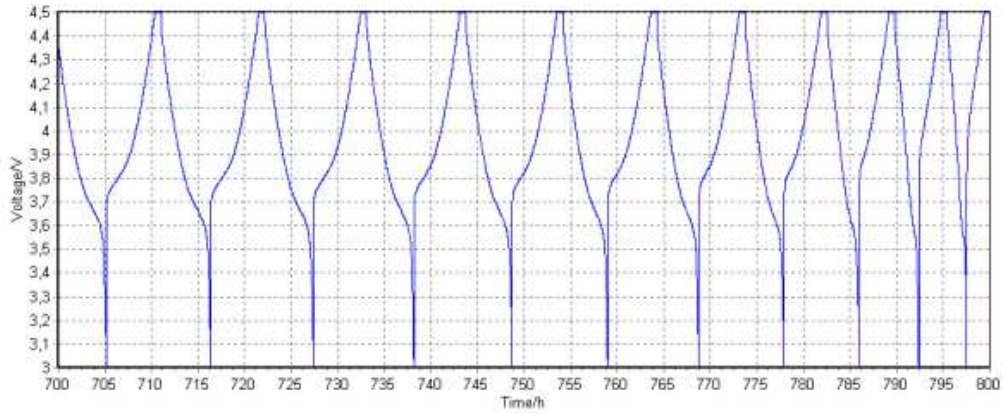


Figure 70. Cell voltage over time for cycles 55 to 65, electrode 9 sample 9.1.3, cycling to 4.5 V.

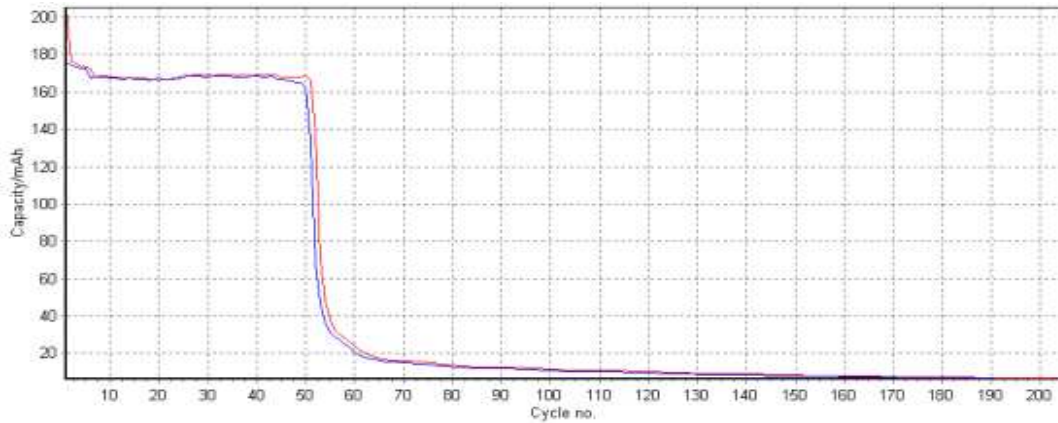


Figure 71. Electric capacity over time, electrode 9 sample 9.2.5, cycling to 4.5 V.

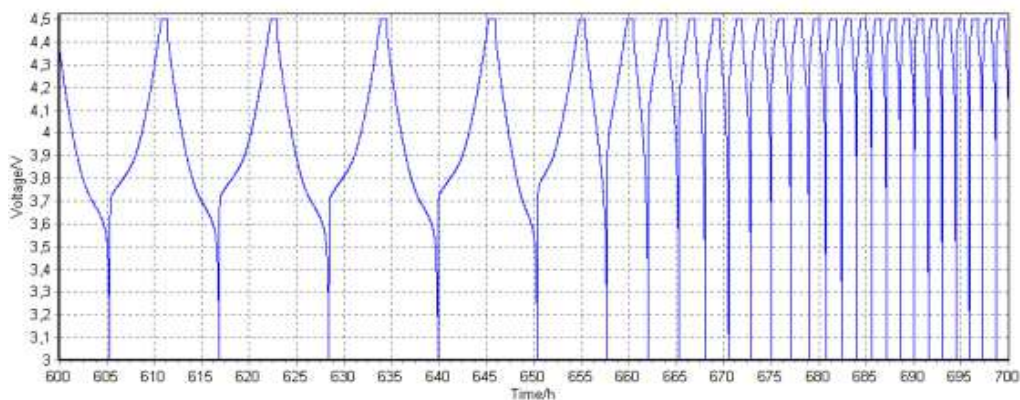


Figure 72. Cell voltage over time for cycles 45 to 60 electrode 9 sample 9.2.5, cycling to 4.5 V.

All experiments with sample 9 seem to behave quite similar and are comparable with results of experiments of sample 4, as well as for cycling to 4.2 V and to 4.5 V.

3.3.6. Cells from electrode 8 (second composition) – NMC 532

Four electrode 8 samples were taken for further examination. Samples named 8.1.1, 8.1.4, 8.2.1 and 8.2.8 were subject for cycling to 4.2 V or 4.5 V and other tests.

3.3.6.1. Samples 8.1.1 and 8.2.8, cycling to 4.2 V

Electrode 8 samples were used to perform cycling tests. Samples 8.1.1 and 8.2.8 were subject for 4.2 V cycling. Results for both samples are illustrated in Figures 73-75. Tests performed in coin cells with cathode material of sample 8 showed, that for about 150-170 cycles, cathode specific capacity is about 145 mAh/g. The obtained capacity is between results of other group using non-aqueous binders⁴⁵, reference sample and results of other groups using aqueous binders.^{39,40} The calculated specific capacity for pure NMC-oxide material in cathode slurry formulation is around 156 mAh/g. Charts illustrate gradual decrease of capacity to about 10 mAh/g after 150-160 cycles. Electric efficiency ranges from 93 to 100 % for both samples for 140 cycles, with an average value of 96% and 99%.

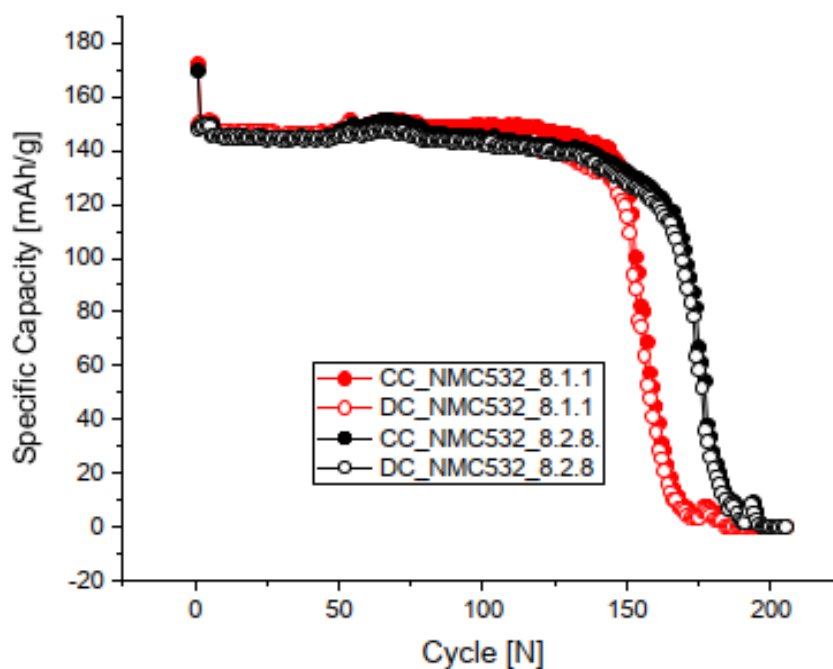


Figure 73. Electric capacity over time, electrode 8 samples 8.1.1 and 8.2.8, cycling to 4.2 V.

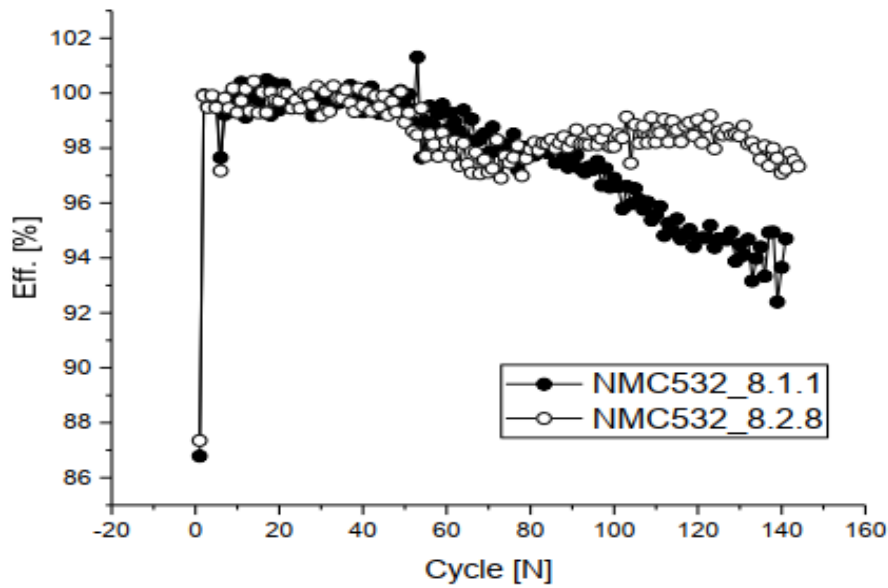


Figure 74. Electric efficiency over time, electrode 8 samples 8.1.1 and 8.2.8, cycling to 4.2 V.

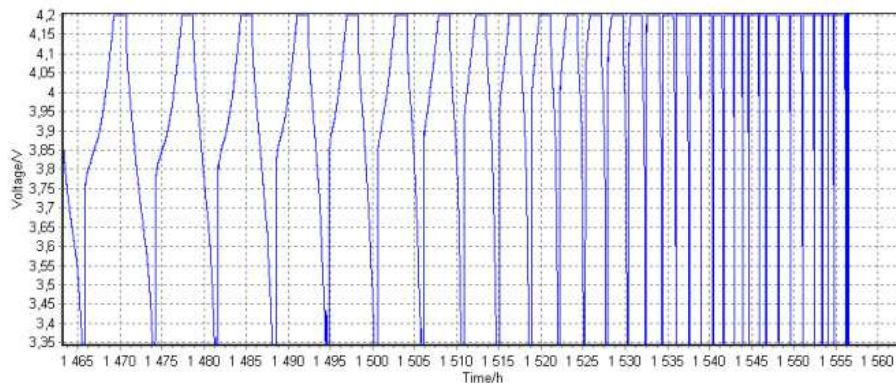


Figure 75. Cell voltage over time for cycles 140 to 160, electrode 8 sample 8.1.1, cycling to 4.2 V.

3.3.6.2. Samples 8.1.4 and 8.2.1, cycling to 4.5 V

Samples 8.1.4 and 8.2.1 were subject for 4.5 V cycling. Results are shown in Figures 76-79. Cathode specific capacity achieved in the first test is about 175 mAh/g for 120 cycles. This value corresponds well to and is even higher than results of other group using non-aqueous binders⁴⁵ and our reference sample. The calculated specific capacity for pure NMC-oxide material in cathode slurry formulation is around 189 mAh/g. After 140 cycles capacity of first sample decreases quickly to about 5 mAh/g. Quite similar trend was observed for the second sample. After 170 cycles capacity decreases rapidly to 5 mAh/g. Electric efficiency ranges from 97 to 100 % for

130 cycles, with an average value of 98 %, and lowers for one sample to 90 % after 130th cycle.

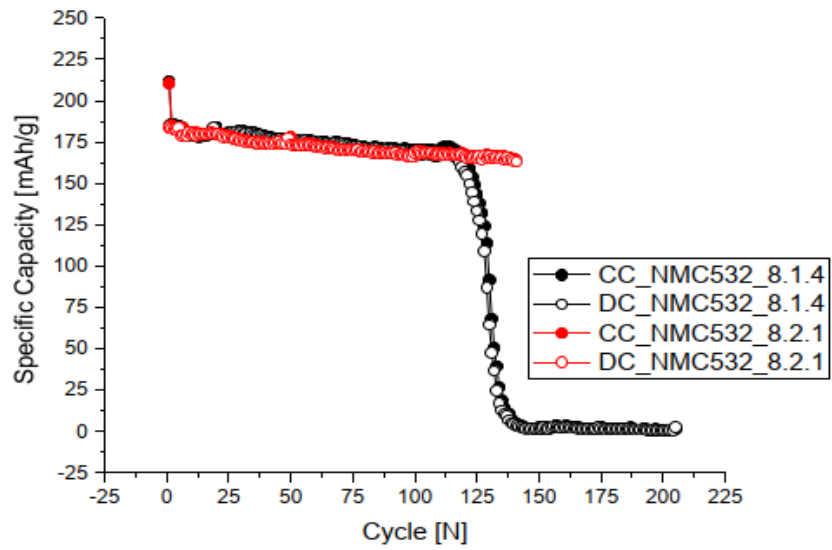


Figure 76. Electric capacity over time, electrode 8 samples 8.1.4 and 8.2.1, cycling to 4.5 V.

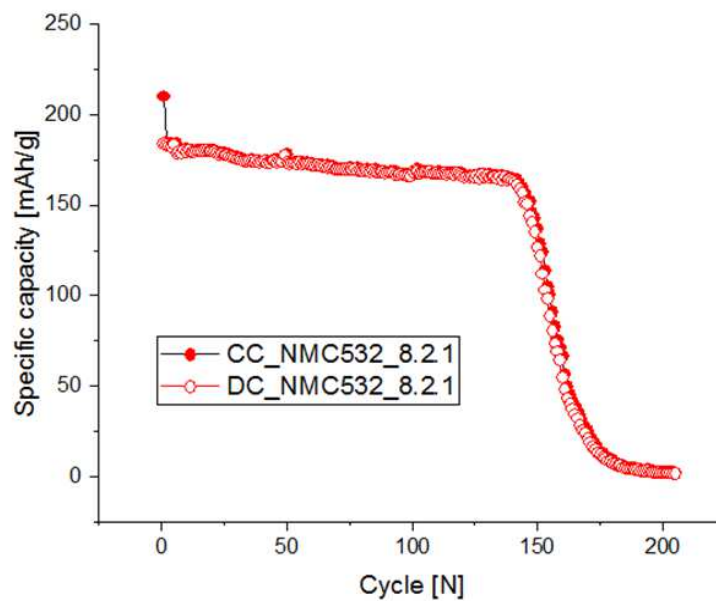


Figure 77. Electric capacity over time, electrode 8 sample 8.2.1, cycling to 4.5 V.

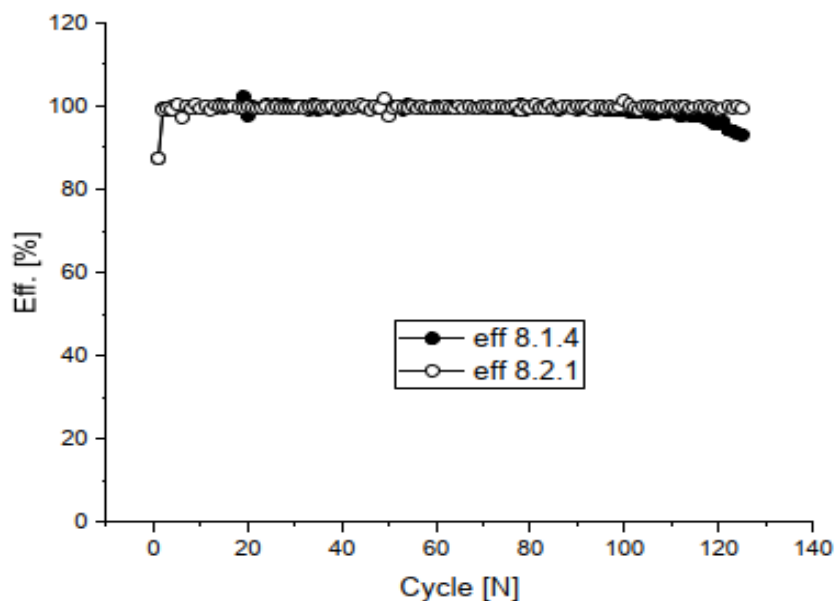


Figure 78. Electric efficiency over time, electrode 8 samples 8.1.4 and 8.2.1, cycling to 4.5 V.

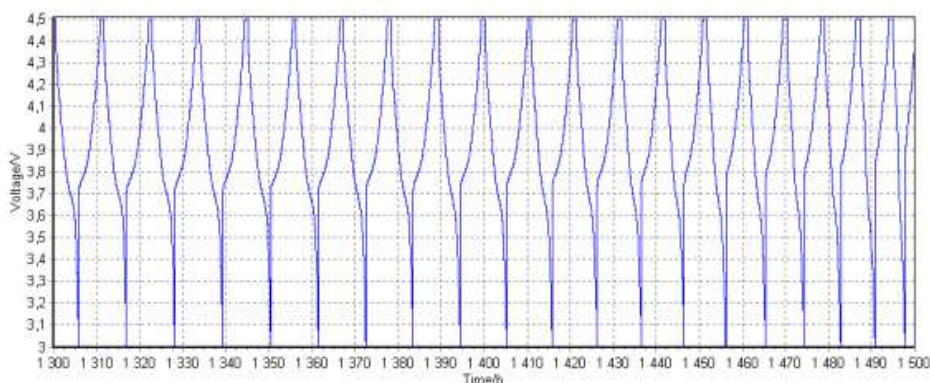


Figure 79. Cell voltage over time for cycles 115 to 125, electrode 8 sample 8.1.4, cycling to 4.5 V.

3.3.7. Cells from electrode 10 (second composition) – NMC 622

Four electrode 10 samples were taken for further examination. Samples named 10.1.2, 10.1.6, 10.1.11 and 10.1.14 were subject for cycling to 4.2 V or 4.5 V and other tests.

3.3.7.1. Samples 10.1.2 and 10.1.14, cycling to 4.2 V

In these experiments our attention was focused on samples 10.1.2 and 10.1.14 cycled with voltage range 4.2 V. Obtained results are presented in Figures 80-82. For

about 65-70 cycles, cathode specific capacity of both samples is about 140 mAh/g, and decreases to about 5 mAh/g in the next 60 cycles. Electric efficiency ranges from 80 to 100 % for both samples for 150 cycles, with an average value of 95 % and 92 %.

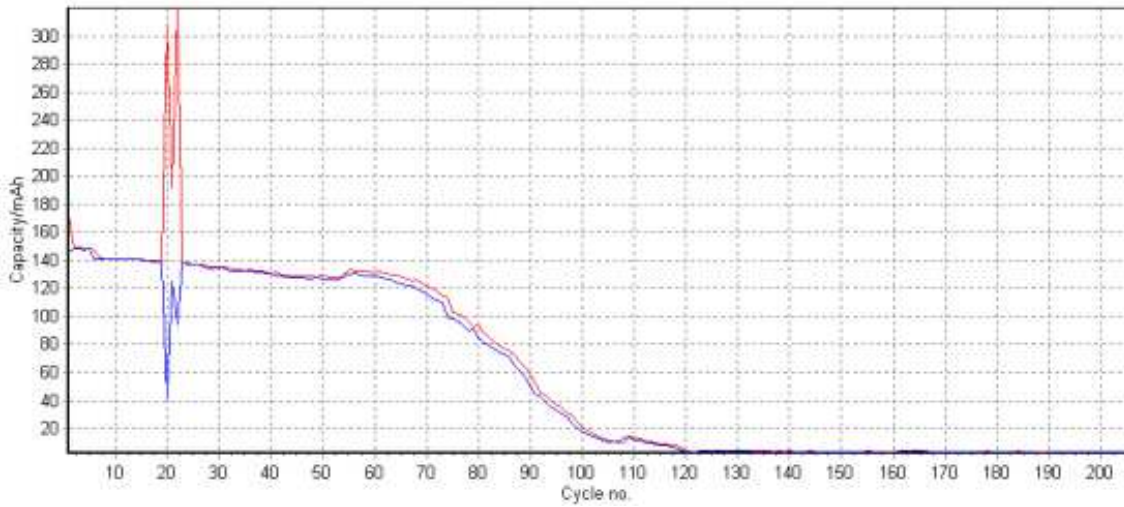


Figure 80. Electric capacity over time, electrode 10 sample 10.1.2, cycling to 4.2 V.

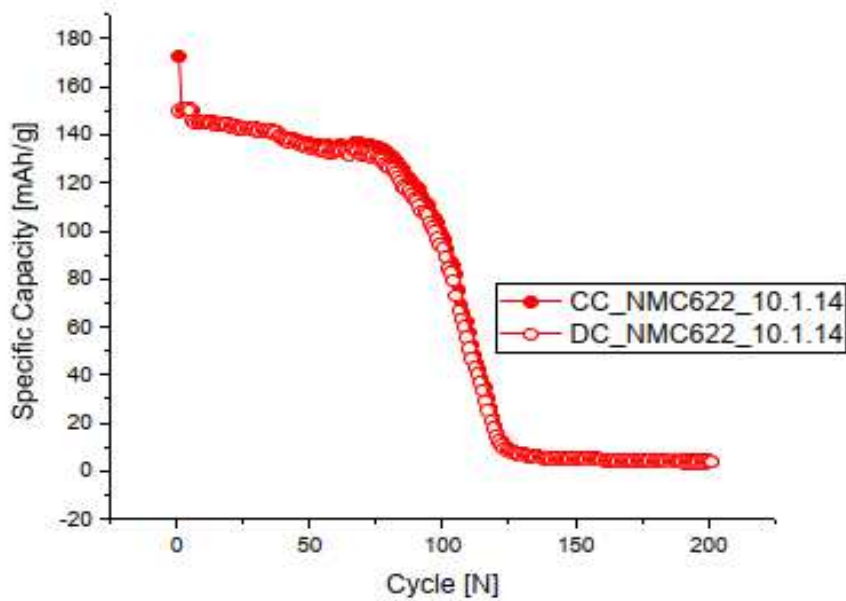


Figure 81. Electric capacity over time, electrode 10 sample 10.1.14, cycling to 4.2 V.

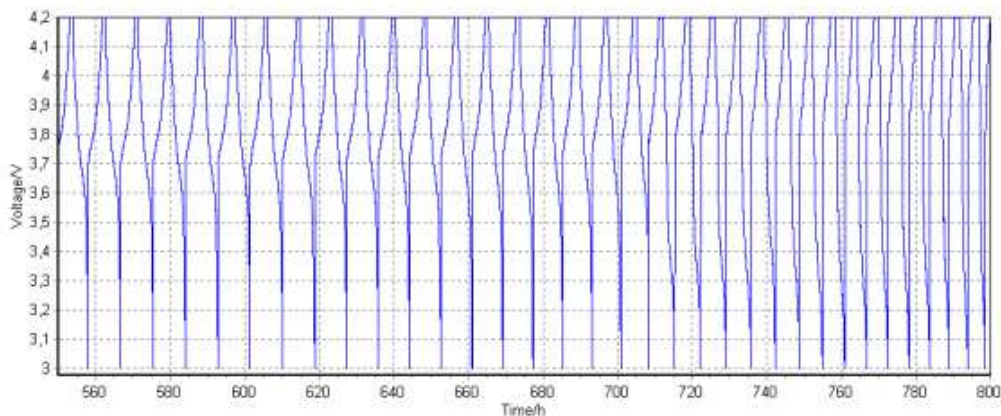


Figure 82. Cell voltage over time for cycles 60 to 85, electrode 10 sample 10.1.2, cycling to 4.2 V.

3.3.7.2. Samples 10.1.6 and 10.1.11, cycling to 4.5 V

Samples 10.1.6 and 10.1.11 were subject for 4.5 V cycling. Results are visible in Figure 83 and 84. For about 120 cycles, cathode specific capacity (of cathode material) is about 176 mAh/g. Unfortunately, after 60 cycles, capacity of one sample declines to about 5 mAh/g, but decreases slower than in other samples (in about 40 cycles). Second sample still shows capacity about 174 mAh/g after 63 cycles, but available results end at 63rd cycle. Electric efficiency ranges from 94 to 100 % for 63 cycles, with average values of 98 %. Here, for those samples it can be observed for about 60 and 63 (without drop) charge/discharge cycles. Further ongoing alterations can lead to loss of properties of active material, especially to drop in charge/discharge capacity, which eventually drops to zero. Slow capacity drop (under about 35 cycles for sample 10.1.6) is somewhat greater in value than slow capacity loss mentioned earlier and leads to almost complete cell degradation. This process is only several times faster than the slow capacity loss; however, the chart shows an observable decrease in capacity during one cycle.

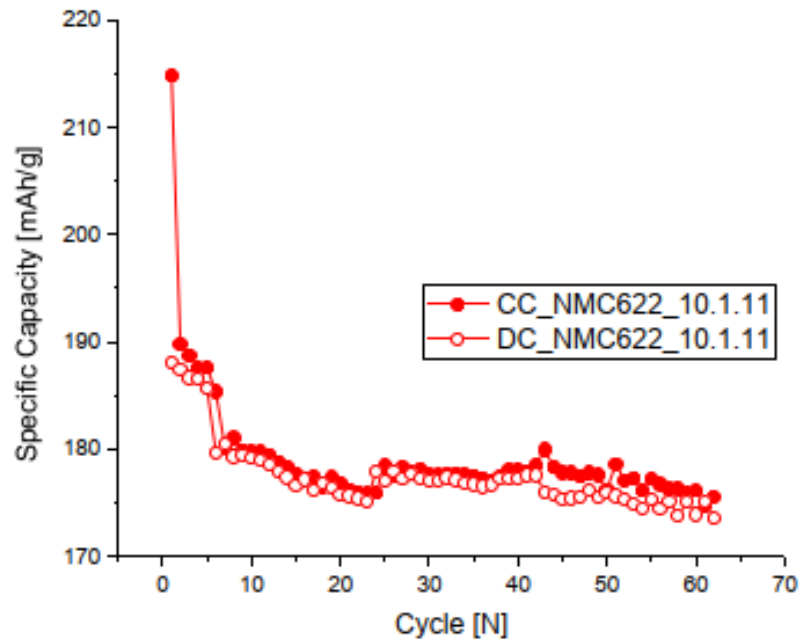


Figure 83. Electric capacity over time, electrode 10 sample 10.1.11, cycling to 4.5 V.

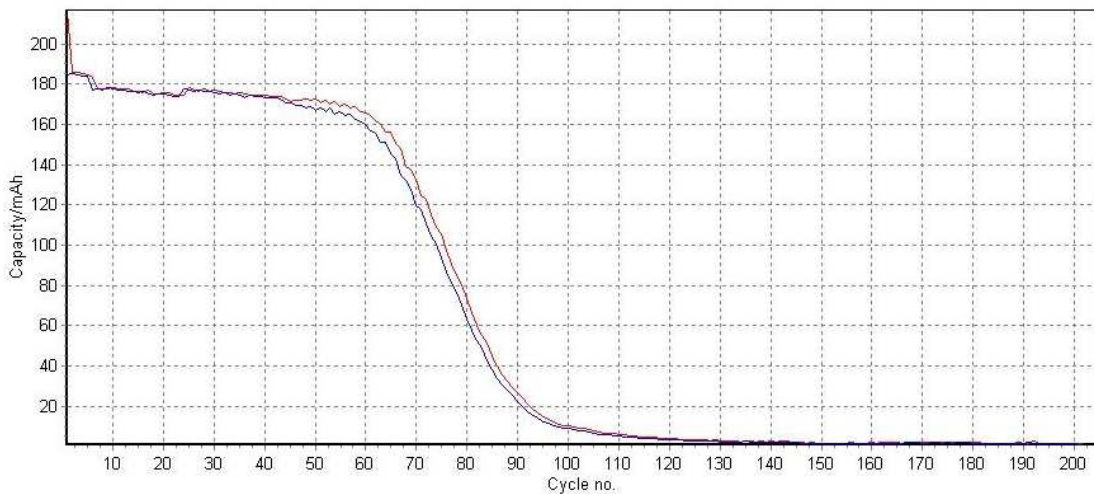


Figure 84. Electric capacity over time, electrode 10 sample 10.1.6, cycling to 4.5 V.

3.4. Comparison of cycling results

Obtained initial capacities for different voltages of different chemical compositions of cathode slurries are shown in Table 6. All six compositions of aqueous cathode slurry samples show smaller capacity when compared to reference non-aqueous cathode slurry sample. Specific capacities of aqueous samples are lower by 4.2-17.0 % than the reference sample capacity (4.2 V cycling). The three highest initial specific capacities of cathode active material was observed in samples: NMC 532 (sample 5, 4.2 V cycling; sample 5, 4.5 V cycling) and NMC 622 (sample 10, 4.5 V cycling). Obtained capacities for tested NMC powders are slightly better than mentioned in other papers,

both for 4.2 V and 4.5 V cycling.^{39,40,44,45} Highest capacity increase for the higher cycling voltage occurred for NMC 111 (sample 9: 27.1%), while lowest occurred for NMC 622 (sample 6: 9.7%). Presented values confirms that higher cycling voltage leads to higher electric capacities.^{10,17,19} It is worth noticing that samples made with higher amount of conductive agent (second composition, samples 8, 9 and 10) have similar specific capacities (calculated for pure active material) to samples made with higher amount of active material (first composition, samples 4, 5 and 6), especially under cycling to 4.2. Capacity is nearly the same for samples of the same active material in different slurry formulations. Only NMC 622 shows higher (21 mAh/g) difference between formulations specific capacities under cycling to 4.5 V, where all other differences are smaller than 10 mAh/g.

Table 6. Initial capacities of different cathode formulations.

Cycling voltage [V]	4.2	4.5	4.2 → 4.5
Slurry composition	Average initial capacity [mAh/g]		Capacity increase [%]
4 (NMC 111)	137	169	23.4
9 (NMC 111)	140	178	27.1
5 (NMC 532)	158	190	20.3
8 (NMC 532)	156	189	21.2
6 (NMC 622)	154	169	9.7
10 (NMC 622)	151	190	25.8
non-aqueous binder sample (reference)	165	---	---

The stability of electric capacity is also an important factor in cells rating. This value depends mainly on active material stability, binder stability and current collector stability. To preserve capacity as high as possible, binder should provide good contact of active material to the aluminium foil. The preparation process with aqueous slurry can affect this strongly. It can lead to corrosion during cycling due to residual water content. Further, the active material should not degrade during operation. Two different behaviors were observed in materials from water-based slurry.

Firstly, a slow capacity loss before rapid capacity drop was observed. Table 7 shows part of the obtained results. Only samples with visible, systematic and slow capacity loss are mentioned there, other are omitted. As reference, at the end of the table four results based on NMC 111 are presented from two different scientific groups.^{39,40} The observed slow capacity fade was used to project capacity losses after 100 and 1000 cycles. In some cases, losses may be higher than real capacities of the mentioned samples. Best results (capacity drop after 1000 cycles less or equal to 100 mAh/g) were noted for NMC 111 (sample 4.8. 4.5 V cycling, 90.9 mAh/g capacity loss) and NMC 532 (samples 8.1.4, 8.2.1, 4.5 V cycling 83.3 mAh/g capacity loss, samples 8.1.1, 8.2.8, 4.2 V cycling, 100 mAh/g capacity loss). Only samples 5.10, 6.2, 6.3, 6.6, 6.7, 6.10 and 10.1.2 have much higher calculated capacity loss than samples from other groups (greater than 250 mAh/g). This capacity loss may be associated with active material degradation due to electrochemical changes during cycling, like changes of chemical composition, mentioned before. Those changes are slow, but relentless, gradually lowering cell electric capacity. Some not mentioned samples, with less visible capacity loss, also suffered the same changes, because they are subject to the same electrochemical restrictions.

Table 7. Comparison of capacity loss depending on number of cycles for different samples.

Sample name	Voltage [V]	Observed drop [mAh/g]	Number of cycles	Calculated drop [mAh/g]	
				for 100 cycles	for 1000 cycles
4.3 (NMC 111)	4.2	10	60	16.7	166.7
4.8 (NMC 111)	4.5	10	110	9.1	90.9
9.1.3 (NMC 111)	4.5	10	60	16.7	166.7
5.10 (NMC 532)	4.5	15	50	30.0	300.0
8.1.1, 8.2.8 (NMC 532)	4.2	15	150	10.0	100.0
8.1.4, 8.2.1 (NMC 532)	4.5	10	120	8.3	83.3
6.2, 6.3, 6.6, 6.7, 6.10 (NMC 622)	4.2	20	50	40.0	400.0
6.11 (NMC 622)	4.5	20	100	20.0	200.0
10.1.2 (NMC 622)	4.2	20	70	28.6	285.7
10.1.14 (NMC 622)	4.2	15	75	20.0	200.0
Sample from [11]	4.2	10	100	10.0	100.0
Sample from [11]	4.2	20	100	20.0	200.0
Sample from [12]	4.2	10	70	14.3	142.9
Sample from [12]	4.2	45	2000	2.3	22.5

Secondly, a rapid capacity drop happened after a certain number of cycles. The cycle numbers for relatively stable capacity until this fast degradation occurs is presented in Table 8 for the different samples. Three samples are marked with ‘not observed (>X)’ comments, because those cells were not tested further than a certain number of cycles and the capacity drop was not observed. Longest durability was observed for NMC 532 (sample 8) – 150 cycles under 4.2 V cycling and 145 cycles under 4.5 V cycling. Also noteworthy are results of sample 4 (4.5 V cycling), sample 9 (4.2 V cycling) and sample 6 (4.5 V cycling) with more than 100 cycles before capacity drop. Worst results were observed for sample 6 (4.2 V cycling and 4.5 V cycling) and slightly better results were noted for sample 5 (4.2 V and 4.5 V cycling) and sample 9

(4.5 V cycling). It is worth noticing that samples made with higher amount of conductive agent (second composition, samples 8, 9 and 10) usually lasts longer than samples made with higher amount of active material (first composition, samples 4, 5 and 6).

Table 8. Number of cycles to rapid capacity drop for different cathode formulations.

Voltage [V]	4.2	4.5
Slurry composition	Number of cycles to rapid capacity drop	
4 (NMC 111)	90, 55	110, not observed (>84)
9 (NMC 111)	110, 88	55, 50
5 (NMC 532)	35, 50, 80	50, 50
8 (NMC 532)	150, 140	145, 115
6 (NMC 622)	30, 50, 50, 50, 45	30, 105
10 (NMC 622)	80, 70	60, not observed (>63)
non-aqueous binder sample (reference)	not observed (>100)	---

The fast capacity drop will be discussed in detail. Term ‘fast’ appoints rapid capacity drop, which leads to nearly entire cell degradation. Obtained results are shown in Table 9, with three groups of samples – with instant capacity drop (up to 9 cycles), with fast capacity drop (in 10-15 cycles) and with rather slow capacity drop (in 16-50 cycles). Duration of capacity drops is similar for samples cycled to 4.2 V and to 4.5 V. Only more samples cycled to 4.2 V suffered instant capacity drop, but it may be totally without relationship to cycling voltage. Similar number of samples, 7 for 4.2 V cycling and 6 for 4.5 V cycling, suffered rather slow capacity drop. Drop duration is also similar for both cycling voltages, being slightly better for 4.2 V cycling, which may favor better longevity of electrodes. It is worth noticing that samples made with higher amount of conductive agent (second composition, samples 8, 9 and 10) usually suffer slower capacity drop than samples made with higher amount of active material (first composition, samples 4, 5 and 6).

Table 9. Comparison of capacity drop duration for different samples.

Voltage [V]	Instant capacity drop (<10 cycles)	Fast capacity drop (10-15 cycles)	Slow capacity drop (16-50 cycles)
4.2	5.1 (NMC 532)	4.1 (NMC 111)	4.3 (NMC 111), >40 cycles
	5.2 (NMC 532)	6.7 (NMC 622)	6.10 (NMC 622), 25 cycles
	5.6 (NMC 532)		9.1.11 (NMC 111), 25 cycles
	6.2 (NMC 622)		8.1.1 (NMC 532), 25 cycles
	6.3 (NMC 622)		8.2.8 (NMC 532), 30 cycles
	6.6 (NMC 622)		10.1.2 (NMC 622), 30 cycles
	9.2.1 (NMC 111)		10.1.14 (NMC 622), 40 cycles
4.5	9.2.5 (NMC 111)	4.8 (NMC 111)	5.3 (NMC 532), 20 cycles
		6.1 (NMC 622)	5.10 (NMC 532), 25 cycles
		9.1.3 (NMC 111)	6.11 (NMC 622), 45 cycles
			8.1.4 (NMC 532), 30 cycles
			8.2.1 (NMC 532), 20 cycles
			10.1.6 (NMC 622), 35 cycles

3.5. Cyclic voltammetry of prepared cathodes

Cathodes samples made with every prepared cathode were taken to check their electrochemical properties during testing in Ametek's program for voltammetric measurements. It is used to obtain information about electrochemical reactions inside the tested material. Cyclic voltammograms of all aqueous binder cathodes samples are presented in Figure 85 and 86. Every plot has only 2 visible peaks, which are associated with NMC active material reduction and oxidation. All six plots show nearly the same oxidation potential (about 3,8 V) and reduction potential (about 3,6 V). With subsequent cycles, the shape of loops is relatively well maintained. The absence of other current peaks means that nothing else takes part in other electrochemical reactions. This suggests that used aqueous binder mixture is electrochemically stable under cell cycling conditions from 3 to 4.5 V – in other words it does not oxidize nor reduce.

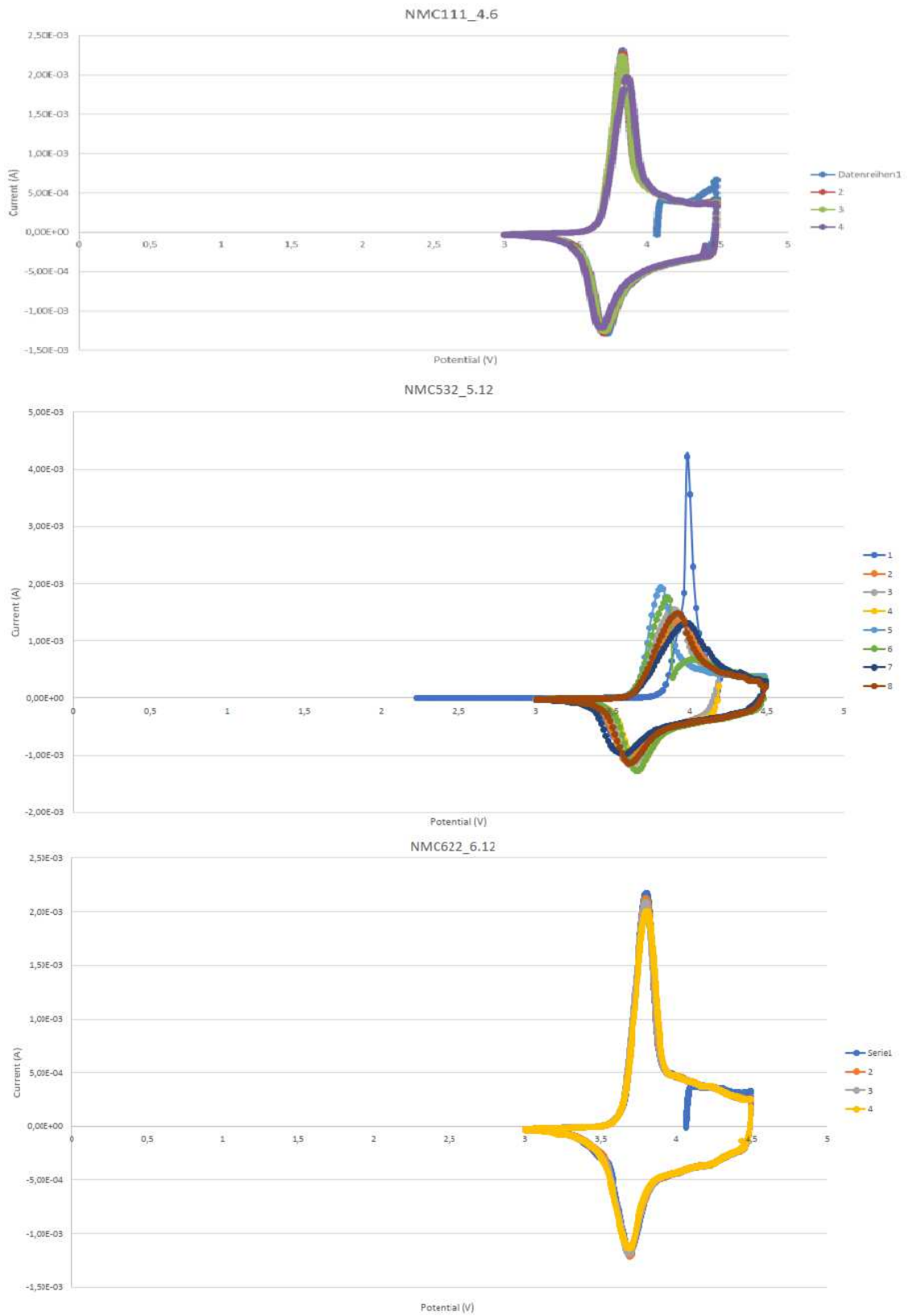


Figure 85. Cyclic voltammograms of samples from 1st composition (4.6, 5.12 and 6.12).

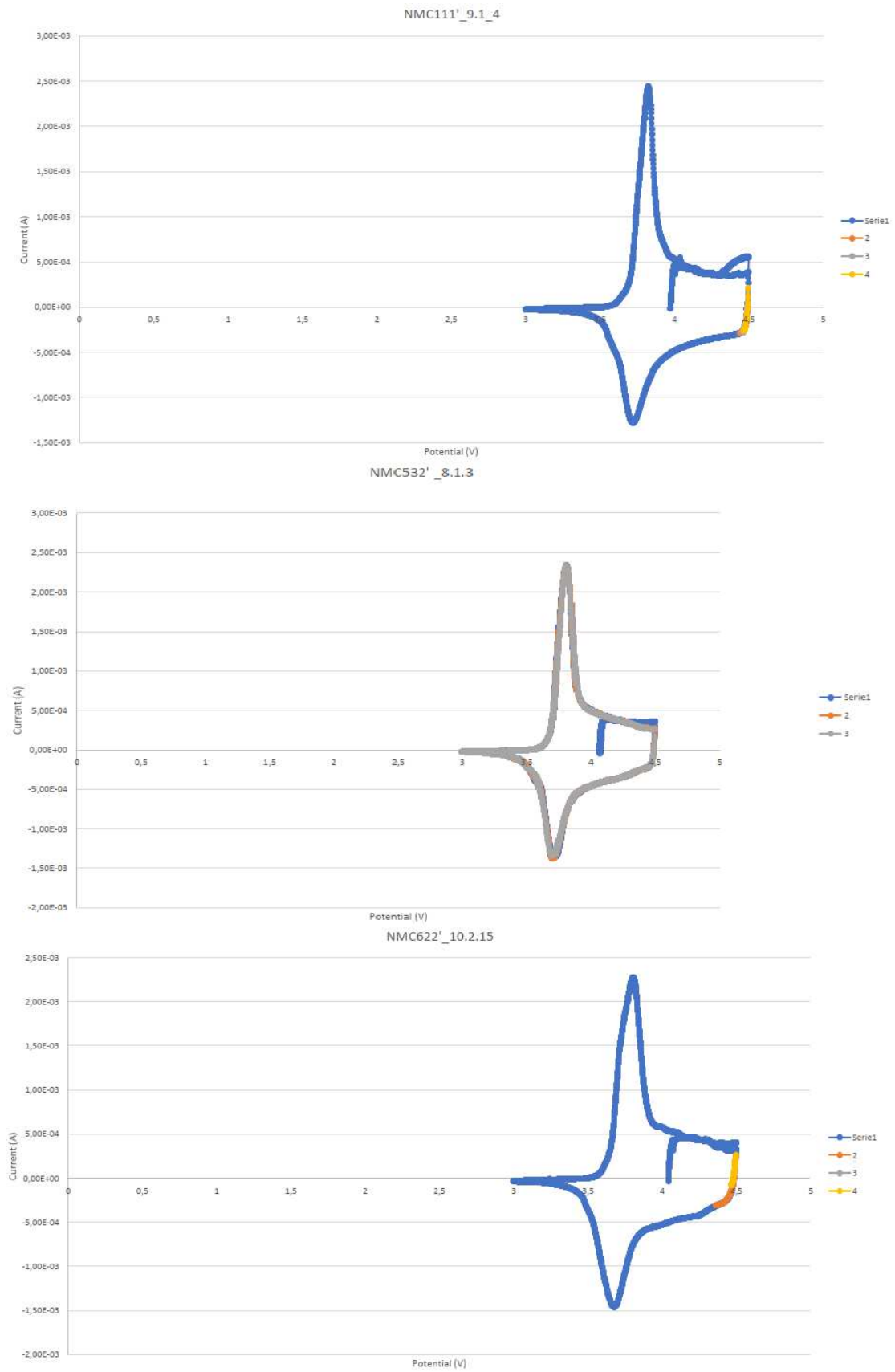


Figure 86. Cyclic voltammograms of samples from 2nd composition (9,1.4, 8.1.3 and 10.2.15).

4. Experimental results summary and conclusions

In this work, the main goal was to show properties and working scheme of Li-Ion batteries, which were based on three well known nickel-manganese-cobalt lithium oxides (NMC 111, NMC 532 and NMC 622) materials with water-soluble binder mixtures of carboxymethyl cellulose (CMC) and fluorine acrylic latex (JSR TRD202A). Based on conducted research and experiments, operation and properties and of Li-Ion batteries were shown. The whole processing of cathodes was presented, starting from slurry preparation, going through slurry casting, cathode drying and cutting, ending on coin cell preparation and examination. Slurry preparation began with adding carbon black (conductive agent) to a CMC solution in water, which was mixed and subsequently blended with NMC-oxide material and at the end modified latex was added under stirring. Then, a slurry film was spread by doctor blade on an aluminum foil and dried first in atmospheric conditions and then at higher temperature under vacuum. Dried foils with coating were hot calandered and afterwards cut into coin-cell shaped electrodes. Two different cathodes formulations with the same binder mass share, but with higher mass share of NMC active material (and hence lower share of conductive agent) and with lower mass share of NMC active material (and hence higher share of conductive agent), for three different oxides – NMC 333 (or NMC 111), NMC 532 and NMC 622, resulting in six different groups of samples. Coin cell were prepared after drying cathodes under vacuum in oven and assembling them with metallic lithium as anode and electrolyte. Properties of cathodes were examined by:

- cycling charge-discharge tests with Maccor Battery & Cell Test Equipment Series 4600 used in CC-CV (constant current, constant voltage) charging with 0.1 C rate during formation and 0.2 C rate during cycling of cells, whose results are cathode capacity and voltage and their changes during full cycle time;
- cyclic voltammograms tests with Ametek's program, whose results are oxidation and reduction potentials of components used to prepare cathodes (active materials, conductive agent, binders and current collectors);
- scanning electron microscopy (SEM) and electron dispersive X-ray spectroscopy/analysis (EDAX/EDS), which were used to examine samples morphology and chemical composition of samples surface;

- some organoleptic tests were used to determine properties of active material coating on current collector by scratching, tapping and bending them before and after cycling tests of cells.

Cycling tests under 0.2 C rate to 4.2 V, performed for samples of all six cathodes showed that cathodes made with aqueous slurries have lower specific capacity than cathode prepared with PVDF (non-aqueous binder) under the same cycling conditions. Under cycling to 4.2 V, NMC 532 showed the highest specific capacity (about 156-158 mAh/g) and NMC 111 showed the lowest specific capacity (about 137-140 mAh/g). Capacity of NMC-622 was about 151-154 mAh/g. Highest specific capacity of aqueous binder electrode was about 158 mAh/g, while PVDF-based electrode showed specific capacity about 165 mAh/g, which means a 4.2% lower value (up to 17.0% for other electrodes) for aqueous binder composition. Under cycling to 4.5 V, specific capacity increased by 9.7-27.1 %, depending of electrode composition, with best result for NMC-532 (about 189-190 mAh/g). The highest increase was noted for NMC 111 sample (27.1 %) with capacity about 169-178 mAh/g. Capacity of NMC-622 was about 169-190 mAh/g. Capacity increase with usage of higher cycling voltage was also proved by other scientific groups,^{17,19,41} which may be useful way to improve cell properties, but may result in shorter cell life cycling. Other scientific groups results are described briefly below:

- group with N. Loeffler³⁹ at the forefront obtained specific capacity of NMC 111 material approx 123-125 mAh/g with use of polyurethane and CMC binder mixture, during cycling to 4.2 V under 1 C rate;
- another group with N. Loeffler⁴⁰ at the forefront obtained specific capacity of NMC 111 material approx 130-134 mAh/g with use of CMC binder, during cycling to 4.2 V under 1 C rate and higher capacity values were obtained for heavier calandered samples;
- group with K. Notake⁴¹ at the forefront obtained specific capacity of own-synthesized Li-rich NMC material approx 260-270 mAh/g with use of fluorine latex and CMC binder mixture, during cycling to 4.8 V;
- group with L. Li⁴⁵ at the forefront obtained specific capacity of own-synthesized NMC 111 material approx 160-181 mAh/g with use of polytetrafluoroethylene binder (pressed electrode, without water processing), during cycling to 4.5 V under 0.109-0.125 C rate.

Longest uninterrupted operation was observed for NMC 532 (sample 8) – 150 cycles under 4.2 V cycling and 145 cycles under 4.5 V cycling. Worst results were observed for NMC 622 sample (4.2 V cycling, no more than 50 cycles for all samples). It is apparent that samples made with more conductive agent (second composition) usually lasts longer than samples made with more active material (first composition). It is assumed that a larger proportion of the conductive agent can improve electrical conductivity between the current collector (aluminium foil) and active oxide material, which is a rather weak electrical conductor. This involves reduction of the stress caused by volume changes during cycling, which can usually cause damage to the cathode material. Unfortunately, none of the scientific groups conducted a direct comparative test of durability of similar compositions with a variable amount of active oxide material and a conductivity improving additive/agent.

During cycling tests, two types of capacity loss were observed. For some samples, slow, continuous capacity loss (less than or equal to 40 mAh/g for 100 cycles) was noted. The calculated rate of capacity decline ranged from 8.3 to 40 mAh/g per 100 cycles. Nine samples had similar capacity loss rate to values obtained by other scientific groups,^{39,40} which used polyurethane and CMC based aqueous binders, with a specific value less than or equal to 20 mAh/g for 100 cycles. During cycling to 4.2 V, the group with N. Loeffler³⁹ at the forefront showed that their two samples of cathode (NMC 111 and polyurethane-CMC binder mixture, cycled with 1 C rate) lost 10 and 20 mAh/g per 100 cycles (calculated values). This is comparable with the results of tests presented in this paper for samples prepared with three different NMC oxides and CMC and fluorine latex binder mixtures, cycled with 0.2 C rate to 4.2 and 4.5 V. Another group, again with N. Loeffler⁴⁰ at the forefront showed that their two samples of cathode (NMC 111 and CMC binder, cycled with 1 C rate) lost 14.3 and 2.3 mAh/g per 100 cycles (calculated values) during cycling to 4.2 V. First value is comparable with the results of tests presented in this paper and second one is far lower than the same value for samples prepared with three different NMC oxides and CMC and fluorine latex binder mixtures, cycled with 0.2 C rate to 4.2 and 4.5 V. The best result was observed for two samples of NMC 532 active material (composition with higher conductive agent mass share) and 4.5 V cycling. The capacity loss was 8.3 mAh/g for 100 cycles. This capacity loss may be associated with active material degradation due to electrochemical changes during cycling, like changes of chemical composition. Those changes are slow,

but relentless, gradually lowering cell electric capacity. Some of those chemical changes were observed during EDAX examination. All samples, also those with less visible capacity loss, suffered the same changes, because they are subject to the same electrochemical working circumstances. Some samples have seen a rapid loss or decrease in performance. This process is a fast drop of capacity within 50 cycles or much less and leads to total cell failure. The specific capacity of the cathode material fell to 0-20 mAh/g, which means that cell is no longer usable. It may indicate that during cycling, binder is losing its properties, especially adhesive and bonding strength, which may affect cell stability and properties. After peeling of the active material coating from current collector during cycling, cell capacity may be severely affected. It is worth noticing that samples made with more conductive agent (second composition, samples 8, 9 and 10) usually show a slower capacity drop than samples made with more active material (first composition, samples 4, 5 and 6). A larger proportion of the mass of conductive medium can improve electrical conductivity between the current collector (aluminium foil) and the active oxide material, which is a rather poor electrical conductor.

Cyclic voltammetry showed that during cycling from 3 to 4.5 V only peaks of reduction and oxidation of active oxide material appear in the graphs. With subsequent cycles, the shape of loops is relatively well maintained. This suggests that the aqueous binder mixture used is electrochemically stable under cell cycling conditions from 3 to 4.5 V – in other words, it does not oxidize nor reduce.

Scanning electron microscopy (SEM) showed that the surface of the examined cathodes is rather smooth, but has evenly distributed mainly spherical holes and cavities. The formation of these cavities can be related to the formation of hydrogen gas bubbles during the preparation process of cathodes. The water from the aqueous slurry/suspension reacts with aluminium current collector foil due to alkaline pH. Thanks to calendaring, surface of electrodes is rather smooth. Even cycled samples have no visible defects, such as an exfoliating or peeling coating of electrode active material. Higher magnification images show cavities with a visible smooth ground, which was subject for EDAX examination. The result is 73,4% atomic content of aluminum and 25.43% atomic content of oxygen, which clearly confirms that the observed area is the current collector aluminium foil, which may be partially affected by reaction with water during casting an alkaline water-based electrode slurry (reaction of aluminum with

water leads to formation of aluminum oxides and hydroxides). Energy dispersive X-ray spectroscopy/analysis (EDS or EDAX) results show unstable chemical composition of the surface layer. When cycled to 4.2 V potential, electrode 5 (NMC 532) experienced increase in manganese and cobalt content or loss in nickel content. When cycled to 4.5 V, the same electrode suffered manganese and probably nickel loss. When cycled to 4.2 V potential, electrode 6 (NMC 622) experienced some cobalt loss and probably nickel loss (suggested by increase in manganese content). When cycled to 4.5 V, the same electrode suffered loss in manganese and cobalt content. Those changes can be explained by reaction of oxide active material with solvent and/or electrolyte during battery cycling. After formation cycles, increased charge/discharge rate (from 0.1 C to 0.2 C) and periodic changes in volume of oxide active material leads to stress of whole electrode complex, also straining cathode electrolyte interphase. Further continuous changes can lead to loss of properties of active material, especially to drop in charge/discharge capacity.

Because SEM and EDAX testing required opening of closed cells, it was also possible to check adhesive strength of coating on aluminium foil. Uncycled cells showed rather good scratch or knock/impact resistance, while cycled samples were much more susceptible to any physical operations, which is seen as coating loss on foil surface. This may suggest that during cycling, binder loses its properties, especially adhesive and bonding strength, which may affect stability and properties of the cell. After peeling off active material coating from current collector during cycling, cell capacity will be severely limited.

Various nickel-manganese-cobalt oxides (NMC 111, NMC 532 and NMC 622) as active materials for cathodes for lithium ion batteries, combined with environmental-friendly, water-soluble binders (mixture of carboxymethyl cellulose and fluorine acrylic latex TRD202A) are promising materials for cathode formation. While other scientific groups reported good cycling stability (small capacity loss during long-term cycling, noteworthy electrochemical potential, high efficiency), all samples prepared in this work showed initially good trend, which unfortunately ended as capacity dropped to zero no later than after 150 cycles. Probably this behavior of cathode active material results from preparation and processing of raw materials to cathode slurry. NMC oxides are prone to leaching and hydrolysis when in contact even with pure water, which results in some properties loss, and reaction products may with aluminum current

collector due to increased pH of suspension. As previously mentioned, this chemical alteration of NMC oxide and the corrosion of the aluminum foil are undesirable, but also impossible to eliminate due to the method of slurry preparation, which involves water as a temporary binder and carrier for the electrode components. There are two possible ways, tested and described by other scientific groups, to limit those unwanted processes – lowering slurry pH value with additives (which prevents aluminum corrosion) or preventing active materials contact with aggressive suspension by use of coatings which blocks hydrolysis or corrosion. Slurry additives were tested by group with N. Loeffler at the forefront – mild acid, and by group with M. Memm at the forefront – amphoteric oxides.^{40,44} Mild acids, here formic acid, added to slurry prevents pH increase, but tends to increase ions leaching from NMC material, which is an unwanted compromise.⁴⁰ Amphoteric oxides (γ -Al₂O₃ and SiO₂) also lowered pH value, but also lowers active material mass fraction in the cathode slurry composition. Different coatings were tested by group with N. Loeffler at the forefront – current collector foil coated with carbon, and by group with K. Notake at the forefront – active material coating with Al₂O₃.⁴¹ Both methods limit contact with water from slurry, which blocks hydrolysis of NMC or corrosion of aluminum foil. Both types of methods proved to be useful and efficient. Probably at least one of those methods should be used to improve long-term stability of the cathodes. It is worth to search for alternatives since lithium nickel-manganese-cobalt oxides are rather cheap and aqueous binders (CMC and fluorine latex) are far more environmentally friendly than PVDF binder, which requires utilization of volatile, organic solvents. NMC oxides show very good properties when it comes to useful discharge/charge capacity and long-term stability. They are sensitive to conditions of slurry processing and cathode manufacturing process, as evidenced by and degradation of oxide active material alkalization of slurry. In future, more interest and attention should be given to the processing of NMC-water slurries. As the law tends to tighten up, and environmental protection is very important, we cannot avoid changing and upgrading our current technology of Li-Ion batteries. The development of new, more advanced technologies, taking into account certain restrictions arising from the materials used, but maximizing their positive characteristics, should be the main goal of scientific research. Due to the use of less harmful agents for the production of new type of cells and huge demand for safe, portable and clean energy sources and batteries, this direction of development has a

great opportunity to develop significantly in the future. This should lead to a stable, efficient and easily obtainable material for new type of cathodes. The environmental impact is also improved, especially when NMC material is combined with water-compatible binders.

5. References

- ¹ Bruno Scrosati Chapter 2. Lithium batteries: From early stages to the future, 2013.
- ² Isidor Buchmann, The power of Li-Ion, *Wireless Review*; Jun 15, 2000; 17, 12; ABI/INFORM Collection, 40.
- ³ Sol Jacobs, Lithium battery basics, *Machine Design*; Mar 6, 75, 5; ABI/INFORM Collection pg. 72, 2003.
- ⁴ R. Koksang, J. Barker, H. Shi, M. Y. Saidi, Cathode Materials for lithium rocking chair batteries, *Solid State Ionics*, Volume 84, Issues 1-2, 1996, 1-21.
- ⁵ M. Wakihara, O. Yamamoto (Eds.), *Lithium Ion Batteries Fundamentals and Performance*, Tokyo, 1998.
- ⁶ K.E. Aifantis, S.A. Hackeny, R.V. Kumar, *High Energy Density Lithium Batteries*, Weinheim: Wiley-VCH, 2009.
- ⁷ S.J. Gerssen-Gondelach, A.P.C. Faaij, Performance of batteries for electric vehicles on short and longer term, *Journal of Power Sources*, 2012.
- ⁸ W. Mocko, E. Szmidt, Recovery Technologies of Co and Li from spent lithium-ion cells, *Archives of Waste Management and Environmental Protection* vol. 14, no.4, 2012;
- ⁹ Bucur Claudiu B., *Challenges of a Rechargeable Magnesium Battery: A Guide to the Viability of this Post Lithium-Ion Battery*, Springer, Switzerland, 2018.
- ¹⁰ K.E. Aifantis, S. A. Hackeny and R. V. Kumar, *High Energy Density Lithium Batteries*, Weinheim: WileyVCH, 2010;
- ¹¹ J.-M. Tarascon, M. Armand, Issues and Challenges Facing Rechargeable Lithium Batteries, *Nature* 414(6861):359-67, 2001.
- ¹² N. Shimbashi, *TechSci Research*, <https://www.techsciresearch.com/blog/manufacturing-lithium-ion-batteries/29.html>, Japan, 16.06.2019.
- ¹³ F. Liu, P.P. Mukherjee, Materials for positive electrodes in rechargeable lithium-ion batteries.
- ¹⁴ Sony Corporation, *Keywords to understanding Sony Energy Devices*, Sony, 1991, archived in 2016.
- ¹⁵ Y. Xianxia, L. Hansan, Z.Jiujun, *Lithium-ion batteries: advanced materials and technologies*, CRC Press, 2012.
- ¹⁶ Patrice Simon, Jean-Marie Tarascon, et al., *Energy Storage – Batteries and Supercapacitors Set*, 2015.
- ¹⁷ A.A. Franco, *Rechargeable lithium battery from fundamentals to applications*, Woodhead Publishing Series in Energy, Elsevier Science, 2015.
- ¹⁸ X. Li, J. Liu, M.N. Banis, A. Lushington, R. Li, M. Cai, X. Sun, Atomic layer deposition of solid-state electrolyte coated cathode materials with superior high-voltage

cycling behaviour for lithium ion battery application, Energy and Environmental Science Royal Society of Chemistry, 2014.

¹⁹ K. Kanamura, Problems and expectancy in lithium battery technologies, Chapter 6, 2013.

²⁰ Zolin L., Large-scale Production of Paper-based Li-ion Cells, 27-28, Springer, Switzerland 2017.

²¹ Buchmann I. and Battery University Group, Types of Lithium-ion, https://batteryuniversity.com/learn/article/types_of_lithium_ion, 22.06.2019.

²² N. Nitta, F. Wu, G. Yushin, Li-ion battery materials: present and future, Elsevier, Volume 18, June 2015.

²³ M. Facada, Li-ion batteries and the years ahead, Industrial Minerals, London 2018.

²⁴ Buchmann I. and Battery University Group, Types of Lithium-ion, https://batteryuniversity.com/learn/article/types_of_lithium_ion, 22.06.2019.

²⁵ NMC Powder, Lithium Nickel Manganese Cobalt Oxide Cathode for Li-ion Batteries, <https://www.targray.com/li-ion-battery/cathode-materials/nmc>, 11.07.2019.

²⁶ D. Aurbach and Y. Cohen, J. Electrochem. Soc., 1996, 143, 3525 -3532 CrossRef CAS PubMed.

²⁷ M. S. Whittingham Proc. IEEE, 2012, 100, 1518 -1534 CrossRef CAS.

²⁸ W. Xu, J. Wang, F. Ding, X. Chen, E. Nasybulin, Y. Zhang, Lithium metal anodes for rechargeable batteries, Energy & Environmental Science, Issue 2, Elsevier B.V, pp.513-537, 2014.

²⁹ K. Kanamura, Problems and expectancy in lithium battery technologies, Chapter 6, 2013.

³⁰ Ch. Julien, A. Mauger, K. Zaghbi, H. Groult, Comparative Issues of Cathode Materials for Li-Ion Batteries, Inorganics 2014, 2, 132-154.

³¹ M. Montanino, S. Passerini, G.B. Appetecchi, *Electrolytes for rechargeable lithium batteries*.

³² M. Xu, S. Dalavi, B.L. Lucht, *Chapter 4. Electrolytes for lithium-ion batteries with high-voltage cathodes*, 2013.

³³ K. Xu, Chemical Review 2004, 104 (10), 4303 – 4417.

³⁴ M. Wang, A. V. Le, D. J. Noelle, Y. Shi, Y. Shirley Meng, Y. Qiao, Internal-short-mitigating current collector for lithium-ion battery, Journal of Power Sources, 2017, Vol.349, pp.84-93.

³⁵ L. Lu, X. Han, J. Li, J. Hua, M. Ouyang, A review on the key issues for lithium-ion battery management in electric vehicles, Journal of Power Sources, 226 (2013), pp. 272-288.

³⁶ M. Morita, T. Shibata, N. Yoshimoto, M. Ishikawa, Electrochim. Acta 2002, 47, 2787-2793.

³⁷ S. Santhanagopalan, Z. Zhang, Batteries for sustainability, Springer, New York, 2013, 135ff.

³⁸ P. Arora, Z. Zhang, Battery Separators, 104, 4419–4462, Chem. Review 2004.

-
- ³⁹ N. Loeffler, T. Kopel, G-T. Kim, S. Passerini, Polyurethane binder for aqueous processing of Li-Ion battery electrodes, *Journal of The Electrochemical Society*, 162 (14) A2692-A2698 (2015).
- ⁴⁰ N. Loeffler, J. Zamory, N. Laszczynski, I. Doberdo, G-T. Kim, S. Passerini, Performance of LiNi_{1/3}Mn_{1/3}Co_{1/3}O₂/graphite batteries based on aqueous binder, *Journal of Power Sources*, 248 (2014) 915-922.
- ⁴¹ K. Notake, T. Gunji, H. Kokubun, S. Kosemura, et al, The application of water-based hybrid polymer binder to a high-voltage and high-capacity Li-rich solid-solution cathode and its performance in Li-ion batteries, *J Appl Electrochem*, (2016) 46:267-278.
- ⁴² D. Versaci, R. Nasi, U. Zubair, J. Amici, M. Sgroi, M. A. Dumitrescu, C. Francia, S. Bodoardo, N. Penazzi, New eco-friendly low-cost binders for Li-ion anodes, 2017, Volume 21, Issue 12, pp 3429–3435.
- ⁴³ S. Lim, S. Kim, K.H. Ahn, S.J. Lee, The effect of binders on the rheological properties and the microstructure formation of lithium-ion battery anode slurries, *Journal of Power Sources*, 299 (2015) 221-230.
- ⁴⁴ M. Memm, A. Hoffmann, M. Wohlfahrt-Mehrens, Water-based LiNi_{1/3}Mn_{1/3}Co_{1/3}O₂-cathodes with good electrochemical performance by use of additives, *Electrochimica Acta*, 260 (2018) 664-673.
- ⁴⁵ L. Li, C. Feng, H. Zheng, P. He, J. Wang, Synthesis and electrochemical properties of LiNi_{1/3}Mn_{1/3}Co_{1/3}O₂ cathode material, *Journal of Electronic Materials*, vol. 43, no. 9 2014.
- ⁴⁶ M. Spreafico, P. Cojocar, L. Magagnin, F. Triulzi, PVDF Latex as a Binder for Positive Electrodes in Lithium-Ion Batteries, *Industrial and Engineering Chemistry Research*, <https://www.solvay.com/sites/g/files/srpend221/files/2018-07/pvdf-latex-as-a-binder-for-positive-electrodes-in-lithium-ion.pdf>, 04.10.2019.